AD-A042 530 ROCKWELL INTERNATIONAL ANAHEIM CALIF F/G 17/9
INVESTIGATION OF SURFACE OPTICAL WAVES FOR OPTICAL SIGNAL PROCE--ETC(U)
JUN 77 J D MCMULLEN, D L MILLS DAHC04-74-C-0024
UNCLASSIFIED C77-464/501 ARO-12120.9P NL

1 OF 2
AD
A042530

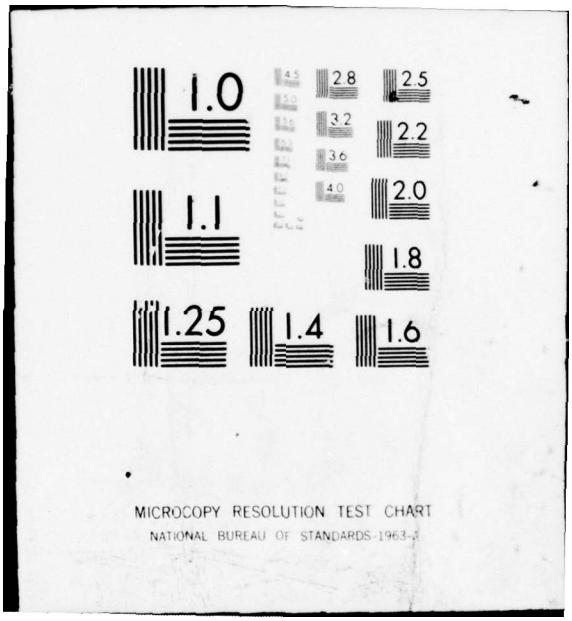
1.0
1.1
1.25
1.4
1.6
1.8
2.0
2.2
2.5
2.8
3.2
3.6
4.0
4.5
5.0
MICROCOPY RESOLUTION TEST CHART
NATIONAL BUREAU OF STANDARDS-1963-A

ARO-12120.9-P

C77-464/501

Final Technical Report

INVESTIGATION OF SURFACE OPTICAL WAVES FOR OPTICAL SIGNAL PROCESSING

by

J. D. McMullen
Principal Investigator
Rockwell International

and

D. L. Mills
Consultant
University of California, Irvine

1 June 1977

U. S. ARMY RESEARCH OFFICE
ARO Contract No. DAHC04-74-C-0024
1 June 1974 to 1 June 1977

Electronics Research Center
Rockwell International Corporation
3370 Miraloma Avenue
Anaheim, California 92803

Unclassified

SECURITY CLASSIFICATION OF THIS PAGE *(When Data Entered)*

REPORT DOCUMENTATION PAGE		READ INSTRUCTIONS BEFORE COMPLETING FORM
1. REPORT NUMBER C77-464/501	2. GOVT ACCESSION NO.	3. RECIPIENT'S CATALOG NUMBER
4. TITLE *(and Subtitle)* INVESTIGATION OF SURFACE OPTICAL WAVES FOR OPTICAL SIGNAL PROCESSING.		5. TYPE OF REPORT & PERIOD COVERED Final Technical Report, 1 June 1974 to 1 June 1977 6. PERFORMING ORG. REPORT NUMBER C77-464/501
7. AUTHOR(s) J. D. McMullen and D. L. Mills		8. CONTRACT OR GRANT NUMBER(s) DAHC04-74-C-0024
9. PERFORMING ORGANIZATION NAME AND ADDRESS<br~~Electronics Research Center~~ Rockwell International 3370 Miraloma Ave., Anaheim, CA 92803		10. PROGRAM ELEMENT, PROJECT, TASK AREA & WORK UNIT NUMBERS D0161102B11B
11. CONTROLLING OFFICE NAME AND ADDRESS Army Research Office Box CM, Duke Station Durham, North Carolina		12. REPORT DATE 1 June 1977 13. NUMBER OF PAGES 139
14. MONITORING AGENCY NAME & ADDRESS *(if different from Controlling Office)*		15. SECURITY CLASS. *(of this report)* Unclassified 15a. DECLASSIFICATION/DOWNGRADING SCHEDULE

16. DISTRIBUTION STATEMENT *(of this Report)*

Approved for public release; distribution unlimited

17. DISTRIBUTION STATEMENT *(of the abstract entered in Block 20, if different from Report)*

18. SUPPLEMENTARY NOTES

The views and conclusions contained in this document are those of the authors, and should not be interpreted as necessarily representing the official policies, either expressed or implied, of the Army Research Office or the United States Government.

19. KEY WORDS *(Continue on reverse side if necessary and identify by block number)*

Surface Polaritons, Surface Optical Waves, Surface Plasmons, CO_2 Pulsed Laser Radar, Frequency Chirped Pulse Compression, Surface Roughness, Dispersive Media, Phase Modulation.

20. ABSTRACT *(Continue on reverse side if necessary and identify by block number)*

NEXT PAGE

DD FORM 1 JAN 73 1473 EDITION OF 1 NOV 65 IS OBSOLETE

Unclassified

SECURITY CLASSIFICATION OF THIS PAGE *(When Data Entered)*

38.9126

ABSTRACT

Propagation and temporal compression of frequency-chirped CO_2 laser pulses has been investigated, wherein a dispersive optical pulse delay line is formed using dispersive surface and bulk phonon-polariton propagation modes in solids. Criteria are developed for the compression of optical pulses, and these criteria are compared to the relevant group-dispersive properties of the propagation modes to determine their suitabilities for performing laser pulse compression. Surface phonon-polariton modes on BeO:air and on BeO:Ge film:air structures, and bulk phonon-polaritons in α -quartz are examined as dispersive media for CO_2 laser pulses.

Absorption in the infrared-active medium has been shown to limit the magnitude of group dispersion available, in addition to limiting the attenuation length of each propagation mode. For the materials considered, absorption limits the application of this approach to CO_2 laser pulses having initial widths of 10 psec or smaller with initial chirp bandwidths in the THz range, if attenuation by absorption is to be limited to 50 dB. Both the narrow pulse width and large chirp bandwidth requirements preclude experimental demonstration with present CO_2 laser technology.

Consequently, attention has been focused in part on other pulse compression schemes appropriate for CO_2 lasers. One method recognized as promising is the grating-pair pulse compression filter in a highly dispersive configuration. An exact analytical solution has been developed for chirped pulses compressed by this type of strongly dispersive filter.

An alternative scheme has been explored, using active modulation of the phase velocity of a medium to compress the pulse envelope.

In earlier work on this program prism and grating coupling were investigated. Attenuation lengths were measured for surface polaritons on metals and BeO, and were found to be macroscopic. Analysis of scattering of surface polaritons by surface roughness showed that acceptable BeO surface quality could be produced by conventional optics polishing technology. Interactions between optical surface waves and surface elastic waves were investigated as a means to produce the desired chirp phase modulation. The influence of dielectric overlayers upon propagation characteristics of surface polaritons was studied, as means to modify the dispersion curves for particular pulse compression applications.

Nonlinear optical interactions among surface polaritons have been studied, including experimental attempts to observe second harmonic generation by a 10.6 μm surface plasmon on a metal surface. Recent theoretical work (Ch. VI) has shown that the second harmonic signal to be expected in the previously attempted experiment was just below the limit of detectability. This experiment is, therefore, being attempted again with appropriate modifications, and may yield the first observation of nonlinear optical interactions among localized surface polaritons. Positive experimental results, if forthcoming, will be reported.

TABLE OF CONTENTS

I. INTRODUCTION

A. Background

The purpose of this program is to investigate those properties of surface polaritons which may be applicable for signal processing at CO_2 laser frequencies, particularly for dispersive optical pulse delay lines to compress frequency chirped CO_2 laser pulses.

In this application, a pulse having just the appropriate amount of of frequency chirp becomes compressed after propagating through a dispersive medium, while background unchirped optical signals become dispersion-broadened and attenuated. The higher peak power of the compressed pulse, along with suppression of background signals, offers improved signal detection, while the narrow width of the compressed pulse gives higher range resolution.

Conventional methods of pulse compression for pulsed laser radars require converting the signal to electrical and acoustic signals, with large insertion losses or bandwidth limitations and sophisticated, power-consuming associated electronics. Pulse compression performed directly at optical frequencies eliminates several of these disadvantages. The present approach, using a dispersive propagation mode in a solid, compares favorably to other optical techniques such as grating pairs or interferometers, because of the relative compactness of the pulse delay line and the possibility of using ultra-wide chirp bandwidths to compress broader laser pulses than previously possible. Further, surface polariton propagation modes in over-layer film structures offer the possibility for constructing a pair of matched filters, so that both chirp and compression may be performed by compact, passive elements at optical frequencies.

The primary problems to be addressed are (1) the efficiency with which a chirped laser pulse can be coupled to the surface propagation mode, and possible distortion of the phase modulation (chirp) and pulse shape during the coupling process, (2) propagation losses arising from absorption and from roughness-induced scattering of the surface polariton, and (3) the amount of group velocity dispersion attainable for surface propagation modes at CO_2 laser frequencies.

B. Significant Results

Both prism and grating couplers were investigated as means to couple a CO_2 laser beam to surface propagation modes on BeO, quartz and metal substrates. Coupling efficiencies of ten percent were measured for prism couplers used to launch surface plasmons on metals, and about one percent for generation of a surface phonon-polariton at 10.6 μm on BeO. Attenuation lengths at 10.6 μm were typically one to 8 mm for surface plasmons on stainless steel, copper and gold, and 120 μm for the ordinary surface phonon-polariton on BeO.

Methods to modulate the phase of a surface optical wave have been investigated, including both electro-optic modulation and interactions with Rayleigh waves. These interactions offer the possibility to chirp the pulse while it is propagating as a surface wave.

Nonlinear optical interactions among surface polaritons have been studied. Experiments to generate a second harmonic surface plasmon by a fundamental surface plasmon at 10.6 μm did not yield a detectable harmonic signal.

The influence of dielectric overlayers upon the dispersion curves of surface phonon-polaritons has been examined in detail as a means to modify the curvature of the dispersion curves of surface phonon-polaritons.

This approach permits the design of a matched-filter pair for expansion and compression of laser pulses.

The theory for chirped pulse compression has been generalized to include strongly frequency-dependent absorption in the dispersive medium. The role of absorption has been quantitatively evaluated for both surface and bulk phonon-polaritons at CO_2 laser frequencies. It has been shown that absorption limits both the attenuation length of the mode and the magnitude of group velocity dispersion attainable. Because of absorption, pulse compression using surface phonon-polaritons on BeO or bulk phonon-polaritons in quartz, requires that the initial CO_2 laser pulse be chirped over a THz range, or an entire P or R branch, and that even then the initial pulse width be 20 psec or less. These parameters preclude experimental demonstration with existing CO_2 laser technology. These results are expanded upon in Section II of this report.

The theory for compression of a chirped pulse in a <u>strongly</u> dispersive medium has been examined, and new, closed-form expressions developed for the shape of the compressed pulse. In this treatment it is assumed that both the group velocity v_{gr} and its first frequency derivative $dv_{gr}/d\omega$ vary significantly with frequency over the bandwidth of the incident chirped pulse. An approach has been identified for compression of CO_2 laser pulses using a grating-pair filter in a highly dispersive configuration. Elements of this analysis follow in Section III of this report.

Active modulation of the refractive index of a crystal has been examined as a means to compress optical pulses, as outlined in Section V. Criteria are developed for active phase modulation and for distortion of the pulse envelope upon passing through a modulator of finite thickness.

C. List of Publications and Technical Reports

The following papers have been published or submitted for publication as results of this program:

D. L. Mills, "Theory of Second Harmonic Generation by Surface Polaritons on Metals, Solid State Communic. (to be published).

J. D. McMullen, "Chirped Pulse Compression in Strongly Dispersive Media," J. Appl. Phys. (to be published).

J. D. McMullen, "Analysis of Frequency-Chirped Optical Pulses using Dispersive Bulk and Surface Phonon-Polariton Propagation Modes at CO_2 Laser Frequencies," J. Appl. Phys. (manuscript No. 1209R, to be published).

D. L. Mills, "Theory of Surface Polariton Generation through Grating Couplers," J. Appl. Phys. (manuscript No. 1210R, to be published).

D. L. Mills, "The Interaction of Surface Polaritons with Periodic Surface Structures; Rayleigh Waves and Gratings," Phys. Rev. B 15, 3097 (1977).

J. D. McMullen, "Recursive Solution of the Dispersion Relation of a Surface Polariton in a Layered Structure," J. Opt. Soc. Am 67, 698 (1977).

J. D. McMullen, "Perturbation Analysis of the Influence of a Thin Dielectric Film on the Propagation Constants of a Surface Optical Wave," J. Opt. Soc. Am. 65, 1253 (1975).

D. L. Mills, "The Attenuation of Surface Polaritons by Surface Roughness," Phys. Rev. B 12, 4036 (1975).

J. D. McMullen, "Propagation Length of Surface Polaritons at 10.6 μm on BeO and Metal Surfaces," Solid State Communic. 17, 331 (1975).

J. D. McMullen, "Surface Polariton Attenuation Length Measurements at 10.6 μm by Direct Excitation and Decoupling and by the Total Internal Reflection Method," Bull. Am. Phys. Soc. 20, 45 (1975).

The following Technical Reports, entitled "Surface Electromagnetic Waves for Optical Signal Processing," have been submitted to A.R.O. during this program:

Final Technical Report, Period 1 June 1974 to 1 June 1977, Report No. C77-464/501 (1 June 1977).

Fifth Semiannual Progress Report, Period 30 June 1976 to 31 December 1976, Report No. C76-700.5-501 (31 Dec. 1976).

Fourth Semiannual Progress Report, Period 31 December 1975 to 30 June 1976, Report No. C76-700-501 (30 June 1976).

Follow-on Proposal, No. T76-275/501 (16 March 1976).

Third Semiannual Progress Report, Period 1 June 1974 to 31 May 1976, Report No. C74-930.5/501 (30 September 1975).

Final Technical Report, Period 1 June 1974 to 31 May 1975, Report No. C74-930.4/501 (31 May 1975).

Third Letter Progress Report, Period 15 December 1974 to 15 March 1975, Report No. C74-930.3/501 (15 March 1975).

Second Quarterly Letter Technical Report, Period 15 September 1974 to 15 December 1974, Report No. C74-930.2/501 (15 December 1974).

Progress Report No. 1, Period 1 June 1974 to 30 September 1974, Report No. C73-930.1/501 (15 September 1974).

D. Abstracts of Publications

Abstracts of papers published during this contract period are listed as follows. Complete copies of papers submitted, but not as yet published, follow as sections II through VI of this report. These sections contain new results obtained during the present reporting period.

Interaction of surface polaritons with periodic surface structures; Rayleigh waves and gratings*

D. L. Mills
Department of Physics
University of California
Irvine, California 92664

ABSTRACT

We describe the interaction of surface polaritons with Rayleigh surface waves for the case of arbitrary angle between the surface-polariton propagation direction and that of the Rayleigh wave. We presume the surface polariton couples to the Rayleigh wave through the periodic displacement of the surface produced by it, and also through the modulation of the dielectric constant of the substrate by the elasto-optic effect. We take the unstressed substrate to be an isotropic dielectric, and no special assumption about its elastic constants is required. The results here may be applied also to the interaction of surface polaritons with periodic gratings, provided the depth of the grooves is small. We obtain expressions for the amplitude of the diffracted electromagnetic waves produced by interaction of the surface polariton with a grating or Rayleigh wave. The diffracted beams may describe either fields localized near the surface or radiation induced by interaction with the periodic distrubance, depending on the kinematics of the interaction process. A small modification of these formulas may be used to compute the amplitude of a surface-polariton wave generated by interaction of incoming electromagnetic radiation with a periodic structure. Finally, we obtain a remarkably simple analytic expression for the surface-polariton dispersion relation in the near vicinity

of gaps opened up by interaction with the periodic surface structure. This expression includes the effect of elasto-optic coupling and may be applied to propagation at an arbitrary angle to a set of grating lines, or to the propagation direction of a Rayleigh wave. The experimental study of these gaps offers the possibility of measuring the magnitude and frequency variation of the elements of the photoelastic tensor of the substrate in situations where these quantities are difficult to measure by conventional methods; i.e., for metals at infrared frequencies.

*Research supported by Contract No. DAHC04-74-C-0024, U. S. Army Research Office, Durham, N. C.

Recursive solution of the dispersion relation of a surface polariton in a layered structure.*

J. D. McMullen
Electronics Research Division
Rockwell International Corporation
Anaheim, California 92803

Abstract

The transcendental equation for the propagation constants of a surface polariton in a layered structure is written in a form which is particularly amenable to solution by a recursive method. A numerical example is given for the surface phonon-polariton on a structure consisting of a Ge film on BeO.

Index Headings: Surface optical waves; films.

---

*This research was supported by the U.S. Army Research Office, under Contract DAHC04-74-C-0024.

PERTURBATION ANALYSIS OF THE INFLUENCE OF A THIN DIELECTRIC FILM ON THE PROPAGATION CONSTANTS OF A SURFACE OPTICAL WAVE*

J. D. McMullen

Rockwell International
Anaheim, California 92803

ABSTRACT

Simplified analytic expressions are obtained for the phase velocity and propagation length of a surface polariton on a layered structure that consists of a dielectric film on a surface-active material.

Index Headings: Surface-guided waves; Films; Integrated optics.

*This research was supported by the U. S. Army Research Office, under Contract No. DAHC04-74-C-0024

THE ATTENUATION OF SURFACE POLARITONS BY SURFACE ROUGHNESS†

D. L. Mills
Department of Physics
University of California
Irvine, California 92664

ABSTRACT

This paper presents a theoretical description of the attenuation of surface polaritons by roughness on the surface. In the presence of surface roughness, and in a frequency region where the dielectric constant is negative, the surface polariton is attenuated by two processes. It may lose energy by radiating into the vacuum or by scattering into other surface polariton states. Through application of a formalism developed recently to describe roughness induced scattering and absorption of a plane electromagnetic wave incident on a surface, we obtain expressions for the contribution to the attenuation rate of the surface polariton from the two processes described above. We examine the relative importance of the two processes for surface polaritons on semiconductor surfaces, and on a nearly free electron metal at infrared frequencies.

†Research supported by Contract DAHC04-74-C-0024, U.S. Army Research Office, Durham, North Carolina

PROPAGATION LENGTHS OF SURFACE POLARITONS AT 10.6 MICRONS ON BeO AND METAL SUBSTRATES*

J. D. McMullen

Electronics Research Division
Rockwell International Corporation
Anaheim, Ca 92803, U. S. A.

ABSTRACT

Propagation lengths at 10.6 μm have been measured to be 120 μm for the surface phonon-polariton on BeO and 5.0, 7.4 and 1.6 mm for surface plasmons on gold, copper and stainless steel. A CO_2 laser beam was coupled to the surface mode, propagated along the surface, and decoupled using the two-prism method.

*Research supported by U. S. Army Research Office Contract DAHC04-74-C-0024.

SURFACE POLARITON ATTENUATION LENGTH MEASUREMENTS AT 10.6 MICRONS BY DIRECT EXCITATION AND DECOUPLING AND BY THE TOTAL INTERNAL REFLECTION METHOD

J. D. McMullen
Rockwell International, Anaheim, CA

ABSTRACT

Propagation lengths were measured for surface polaritons by two methods. CO_2 laser radiation at 10.6 microns was used to directly excite surface polaritons by total internal reflection from an adjacent dielectric prism.[1] For one type of experiment, damping of the surface polariton is deduced from the angular width of the coupling angle for which the totally reflected intensity is minimum. In the other measurements, the surface polariton is launched by coupling from a right-angle prism and decoupled by another prism in the manner introduced by Schoenwald, et al.[2] Results of the two methods are compared for surface plasmons on metals and the ordinary surface phonon-polariton on BeO.

[1] A. Otto, Z. Physik 216, 399 (1968).

[2] J. Schoenwald, E. Burstein and J. M. Elson, Solid St. Commun. 12, 185 (1973).

II. ANALYSIS OF COMPRESSION OF FREQUENCY-CHIRPED OPTICAL PULSES USING DISPERSIVE BULK AND SURFACE PHONON-POLARITON PROPAGATION MODES AT CO_2 LASER FREQUENCIES*

J. D. McMullen
Electronics Research Center
Rockwell International Corporation
Anaheim, California 92803

Abstract

An analysis is given for the compression of linearly chirped optical pulses propagating in dispersive, absorbing media. Numerical calculations are reported for frequency-chirped CO_2 laser pulses which propagate as phonon-polaritons in α -quartz or as surface phonon-polaritons on BeO, including the influence of thin dielectric films on the surface propagation mode. Quantitative evaluation is made of the use of these modes to form dispersive optical pulse delay lines. It is shown that absorption limits both the attenuation length and the curvature of the dispersion curves. For the materials considered, this approach is restricted to 10 picosecond pulses having THz chirp bandwidths, with large accompanying absorption losses.

*This research was supported by the U. S. Army Research Office under Contract No. DAHC04-74-C-0024

It is well recognized that a pulse may be temporally compressed by appropriately modulating its carrier frequency, then propagating it through a dispersive medium.[1-4] The purpose of this paper is to evaluate the suitability of using surface and bulk phonon-polariton propagation modes in crystals to form dispersive pulse delay lines at infrared frequencies. Particular attention is given to the possibility of compressing CO_2 laser pulses at frequencies between 900 cm^{-1} and 1100 cm^{-1}.

Phonon-polaritons are the electromagnetic modes of propagation in a crystal at frequencies close to the transverse optic (TO) phonon frequency of the lattice.[5] The dispersion curve for the coupled excitation, or phonon-polariton, bends asymptotically toward large values of wave vector for frequencies increasing toward the propagation stopband, because of near-resonant coupling between the optical electric field and the infrared active phonon. A surface optical wave may propagate nonradiatively along the surface of the infrared active crystal at frequencies just above the TO phonon frequency.[6,7] The dispersion curve for the surface phonon-polariton also bends toward large values of wave vector, with a limiting frequency just below the longitudinal optic (LO) phonon frequency of the crystal. The bending of the dispersion curves indicates that group velocity varies strongly with frequency over these ranges of frequency. Therefore, different frequency components within the spectrum of an incident pulse are delayed by different amounts as the pulse propagates through the dispersive medium. The output pulse envelope is then distorted and, under certain conditions, may be temporally compressed.

COMPRESSION OF LINEARLY CHIRPED PULSES IN DISPERSIVE, ABSORBING MEDIA

Compression of frequency chirped pulses is used to improve the detection sensitivity and range resolution of pulsed radar.[1-4] Recently, emphasis has been placed upon extending pulse compression methods to optical frequencies for laser communications and radar.[8-27] Frequency modulated laser pulses suitable for compression have been produced by electro-optic phase modulation,[8,9] and by self-phase modulation of a pulse propagating in a nonlinear medium.[10-15] Compression of frequency chirped laser pulses has been investigated using dispersion of the refractive index of a liquid [9] or of an alkali vapor.[14,16-18] Pulse compression filters have also been demonstrated using diffraction gratings [15, 19-22] or a Gires-Tournois interferometer.[23,24] Other methods for obtaining compressed laser pulses have included active modulation of the refractive index and its dispersion using a Stark cell,[25,26] and an intra-cavity saturable absorber in a mode-locked CO_2 laser.[27]

In this paper the propagation of a frequency-chirped optical pulse through an absorbing, dispersive medium is discussed within the framework of linear dispersion theory. The theoretical approach is similar to that given previously for a non-chirped incident pulse,[28-30] and for dispersive but non-absorbing media.[1-3,9,12] The present treatment is generalized to include the possibilities of a non-optimized initial chirp, a finite attenuation length in the absorbing medium, and the temporal shaping influence of strongly frequency-dependent absorption as well as dispersion.[31-33] Criteria are established for the

initial chirp rate required to obtain a given pulse-width compression ratio, in terms of the incident pulse width and the frequency dependence of the complex wave vector $k(\omega)$. Quantitative evaluation is then given for chirped CO_2 laser pulses propagating as bulk phonon-polaritons in α-quartz or as surface phonon-polaritons on BeO.

Consider an optical pulse having electric field $E(x,t)$ which propagates in the +x direction in a linear, dispersive medium. The linearly chirped incident pulse, specified at a point x=0 just inside the boundary of the dispersive medium, is of the form:

$$E(0,t) = E_o \exp\left(\frac{-2t^2}{T^2}\right) \cos\left(\omega_o t + \frac{\delta\omega_m}{2T^2} t^2\right) \tag{1}$$

where ω_o (rad./sec) is the average optical carrier frequency, and $\delta\omega_m$ (rad./sec) is the applied range of linear frequency modulation (chirp) over the full width T of the intensity envelope. The assumption of a Gaussian envelope greatly simplifies the analysis, permitting a closed-form solution for the output field $E(x,t)$ while retaining the important aspects of chirped pulse propagation and compression. The frequency spectrum $\tilde{E}(0,\omega)$ of the incident pulse, given by the Fourier transform of $E(0,t)$, is:

$$\tilde{E}(0,\omega) = \left(\frac{2\pi}{\delta\omega_o\,\delta\omega}\right)^{1/2} E_o \left\{ \exp\left[\frac{-2(\omega-\omega_o)^2}{\delta\omega_o(\delta\omega_o + i\,\delta\omega_m)} - i\,\frac{1}{2}\,\tan^{-1}\left(\frac{\delta\omega_m}{\delta\omega_o}\right)\right] + \exp\left[\frac{-2(\omega+\omega_o)^2}{\delta\omega_o(\delta\omega_o - i\,\delta\omega_m)} + i\,\frac{1}{2}\tan^{-1}\left(\frac{\delta\omega_m}{\delta\omega_o}\right)\right]\right\}, \tag{2}$$

where

$$\delta\omega \equiv \left[(\delta\omega_o)^2 + (\delta\omega_m)^2\right]^{1/2} \tag{3}$$

is the full width at e^{-1} of peak for the power spectrum $|\tilde{E}(0,\omega)|^2$, and $\delta\omega_o \equiv 4/T$ is the full width at e^{-1} of peak for the power spectrum of the unmodulated pulse envelope.

According to linear dispersion theory, the electric field E(x,t) after propagating a distance x through the dispersive medium is given by:

$$E(x,t) = \frac{1}{2\pi}\int_{-\infty}^{\infty} d\omega\, \tilde{E}(0,\omega)\, \exp[\pm ik(\omega)x - i\omega t] \quad . \tag{4}$$

It is assumed that $\tilde{E}(0,\omega)$ is localized to frequencies in the vicinities of $\omega\simeq+\omega_o$ and $\omega\simeq-\omega_o$. In order to ensure that the pulse amplitude diminishes to zero in the limit $x\to+\infty$ in an absorbing medium, the positive sign for $+k(\omega)$ must be chosen when performing the integral of Eq. (4) over the term in $\tilde{E}(0,\omega)$ peaked about $\omega\simeq+\omega_o$ and $-k(\omega)$ is chosen for the term in $\tilde{E}(0,\omega)$ peaked about $\omega\simeq-\omega_o$. For most cases of interest the variation of $k(\omega)$ with frequency is sufficiently weak that $k(\omega)$ may be expanded in a Taylor series of the form

$$k(\omega)x = k_o x + \tau_1(\omega-\omega_o) + \frac{1}{8}\tau_2{}^2(\omega-\omega_o)^2 + \ldots. \tag{5a}$$

about $\omega\simeq+\omega_o$, and

$$k(\omega)x = k_o x - \tau_1(\omega+\omega_o) + \frac{1}{8}\tau_2{}^2(\omega+\omega_o)^2 + \ldots. \tag{5b}$$

about $\omega=-\omega_o$, where $k_o \equiv k(\omega_o)$ and the complex parameters τ_1 and τ_2 are defined by:

$$\tau_1 \equiv \frac{dk}{d\omega}\bigg|_{\substack{x \\ \omega=+\omega_o}} , \tag{5c}$$

and

$$(\tau_2)^2 \equiv 4\,\frac{d^2k}{d\omega^2}\bigg|_{\substack{x \\ \omega=+\omega_o}} . \tag{5d}$$

In the absence of absorption, τ_1 is simply the group delay time for the pulse envelope, while τ_2, defined here as the "quadratic dispersion parameter," characterizes the relative delay time among frequency components after propagation through the dispersive medium. At frequencies for which $\mathrm{Im}[k(\omega)]$ varies rapidly with frequency, τ_1 and τ_2 are more generally complex constants which are related to the slope and curvature of the curves for $\mathrm{Re}[k(\omega)]$ and $\mathrm{Im}[k(\omega)]$, respectively.

For many cases of interest the series expansions for $k(\omega)$ may be truncated after the second-order term. If the frequency dependence of $\mathrm{Im}[k(\omega)]$ is negligibly small, then the electric field waveform at position x is evaluated to be:

$$E(x,t) = \mathrm{Real}\; E_o \left(\frac{T}{T_x}\right)^{1/2} \exp\left(i \left[k_o x - \omega_o t + \frac{1}{2}\tan^{-1}\left(\frac{(\tau_2/T)^2}{1 + \frac{\delta\omega_m}{\delta\omega_o}\left(\frac{\tau_2}{T}\right)^2} \right) \right] \right)$$

$$\exp\left(\frac{-2(\tau_1 - t)^2}{T_x^{\,2}} \left[1 + i\left(\frac{\delta\omega_m}{\delta\omega_o}\left[1 + \frac{\delta\omega_m}{\delta\omega_o}\left(\frac{\tau_2}{T}\right)^2 \right] + \left(\frac{\tau_2}{T}\right)^2 \right) \right] \right) \tag{6}$$

In the absence of strongly frequency-dependent absorption, so that $\mathrm{Im}[k(\omega)] \simeq \mathrm{Im}[k_o]$, the envelope and phase portions of $E(x,t)$ in Eq. (6) are readily distinguishable. $E(x,t)$ has a Gaussian envelope of full width T_x at e^{-1} of peak intensity given by:

$$T_x^2 = T^2 \left\{ \left[1 + \frac{\delta\omega_m}{\delta\omega_o} \left(\frac{\tau_2}{T} \right)^2 \right]^2 + \left(\frac{\tau_2}{T} \right)^4 \right\} \quad , \tag{7}$$

in agreement with Eq. (22) of Reference 12. The peak intensity of the pulse at position x decreases or increases by the factor T/T_x as the pulse becomes either dispersion-broadened or temporally compressed, respectively. Additionally, the pulse intensity is reduced by a factor $\exp(-2\mathrm{Im}(k_o)x)$ because of absorption by the medium.

It is apparent from Eq. (7) that if no frequency chirp is applied to the incident pulse ($\delta\omega_m=0$), the output pulse $E(x,t)$ becomes dispersion-broadened, as illustrated by the dashed curves in Figure 1. The phase of $E(x,t)$ then contains a linear frequency chirp covering a range of frequencies $\delta\omega_o\left[1-(T/T_x)^2\right]$ within the full width T_x of the output pulse intensity envelope. However, when a frequency chirp $\delta\omega_m=-\delta\omega_o(T/\tau_2)^2$ is applied to the incident pulse, the output pulse becomes compressed to a minimum possible width upon propagation through the dispersive medium, [1,3,12] as illustrated by the dotted limiting curve in Fig. 1. The width of the optimally compressed pulse is $T_x \approx 4/|\delta\omega_m|$, and the phase of $E(x,t)$ contains a linear frequency chirp during full width T_x over a range of frequencies $\delta\omega_o$. The rate of chirp of the optimally compressed pulse is equal in magnitude but opposite in sign to the rate of chirp for the incident pulse. The intermediate cases for $\delta\omega_m<0$ represented in Fig. 1 by solid curves show that large compression ratios can be obtained for sufficiently large

chirp bandwidths and sufficiently small quadratic dispersion parameter τ_2. However, optimum compression requires an increasingly delicate balance among the parameters $\delta\omega_m$ and T of the incident pulse and τ_2 of the dispersive medium if large compression ratios are to be attained.

When the average carrier frequency ω_o is very close to the propagation stopband for either a bulk or surface phonon-polariton, the frequency dependence of $\mathrm{Im}[k(\omega)]$ may also contribute significantly to pulse shaping. The output pulse width T_x is then given more generally by:

$$\left(\frac{T_x}{T}\right)^2 = \frac{\left[1 + \frac{\delta\omega_m}{\delta\omega_o}\,\frac{\mathrm{Re}(\tau_2^2)}{T^2} + \frac{\mathrm{Im}(\tau_2^2)}{T^2}\right]^2 + \left[\frac{\delta\omega_m}{\delta\omega_o}\,\frac{\mathrm{Im}(\tau_2^2)}{T^2} - \frac{\mathrm{Re}(\tau_2^2)}{T^2}\right]^2}{\left[1 + \frac{\mathrm{Im}(\tau_2^2)}{T^2} + \left(\frac{\delta\omega_m}{\delta\omega_o}\right)^2 \frac{\mathrm{Im}(\tau_2^2)}{T^2}\right]} \quad . \tag{8}$$

The minimum possible output pulse width is then given by:

$$\mathrm{Min}\left[\left(\frac{T_x}{T}\right)^2\right] = -1 - \frac{\mathrm{Re}(\tau_2^2)}{T^2}\left[\frac{\delta\omega_m}{\delta\omega_o} + \frac{\delta\omega_o}{\delta\omega_m}\right] \quad , \tag{9a}$$

when the input chirp is adjusted to an optimum value of:

$$\delta\omega_m\Big|_{\text{opt.}} = -\delta\omega_o\,\frac{T^2}{\mathrm{Re}(\tau_2^2)}\left[1 + \frac{\mathrm{Im}(\tau_2^2)}{T^2}\right] \tag{9b}$$

This reduces to the previously discussed result for optimum compression in the limit that frequency-dependent absorption becomes sufficiently weak, or $\mathrm{Im}[k(\omega)] \simeq \mathrm{Im}(k_o)$.

When $Im(\tau_2^2)$ becomes comparable to T^2, as may occur when ω_o is just below the propagation stopband, then the chirp bandwidth required for optimum compression is larger and the attainable pulse compression ratio is reduced because of frequency-dependent absorption.

BULK PHONON-POLARITON MODES IN QUARTZ

The preceding discussion has shown how the curvatures of the curves for $Re[k(\omega)]$ and $Im[k(\omega)]$ are related to temporal shaping of the pulse envelope. For example, Fig. 1 illustrates that the quadratic dispersion parameter must be comparable to the initial pulse width if a non-chirped pulse is to be significantly dispersion-broadened. Also, when the chirp rate in the incident pulse is optimized Eq. (7) shows the minimum pulse width obtainable is τ_2^2/T. Therefore, the quadratic dispersion parameter τ_2 must be calculated for bulk and surface phonon-polariton propagation modes in order to evaluate their potential use for optical pulse compression.

Consider first the ordinary phonon-polariton modes in α-quartz. The dispersion curves illustrated in Fig. 2 are given by:

$$k(\omega) = \frac{\omega}{c}\,\varepsilon(\omega)^{1/2} \quad , \tag{10}$$

where the complex, frequency-dependent dielectric constant $\varepsilon(\omega)$ for the ordinary ray is of the form:

$$\varepsilon(\omega) = \varepsilon(\infty) + \sum_{m=1}^{N} \frac{S_m \omega_m^2}{(\omega_m^2 - \omega^2 - i\gamma_m\omega)} \quad . \tag{11}$$

S_m, ω_m and γ_m are the oscillator strength, transverse optic phonon frequency, and anharmonic damping rate, respectively, for the m'th of N ordinary phonon-polariton branches, and $\varepsilon(\infty)$ is the ordinary optical dielectric constant at frequencies well above the lattice resonance but still well below electronic bandgap transitions. Data for the parameters used to calculate $\varepsilon(\omega)$ are taken from infrared reflectivity measurements by Spitzer and Kleinman.[34] The solid curves of Fig. 2 represent phonon-polariton dispersion in the limit of no damping (γ_m=0; m=1, 2,...7), while the dashed curve for Re[$k(\omega)$] and the dotted curve for Im[$k(\omega)$] include the influence of anharmonic damping at 300°K. The undamped case is presented as a limiting case of theoretical interest, since the strong bending of the undamped dispersion curve stimulated the present study. However, an assessment of practical applications clearly must include the influence of absorption.

The parameter τ_2 was calculated by computer, using analytic expressions for the derivatives $dk/d\omega$ and $d^2k/d\omega^2$ derived from Eqs. 10 and 11. These expressions are somewhat lengthy, and are therefore not reproduced here. Figure 3 illustrates the variation of τ_2 with average carrier frequency for an assumed propagation distance of x=1cm. For a smaller propagation distance x, as may be required by a small attenuation length, the value of the ordinate must be multiplied by a factor $[x(cm)]^{1/2}$. The solid curve of Fig. 3 represents the limit of no damping. With absorption included, the quantities $|Re(\tau_2^2)|^{1/2}$ and $|Im(\tau_2^2)|^{1/2}$ are illustrated by dashed and dotted curves, respectively. The dashed curve for $|Re(\tau_2^2)|^{1/2}$ follows closely the solid limit curve at frequencies well below the TO phonon frequency, and displays maxima for positive values of $Re(\tau_2^2)$ at 1064 cm^{-1} and

1075 cm^{-1} in addition to a peak for negative values of $Re(\tau_2^2)$ at 1071 cm^{-1}. Negative values for $Re(\tau_2^2)$ occur between 1067 and 1073 cm^{-1} and for a range of frequencies below 889 cm^{-1}, for which the $Re[k(\omega)]$ curve in Fig. 2 is concave toward decreasing values of k. Maxima occur for positive values of $Im(\tau_2^2)$ at 1069 and 1080 cm^{-1} and a peak for negative values at 1073 cm^{-1} frequency.

As an example, consider the propagation of a chirped laser pulse having an average carrier frequency of 925 cm^{-1}, corresponding to the (00°1)-(10°0) P(40) emission line of a CO_2 laser. The attenuation length $[2Im(k)]^{-1}$ at this frequency is 46 μm, while, from Fig. 3, $|Re(\tau_2^2)|^{1/2} = 5.0\times10^{-12}$ sec and $|Im(\tau_2^2)|^{1/2} = 2.7\times10^{-12}$ sec for x=1cm. A quartz crystal 0.5 mm thick then gives $|Re(\tau_2^2)|^{1/2} = 1.1\times10^{-12}$ sec and $|Im(\tau_2^2)|^{1/2} = 0.6\times10^{-12}$ sec, along with a reduction in peak intensity by a factor $exp[-2Im(k_o)x] = 2\times10^{-5}$ due to absorption. It is apparent from the magnitude of τ_2 that a pulse which is to be optimally compressed in this medium should have an initial width of a few picoseconds and requires a chirp bandwidth of the order of a few THz. A chirp bandwidth of this magnitude would require a high-pressure CO_2 laser, for which the emission lines of the (00°1)-(10°0) band P branch are broadened sufficiently to merge into a continuous gain spectrum.[35-39] For a chirp range of -1.5 THz, a 2.9 psec pulse can be compressed to 0.43 psec in width, with a gain factor $T/T_x = 6.7$ in peak intensity. If a broader incident pulse is used, so that conditions for pulse compression are no longer optimized, the same chirp bandwidth will cause a 5.7 psec incident pulse to be compressed by a factor of $T_x/T = 0.5$ in width. Clearly, larger values of τ_2 are required

to extend this method to the compression of CO_2 laser pulses of the order of 0.1 nsec in width. Calculations show that significantly larger values of τ_2 cannot be realized in practice by increasing the average carrier frequency above 925 cm^{-1}, because the attentuation length decreases rapidly as ω_o approaches the TO phonon frequency at 1072 cm^{-1}.

It is reasonable to inquire whether the quadratic dispersion parameter might be significantly increased by cooling the crystal in order to decrease anharmonic damping of the TO phonon and thereby obtain a larger attenuation length. However, at lower temperatures, with correspondingly smaller damping rates γ_m, the curves for $Re[k(\omega)]$ become more nearly linear at frequencies for which the attenuation length may be suitably large. Calculations indicate $|Re(\tau_2^2)|^{1/2}$ can be increased by only a factor of about 1.3 at frequencies from 925 cm^{-1} to 1060 cm^{-1} upon cooling the crystal from 300°K to 80°K.

Additionally, it should be noted that the magnitude of τ_2 varies significantly over the large THz chirp bandwidths considered in the present example. Further analysis, to be published separately, reveals that this higher order variation of $k(\omega)$ with frequency over the incident pulse bandwidth gives an asymmetrically shaped compressed pulse of slightly greater width than calculated for the above examples.

SURFACE PHONON-POLARITON MODES ON BeO:

Experimental measurements have shown that the attenuation length for a surface polariton may be several times greater than its wavelength.[40,41] Therefore, surface propagation modes may also be considered for dispersive

optical pulse delay lines. The theory for scattering of surface polaritons by surface roughness has shown that the quality of surface required to reduce scattering to acceptable limits is well within the capabilities of optics polishing technology.[42] Theoretical work on coupling an optical pulse to the surface mode by using grating structures has yielded criteria for launching a frequency-chirped surface polariton pulse without distorting its shape or time-dependent phase.[43, 44]

Single-Interface Structure: A surface optical wave may propagate nonradiatively along the interface between two materials having dielectric constants ε_p and ε_s, provided the real part of the dielectric constant of one medium, $\mathrm{Re}(\varepsilon_s)$, is negative and greater in magnitude than the positive dielectric constant ε_p of the transparent medium.[5-7] This condition may be satisfied for frequencies just above the TO phonon frequency of an infrared-active crystal. The dispersion relation for a surface polariton is of the same form as given by Eq. (10), if $k(\omega)$ is understood to be the wave vector parallel to the surface and the "effective dielectric constant" $\varepsilon(\omega)$ for the surface mode is defined as:

$$\varepsilon(\omega) = \varepsilon_p \, \varepsilon_s(\omega)/[\varepsilon_p + \varepsilon_s(\omega)] \qquad (12)$$

The dielectric constant $\varepsilon_s(\omega)$ of the infrared-active medium varies with frequency in the manner prescribed by Eq. (11). If damping in the infrared-active material is neglected, then the phase velocity of the surface wave varies from $c/\varepsilon_p^{1/2}$ at the TO phonon frequency to zero at a limiting frequency ω_{SF} for which $\varepsilon_s(\omega_{SF})=-\varepsilon_p$. The dispersive character of undamped surface phonon-polariton modes is illustrated by solid curves in Fig. 4 for a BeO:air ($\varepsilon_p=1$) surface and for a BeO:CsI ($\varepsilon_p=2.59$) interface. The $\hat{c}$

axis of the BeO crystal is assumed to be perpendicular to the surface wave vector $\underset{\sim}{k}$ and the electric vector $\underset{\sim}{E}$, so that parameters for the ordinary ray in BeO are appropriate for calculating $\varepsilon_s(\omega)$. It is apparent from the slopes of the solid curves that group-velocity dispersion may be made large over any desired range of frequencies just above ω_{TO} by appropriate choice of the transparent medium of dielectric constant ε_p. For example, if ε_p=2.59, the surface mode exhibits large group-velocity dispersion for a range of frequencies coincident with the strong (00°1)-(10°0) band P branch emission lines from a CO_2 laser.

Analytic expressions derived from Eqs. (10) and (12) for the derivatives $dk/d\omega$ and $d^2k/d\omega^2$ were used to calculate the expansion parameters τ_1 and τ_2 for $k(\omega)$ of the surface mode. The frequency-dependent dielectric constant $\varepsilon_s(\omega)$ for the ordinary ray in BeO was calculated from Eq. (11), using $\varepsilon(\infty)$=2.95, S=3.94, and ω_{TO}=725. cm^{-1}.[45] The solid curve of Fig. 5 illustrates the dependence of τ_2 upon average carrier frequency for the surface phonon-polariton on a BeO:air surface, with damping neglected. As expected, τ_2 diverges as the average carrier frequency asymptotically approaches the maximum frequency ω_{SF} of the surface mode.

When absorption in the BeO substrate is included, the solid dispersion curve in Fig. 4 is replaced by the dashed curve for $Re[k(\omega)]$ and the dotted curve for $Im[k(\omega)]$. The damping rate γ=7.5 cm^{-1} was used in Eq. (11) to calculate $\varepsilon_s(\omega)$.[45] The curvatures of the broken curves in Fig. 4 indicate that real and imaginary components of τ_2^2 display maxima at frequencies close to the limiting surface frequency ω_{SF}. Therefore, as for bulk phonon-polaritons, the effects of absorption in the BeO substrate are to limit both the maximum attainable value of τ_2 and the attenuation length.

The dependence of components of τ_2^2 upon average carrier frequency is illustrated in Fig. 5 for a BeO:air structure with x=1 cm. The dashed curve displays maxima for positive values of $Re(\tau_2^2)$ at 1017 cm^{-1} and 1028 cm^{-1} frequency, and a peak negative value for $Re(\tau_2^2)$ at 1024 cm^{-1} frequency. Similarly, the dotted curve for $Im(\tau_2^2)$ displays positive maxima at 1022 cm^{-1} and 1032 cm^{-1} and a peak negative value at 1026 cm^{-1} frequency.

As an example, consider a pulse having an average carrier frequency of 980 cm^{-1}, corresponding to the (00°1)-(10°0) band R(26) emission line of a CO_2 laser, for which the attenuation length of a BeO:air surface mode is 20 μm, $|Re(\tau_2^2)|^{1/2} = 2\times10^{-11}$ for x = 1cm, and $Im(\tau_2^2)=0.23Re(\tau_2^2)$. Propagation a distance of 0.2 mm then gives a quadratic dispersion parameter $|Re(\tau_2^2)|^{1/2}=2.8\times10^{-12}$ sec, with a reduction in peak intensity by a factor $\exp[-2Im(k_o)x] = 4\times10^{-5}$ due to absorption. As was the case for the bulk phonon-polariton in quartz, a quadratic dispersion parameter of this magnitude requires that the initial chirp bandwidth be a few THz and the incident pulse width of the order of a few picoseconds. If, for example, the frequency chirp covers a range of -0.9 THz, corresponding to the entire (00°1)-(10°0) band R branch of a highly pressure broadened CO_2 laser, then an 11 psec pulse may be optimally compressed to 0.7 psec in width, with gain in peak intensity by a factor of $T/T_x=16$. A 22 psec pulse will be compressed by a factor $T_x/T=0.5$, using the same initial chirp bandwidth. As previously noted, additional pulse shaping is anticipated due to variation of τ_2 with frequency over the large chirp bandwidth. However, it is clear that pulse compression is limited by the magnitudes of τ_2 and $Im(k_o)$ to incident pulses of the order of 20 psec in width.

Layered Structure: Another configuration of interest is a layered structure formed by depositing a thin film of transparent dielectric onto a surface-active material such as BeO. The surface polariton in this layered structure has a dispersion relation of the form given by Eq. (10), but for this case the "effective dielectric constant $\varepsilon(\omega)$" for the surface mode is given by the root of the following transcendental equation:[46,47]

$$\left\{\varepsilon_p\varepsilon_s(\varepsilon_f-\varepsilon) - \varepsilon_f^2(\varepsilon-\varepsilon_p)^{1/2}(\varepsilon-\varepsilon_s)^{1/2}\right\} \tan\left(\frac{\omega\ell}{c}(\varepsilon_f-\varepsilon)^{1/2}\right) - \tag{13}$$

$$\varepsilon_f(\varepsilon_f-\varepsilon)^{1/2}\left\{\varepsilon_s(\varepsilon-\varepsilon_p)^{1/2} + \varepsilon_p(\varepsilon-\varepsilon_s)^{1/2}\right\} = 0 \ ,$$

where ε_p, ε_f and $\varepsilon_s(\omega)$ are the dielectric constants for the semi-infinite transparent medium (air), the thin dielectric overlayer film of thickness ℓ, and the surface-active medium (BeO), respectively. The detailed configuration and expressions for the surface polariton fields are outlined in reference 46, along with the derivation of the transcendental equation. We are presently interested in that portion of the dispersion curve for which $\varepsilon_p<\varepsilon<\varepsilon_f$, for which the electric field amplitude varies sinusoidally through the film region in the direction perpendicular to the surfaces. When absorption is neglected, the solid dispersion curve in Fig. 4 increases to a maximum allowed frequency, then bends downward for larger values of surface wave vector k. At frequencies near the maximum in the dispersion curve, large values for τ_2 occur at relatively small values of wave vector. Therefore, it should be possible to couple an optical beam to the surface mode at a point on the dispersion curve where $k(\omega)$ varies rapidly with frequency, using either the prism-coupling method or a grating

coupler with reasonably large period. The layered structure also offers the potential advantage that both the dielectric constant and the thickness of the overlayer film are experimental variables which may be used to optimize the design of a dispersive pulse delay line.

Figure 4 illustrates the dispersion curve for a layered structure consisting of a germanium film on a BeO crystal, with a germanium film thickness of 500 Å. The $\hat{c}$ axis of the Beo crystal is assumed parallel to the plane of the interface and perpendicular to the direction of propagation, so that parameters for the ordinary phonon-polariton of BeO are used to calculate $\varepsilon_s(\omega)$. The solid curve is calculated for the limit of no absorption in the BeO substrate. Similar calculations show that a thicker Ge film lowers the maximum allowable frequency and causes the dispersion curve to bend more sharply in the vicinity of this maximum. The solid dispersion curve bends downward and asymptotically approaches from above the limiting surface frequency for a single-interface structure of BeO:Ge at very large values of wave vector.

The dispersion parameters for a surface polariton in a layered structure are calculated from analytic expressions derived from Eqs. (10) and (13). Formulation of expressions for $d\varepsilon/d\omega$ and $d^2\varepsilon/d\omega^2$ from Eq. (13) is much less straightforward than for the previous configurations, so that the calculation for the layered structure deserves special comment. It should be noted that the implicit dependence of ε upon frequency through $\varepsilon_s(\omega)$ must be included, in addition to the explicit dependence upon ω in the argument of $\tan(\omega\ell(\varepsilon_f-\varepsilon)^{1/2}/c)$ in Eq. (13). Further details of the computation are deferred to Appendix A, since the expressions are lengthy and do not contribute insight to the present discussion.

Variation of τ_2 with average carrier frequency is illustrated in Fig. 6 for Ge overlayer thicknesses ℓ=100 Å and ℓ=500 Å and x=1 cm. The case for no absorption (γ=0) is not represented in Fig. 6 because, as is evident from the solid dispersion curve in Fig. 4, the frequency dependence of $k(\omega)$, and therefore of τ_2, is double-valued. However, it is clear from Fig. 4 that for no damping τ_2 diverges at frequencies approaching the region of zero slope in the solid dispersion curve, at 943 cm^{-1} for ℓ=500 Å. Positive values of τ_2 occur for wave vector values below this point, and negative values of τ_2 for larger values of $k(\omega)$.

When absorption in the BeO region is included, Fig. 6 shows that $|Re(\tau_2^2)|^{1/2}$ for the 100 Å thick film displays maxima in its frequency dependence, with $Re(\tau_2^2)<0$ at frequencies between 995 cm^{-1} and 1014 cm^{-1} and $Re(\tau_2^2)>0$ otherwise; while $Im(\tau_2^2)$ is negative for frequencies above 999 cm^{-1} and positive below 999 cm^{-1}. The 500 Å thick Ge film gives similar structure, with $Re(\tau_2^2)<0$ between 940 cm^{-1} and 983 cm^{-1} and $Re(\tau_2^2)>0$ above 945 cm^{-1} frequency. The maximum value of τ_2 attainable for the layered structure is about an order of magnitude smaller than for the single-interface surface polariton on BeO:air or the bulk phonon-polariton in α-quartz, because of the influence of absorption.

As an example, consider a pulse having an average carrier frequency of 900 cm^{-1}, corresponding to the $(01^{\circ}1)$-$(03^{1}0)$ band P(31) emission line of a CO_2 laser, propagating as a surface polariton in a BeO:Ge film:air structure with a film thickness ℓ=100 Å. The attenuation length for this frequency is 55μm and, for x=1 cm, $|Re(\tau_2^2)|^{1/2}=6\times10^{-12}$ sec, with $|Im(\tau_2^2)|^{1/2} = 0.07\ |Re(\tau_2^2)|^{1/2}$. A propagation distance of 0.63 mm then gives

$|Re(\tau_2^2)^{1/2}=1.5x10^{-12}$ sec, along with an attenuation factor $exp[-2Im(k_o)x]\simeq 10^{-5}$ due to absorption. Therefore, τ_2 for the layered structure is comparable to values obtained with similar attenuation for a single BeO:air surface, and pulse compression is limited to pulses of a few picoseconds initial width using THz chirp bandwidths.

SUMMARY AND CONCLUSIONS

An analysis has been presented within the framework of linear dispersion theory for the propagation and temporal compression of linearly chirped pulses in dispersive, absorbing media. The relative delay among frequency groups in the incident pulse is characterized in terms of the frequency dependence of wave vector $k(\omega)$ for each type of propagation mode considered. Specific calculations are presented for CO_2 laser pulses which propagate as bulk phonon-polaritons in quartz, as surface phonon-polaritons on a BeO:air surface, and as surface phonon-polaritons in a BeO:Ge film:air layered structure.

For attenuation losses of 50 dB or smaller significant pulse compression may be demonstrated for optical pulses 20 psec or less in width having applied chirp bandwidths in the THz range. Larger group dispersion and smaller absorption loss are required for this method to become competitive with other types of optical pulse compression filters, such as the grating pair[15, 19-22] or a Gires-Tournois interferometer,[23, 24] or to extend this method to the compression of nanosecond CO_2 TEA-laser pulses using experimentally

realizable chirp bandwidths. Appropriate materials must have larger TO phonon oscillator strengths and smaller anharmonic damping rates at the appropriate frequencies. Further, the limitations imposed by laser-induced damage upon peak and average laser power should be considered when assessing particular applications. However, if a suitably dispersive medium can be identified, the simplicity and compactness of this type of pulse compression filter may become important design considerations.

ACKNOWLEDGEMENTS

The author gratefully acknowledges Professor D. L. Mills of The University of California, Irvine, for stimulating and helpful discussions during the course of this work.

APPENDIX A

COMPUTATIONAL METHOD FOR LAYERED STRUCTURES

Analytic expressions for the propagation constants for bulk phonon-polaritons and for surface phonon-polaritons on a single-interface structure may be derived in a straightforward manner from the dispersion relation for $k(\omega)$. However, for the layered structure the propagation constants must satisfy the transcendental equation (13), so that the development of analytic expressions for τ_2 is much less straightforward. Therefore, the method used to calculate $k(\omega)$ and its frequency derivatives for layered structures is briefly outlined here.

The transcendental equation (13) is of the general form

$$F[\varepsilon(\omega, \varepsilon_s(\omega))] = 0 \qquad \text{(A-1)}$$

The wave vector $k(\omega)$ and its frequency derivatives are calculated using the complex root $\varepsilon(\omega)$, for which both real and imaginary parts of $F(\varepsilon)$ equal zero. The roots $\varepsilon(\omega)$ are conveniently found by mapping the root locus $F(\varepsilon)=0$ in the complex ε plane. The root $\varepsilon(\omega)$ is calculated first at a frequency $\delta_{TO}+\delta\omega$ just above the TO phonon frequency, where $Re(\varepsilon_s)$ is large in magnitude and $\varepsilon(\omega_{TO}+\delta\omega)$ is very nearly equal to the value calculated directly from Eq. (12) without the thin overlayer film. Equation (12) provides a first approximation for $\varepsilon(\omega_{TO}+\delta\omega)$, valid for very thin dielectric overlayers. Based upon this initial estimate, the exact root at $\omega_{TO}+\delta\omega$ is calculated by a Newton-Raphson iteration in complex variables, using analytic expressions formed for $F(\varepsilon)$ and $dF/d\varepsilon$. The frequency is then incremented to $\omega_{TO}+2\delta\omega$, usually by $\delta\omega = 5\ cm^{-1}$ or less,

and $\varepsilon(\omega)$ is calculated for the new frequency using $\varepsilon(\omega_{TO}+\delta\omega)$ as an initial value for the Newton-Raphson iteration. In this manner, the root locus of solutions $\varepsilon(\omega)$ is traced out step-wise over the entire range of surface polariton frequencies, and each solution rapidly converges in a small number of iterations.

Calculation of τ_2 requires the derivation of expressions for the derivatives $d\varepsilon/d\omega$ and $d^2\varepsilon/d\omega^2$. The transcendental function $F(\varepsilon)$ is a function of frequency through $\varepsilon(\omega)$ which, in turn, varies with $\varepsilon_s(\omega)$ and also explicitly with ω in the argument of $\tan(\omega\ell(\varepsilon_f-\varepsilon)^{1/2}/c)$. If the partial derivative with respect to ε is denoted by a prime (') notation and the partial derivative with respect to frequency by a dot (˙) notation, then the frequency derivative of F is written:

$$\frac{dF}{d\omega} = F' \frac{d\varepsilon}{d\omega} + \dot{F} = 0, \qquad \text{(A-2)}$$

which yields a direct analytic expression for $d\varepsilon/d\omega$. Differentiation a second time gives:

$$\frac{d^2F}{d\omega^2} = \ddot{F} + 2\,\dot{F}'\,\frac{d\varepsilon}{d\omega} + F''\left(\frac{d\varepsilon}{d\omega}\right)^2 + F'\,\frac{d^2\varepsilon}{d\omega^2} = 0 \qquad \text{(A-3)}$$

which similarly yields a direct analytic expression for $d^2\varepsilon/d\omega^2$. The partial derivatives F' and F" are formed from the explicit appearance of ε in Eq. (A-1), while derivatives $\dot{F}$ and $\ddot{F}$ must include the frequency dependence of $\varepsilon_s(\omega)$ as well as an explicit dependence on frequency.

$$\dot{F} = \frac{\partial F}{\partial \varepsilon_s} \frac{d\varepsilon_s}{d\omega} + \frac{\partial F}{\partial \omega}$$

(A-4)

and $$\ddot{F} = \frac{\partial \dot{F}}{\partial \varepsilon_s} \frac{d\varepsilon_s}{d\omega} + \frac{\partial \dot{F}}{\partial \omega}$$

Having now formed analytic expressions for $\varepsilon(\omega)$, $d\varepsilon/d\omega$ and $d^2\varepsilon/d\omega^2$, the propagation constant $k(\omega)$ and its frequency derivatives are evaluated from Eq. (10) to give:

$$\tau_1 = \varepsilon(\omega)^{1/2} \frac{x}{c} \left[1 + \frac{\omega}{2\varepsilon(\omega)} \frac{d\varepsilon}{d\omega} \right] \Bigg|_{\omega_o} \qquad \text{(A-5)}$$

and

$$\tau_2^2 = 4\varepsilon(\omega)^{-1/2} \frac{x}{c} \left\{ \frac{d\varepsilon}{d\omega} - \frac{\omega}{2} \left[(2\varepsilon(\omega))^{-1} \left(\frac{d\varepsilon}{d\omega}\right)^2 - \frac{d^2\varepsilon}{d\omega^2} \right] \right\} \Bigg|_{\omega_o} \qquad \text{(A-6)}$$

References

1. J. R. Klauder, A. C. Price, S. Darlington and W. J. Albersheim, Bell System Tech. J. 39, 745 (1960).
2. J. R. Klauder, Bell System Tech. J. 39, 809 (1960).
3. C. E. Cook, Proc. IRE 48, 310 (1960).
4. M. I. Skolnik, Introduction to Radar Systems (McGraw-Hill, New York, 1962) p. 493.
5. U. Fano, Phys. Rev. 103, 1202 (1956).
6. D. L. Mills and E. Burstein, Rep. Progr. Phys. 37, 817 (1974).
7. U. Fano, J. Opt. Soc. Am. 31, 213 (1941).
8. M. A. Duguay, L. E. Hargrove and K. B. Jefferts, Appl. Phys. Letters 9, 287 (1966).
9. J. A. Giordmaine, M. A. Duguay and J. W. Hansen, IEEE J. Quant. Electron. QE-4, 252 (1968).
10. R. A. Fisher, P. L. Kelley and T. K. Gustafson, Appl. Phys. Letters 14, 140 (1969).
11. A. Laubereau, Phys. Letters 29A, 539 (1969).
12. A. Laubereau and D. von der Linde, Z. Naturforsche 25A, 1626 (1976).
13. R. A. Fisher and W. Bischel, Appl. Phys. Letters 23, 661 (1973).
14. D. Grischkowsky, E. Courtens and J. A. Armstrong, Phys. Rev. Letters 31, 422 (1973).
15. R. H. Lehmberg and J. M. McMahon, Appl. Phys. Letters 28, 204 (1976).
16. D. Grischkowsky, Phys. Rev. A 7, 2096 (1973).
17. D. Grischkowsky, Appl. Phys. Letters 25, 566 (1974).
18. D. Grischkowsky, 1974 International Quantum Electronics Conference, Digest of Technical Papers (IEEE, New York, 1974) p. 47.

19. E. B. Treacy, Phys. Letters 28A, 34 (1968).

20. E. B. Treacy, Appl. Phys. Letters 14, 112 (1969).

21. E. B. Treacy, IEEE J. Quant. Electron. QE-5, 454 (1969).

22. E. P. Ippen and C. V. Shank, Appl. Phys. Letters 27, 488 (1975).

23. F. Gires and P. Tournois, Compt. Rend. 258, 6112 (1964).

24. M. A. Duguay and J. W. Hansen, Appl. Phys. Letters 14, 14 (1969).

25. M. M. T. Loy, Appl. Phys. Letters 26, 99 (1975).

26. D. Grischkowsky and M. M. T. Loy, Appl. Phys. Letters 26, 156 (1975).

27. B. J. Feldman and J. F. Figueira, Appl. Phys. Letters 25, 301 (1974).

28. D. G. Anderson and J. I. H. Askne, Proc. IEEE 62, 1518 (1974).

29. D. Anderson, J. Askne and M. Lisak, Proc. IEEE 63, 715 (1975).

30. D. Anderson, J. Askne and M. Lisak, Phys. Rev. A 12, 1546 (1975).

31. D. Rader, Am. J. Phys. 41, 420 (1973).

32. R. A. Fisher, Am. J. Phys. 44, 1002 (1976).

33. D. Rader, Am. J. Phys. 44, 1005 (1976).

34. W. G. Spitzer and D. A. Kleinman, Phys. Rev. 121, 1324 (1961).

35. T. Y. Chang and O. R. Wood, Appl. Phys. Letters 23, 370 (1973).

36. A. J. Alcock, K. Leopold and M. C. Richardson, Appl. Phys. Letters 23, 562 (1973).

37. N. G. Basov, E. M. Belenov, V. A. Danilychev, O. M. Kerimov, I. B. Kovsh, A. S. Podsosonnyl and A. F. Suchkov, Sov. Phys.--JETP 37, 58 (1973).

38. F. O'Neil and W. T. Whitney, Appl. Phys. Letters 26, 454 (1975).

39. I. M. Beterov, V. P. Chebotayev and A. S. Provorov, IEEE J. Quant. Electron. QE-10, 245 (1974).

40. J. Schoenwald, E. Burstein and J. M. Elson, Sol. St. Commun. 17, 331 (1975).

41. J. D. McMullen, Sol. St. Commun. 17, 331 (1975).

42. D. L. Mills, Phys. Rev. B 12, 4036 (1975).

43. D. L. Mills, Phys. Rev. B 15, 3097 (1977).

44. D. L. Mills, J. Appl. Phys. (to be published, manuscript No. 2510R).

45. E. Loh, Phys. Rev. 166, 673 (1968).

46. J. D. McMullen, J. Opt. Soc. Am. 65, 1253 (1975).

47. J. D. McMullen, J. Opt. Soc. Am. 67, 698 (1977).

Figure Captions

II-1. Pulse-width compression ratio T_x/T versus normalized quadratic dispersion parameter τ_2 for various ratios of $\delta\omega_o/\delta\omega_m$. Dashed curves (----) show only pulse broadening for $\delta\omega_m \geq 0$, while solid curves illustrate pulse compression when $\delta\omega_m < 0$. Optimum pulse compression, illustrated by the dotted curve (••••), occurs when $\delta\omega_o/\delta\omega_m = -(\tau_2/T)^2$.

II-2. Dispersion curves for ordinary ($\underset{\sim}{E} \perp \hat{c}$) bulk phonon-polaritons in α -quartz. Solid curve gives dispersion in the limit of no anharmonic damping $\gamma_m = 0$; and broken curves give Real$[k(\omega)/2\pi]$ (----) and Im$[k(\omega)/2\pi]$ (••••) at 300°K.

II-3. Variation with average carrier frequency of the quadratic dispersion parameter τ_2 for the ordinary bulk phonon-polariton of α -quartz, normalized to a propagation distance $x = 1$ cm. Solid curve illustrates the limit for no damping, while the components when absorption at 300°K is included are shown for $|\mathrm{Re}(\tau_2^2)|^{1/2}$ by the dashed curve (----) and for $|\mathrm{Im}(\tau_2^2)|^{1/2}$ by the dotted curve (••••).

II-4. Dispersion curves for ordinary ($\underset{\sim}{E} \perp c$) surface phonon-polaritons on single-interface structures of BeO:air ($\varepsilon_p = 1.$) and BeO:CsI ($\varepsilon_p = 2.59$), and on a layered structure of BeO:Ge film:air with Ge film thickness $\ell = 500$ Å. Solid curves are for the limit of no anharmonic damping. With absorption in BeO included, components of complex $k(\omega)$ are indicated by the dashed curves (----) for Re$[k(\omega)]$ and the dotted curves (••••) for Im$[k(\omega)]$.

II-5. Variation with carrier frequency of the quadratic dispersion parameter τ_2 for the ordinary surface phonon-polariton on a BeO:air interface,

normalized to a propagation distance x=1 cm. Solid curve illustrates the limit for no damping, while the components when absorption at 300°K is included are shown for $|Re(\tau_2^2)|^{1/2}$ by the dashed curve (----) and for $|Im(\tau_2^2)|^{1/2}$ by the dotted curve (••••).

II-6. Variation with carrier frequency of the quadratic dispersion parameter τ_2 for the ordinary surface phonon-polariton in layered structures of BeO:Ge film:air, with Ge film thicknesses ℓ=100 Å and ℓ=500 Å. Absorption in the BeO region is included, with components $|Re(\tau_2^2)|^{1/2}$ indicated by the dashed (----) curves and $|Im(\tau_2^2)|^{1/2}$ by the dotted (••••) curves.

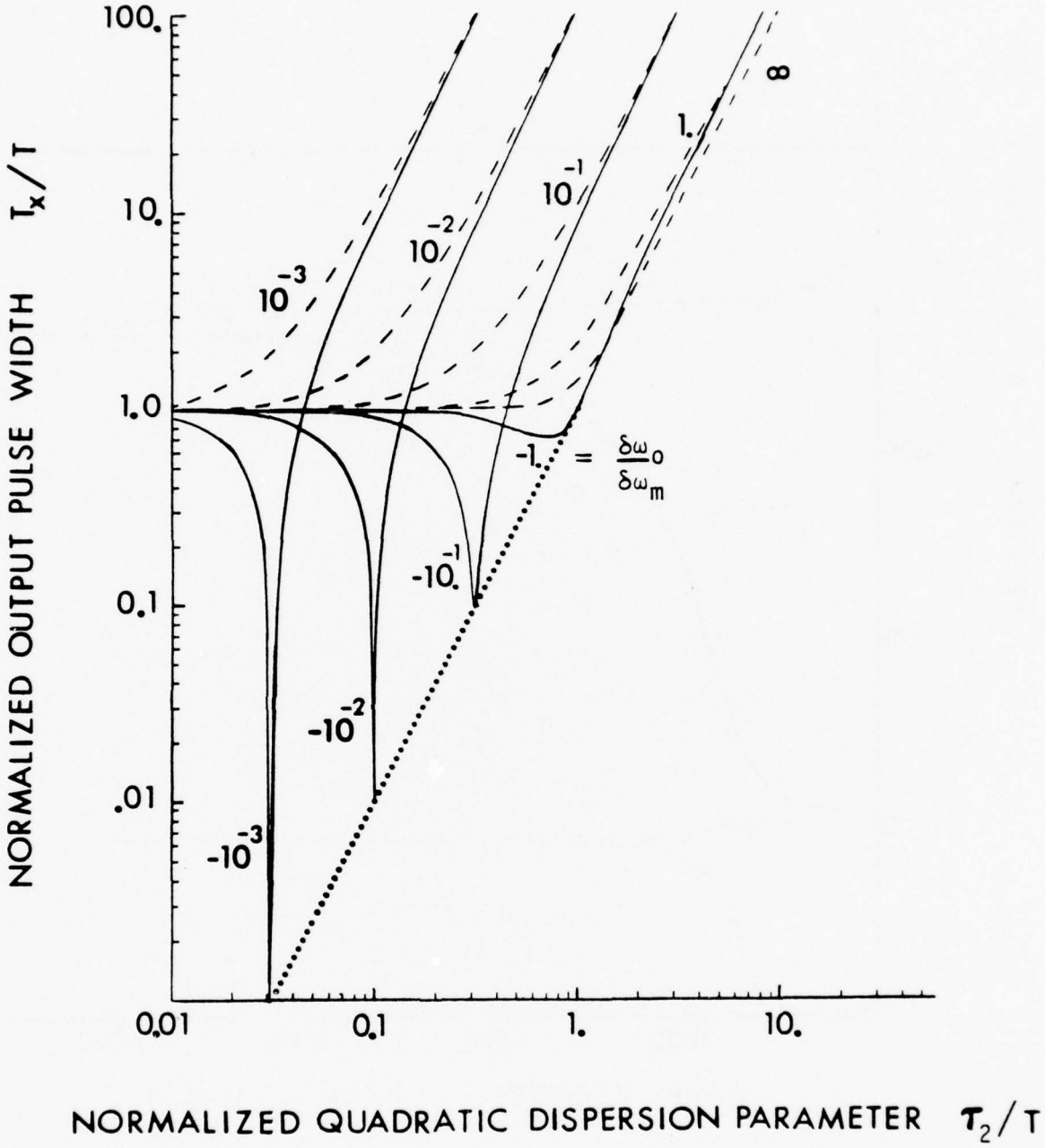
100.
10.
1.0
0.1
.01
0.01
0.1
1.
10.
NORMALIZED OUTPUT PULSE WIDTH τ_x/T
NORMALIZED QUADRATIC DISPERSION PARAMETER τ_2/T
10^{-3}
10^{-2}
10^{-1}
1.
∞
-1. = $\frac{\delta\omega_o}{\delta\omega_m}$
-10^{-1}
-10^{-2}
-10^{-3}

Figure II-1

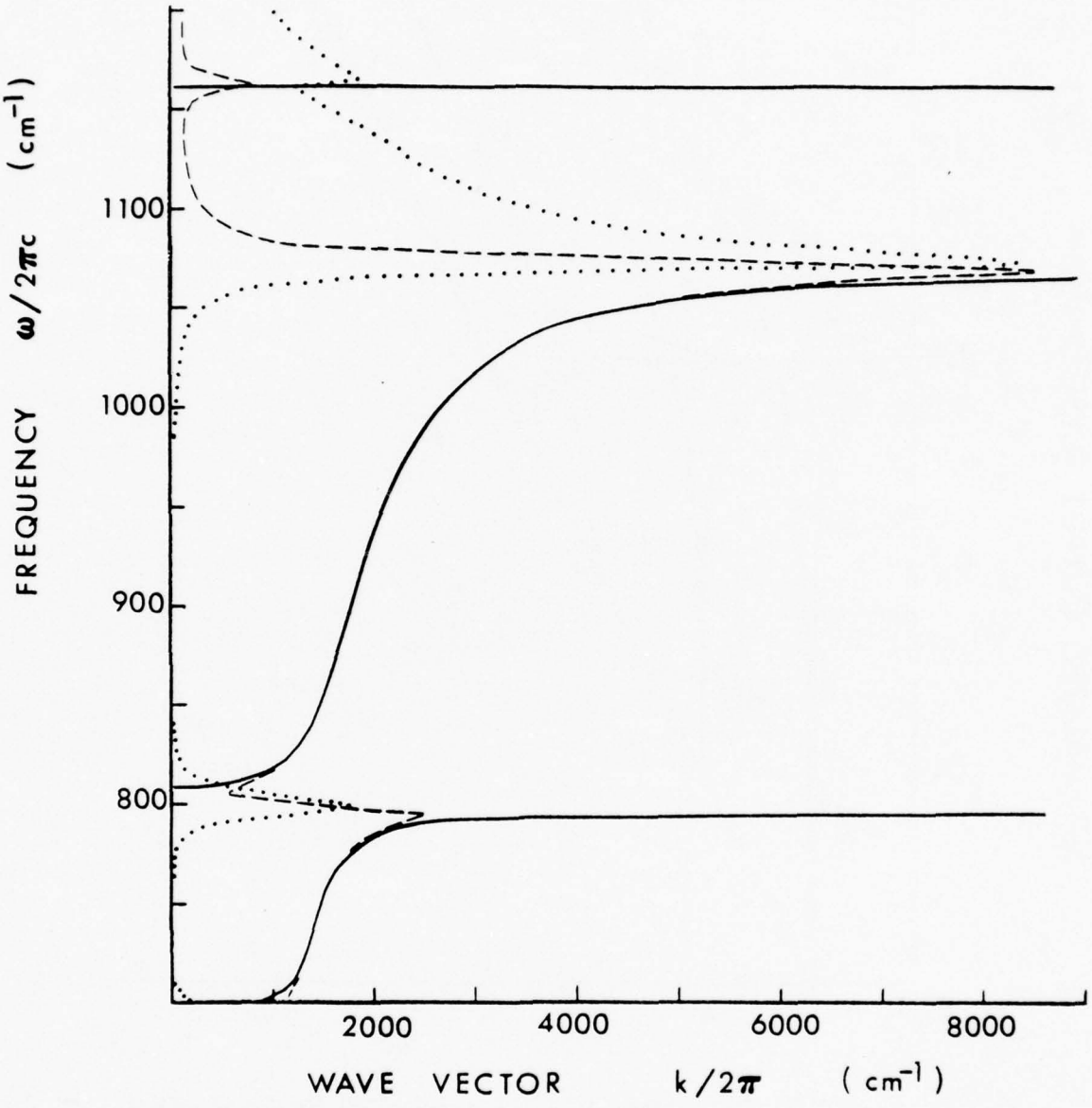
FREQUENCY ω/2πc (cm⁻¹)
1100
1000
900
800
2000
4000
6000
8000
WAVE VECTOR k/2π (cm⁻¹)

Figure II-2

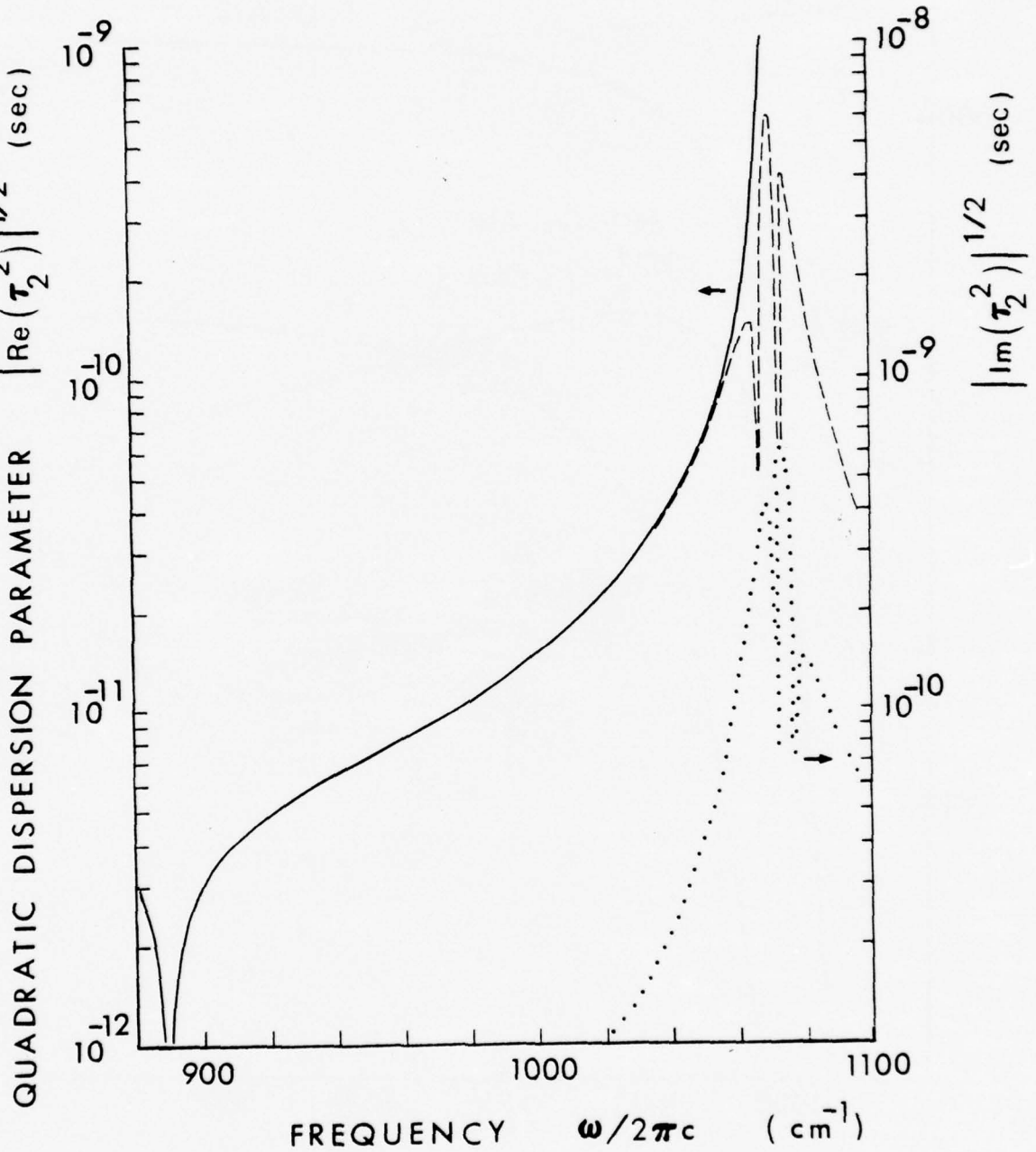
QUADRATIC DISPERSION PARAMETER
$|Re(\tau_2^2)|^{1/2}$ (sec)
$|Im(\tau_2^2)|^{1/2}$ (sec)
10^{-9}
10^{-10}
10^{-11}
10^{-12}
10^{-8}
10^{-9}
10^{-10}
900
1000
1100
FREQUENCY $\omega/2\pi c$ (cm^{-1})

Figure II-3

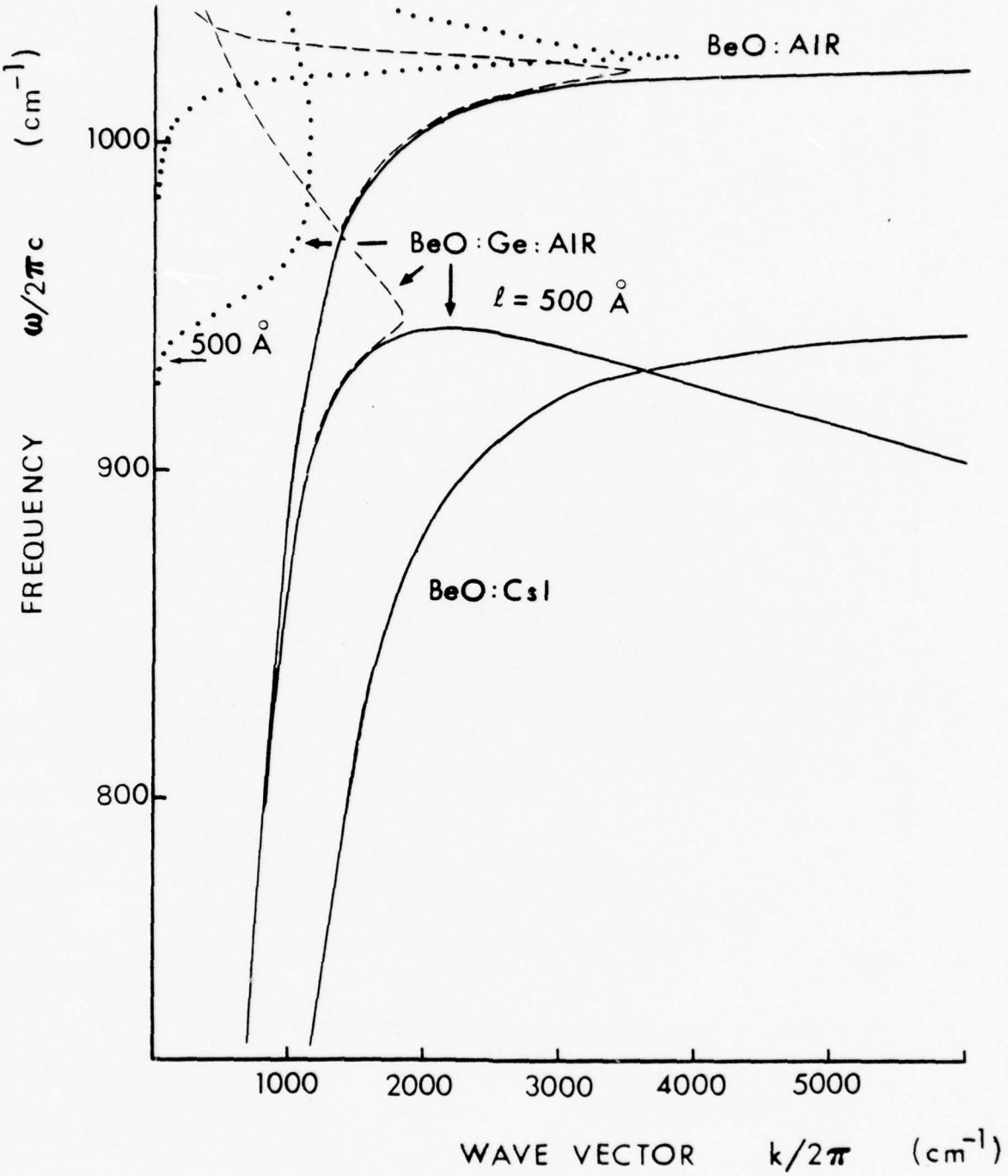
BeO : AIR
BeO : Ge : AIR
ℓ = 500 Å
500 Å
BeO : CsI
FREQUENCY ω/2πc (cm⁻¹)
1000
900
800
1000
2000
3000
4000
5000
WAVE VECTOR k/2π (cm⁻¹)

Figure II-4

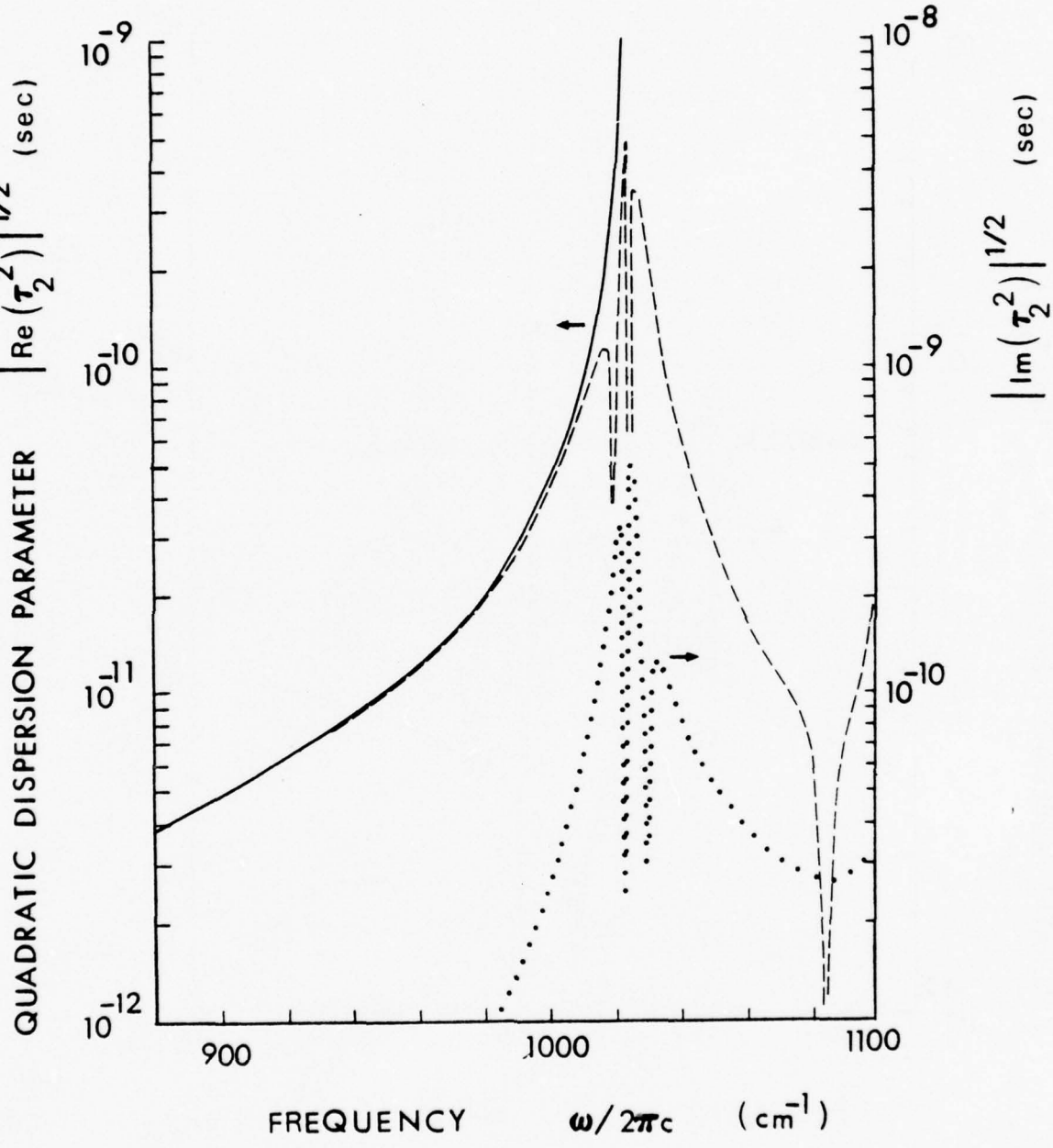
QUADRATIC DISPERSION PARAMETER
$|Re(\tau_2^2)|^{1/2}$ (sec)
$|Im(\tau_2^2)|^{1/2}$ (sec)
10^{-9}
10^{-10}
10^{-11}
10^{-12}
10^{-8}
10^{-9}
10^{-10}
900
1000
1100
FREQUENCY $\omega/2\pi c$ (cm^{-1})

Figure II-5

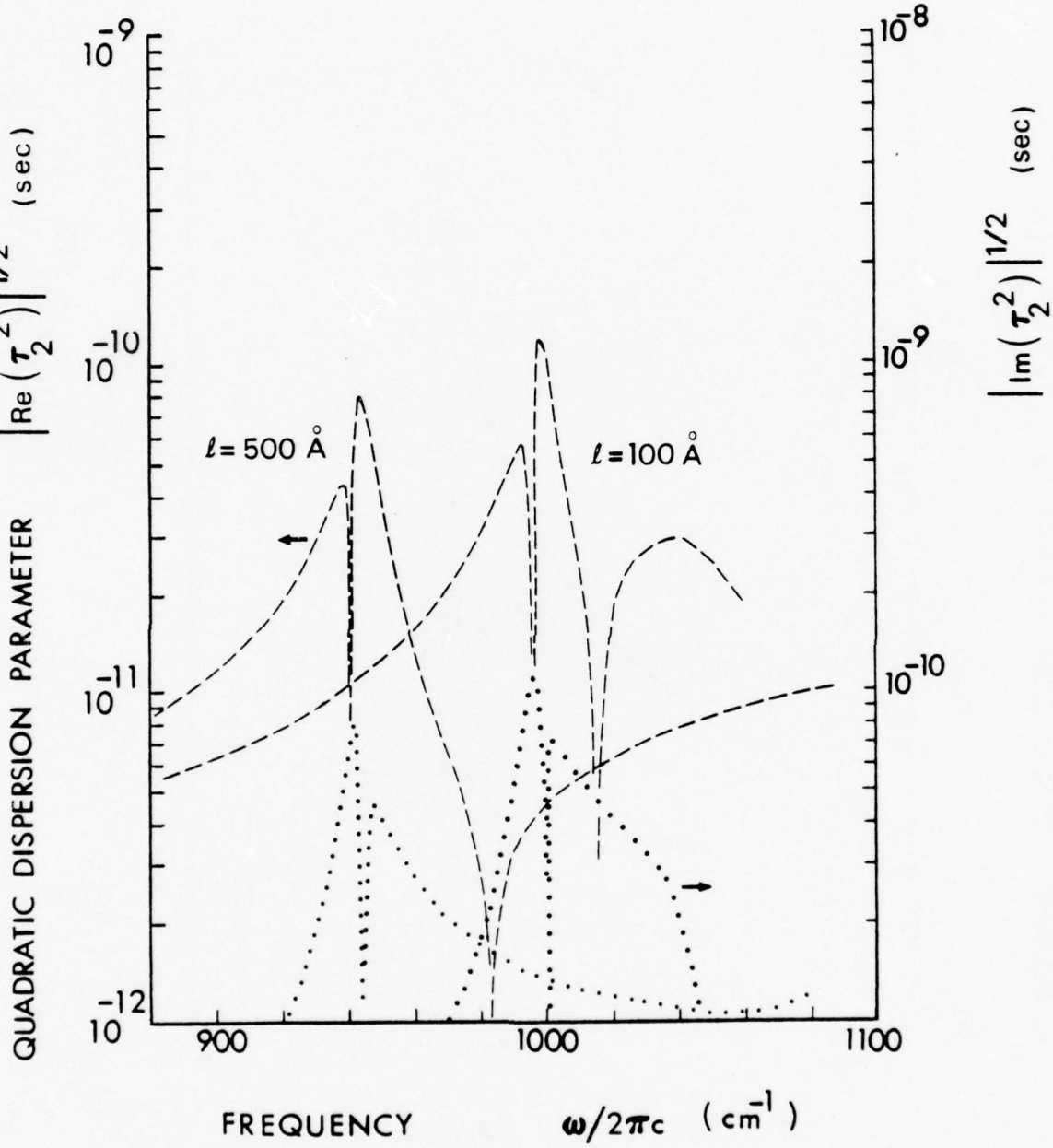
QUADRATIC DISPERSION PARAMETER
$|Re(\tau_2^2)|^{1/2}$ (sec)
$|Im(\tau_2^2)|^{1/2}$ (sec)
10^{-9}
10^{-10}
10^{-11}
10^{-12}
10^{-8}
10^{-9}
10^{-10}
$\ell = 500$ Å
$\ell = 100$ Å
900
1000
1100
FREQUENCY $\omega/2\pi c$ (cm^{-1})

Figure II-6

III. Chirped Pulse Compression In Strongly Dispersive Media*

J. D. McMullen
Electronics Research Center
Rockwell International Corporation
Anaheim, California 92803

ABSTRACT

An analysis is given for the temporal compression of linearly chirped pulses in strongly dispersive media. Terms cubic in frequency are included in the frequency dependent wave vector $k(\omega)$ of the dispersive medium. Analytical expressions are developed for the compressed pulse envelope, and numerical examples given for the influence of the cubic frequency contribution. The strong dispersion term is found to give asymmetric broadening of the compressed pulse envelope.

---

*This research was supported by the U. S. Army Research Office, under Contract No. DAHC04-74-C-0024.

Introduction

A pulse with a linearly chirped carrier frequency may be temporally compressed upon propagating through a suitably dispersive medium.[1-13] Previous analyses have been given for chirped pulses propagating in dispersive but nonabsorbing media,[1-5] and for chirped pulses in absorbing, moderately dispersive media.[6] These treatments are valid when the dispersion is sufficiently weak that the group velocities change only linearly with frequency across the bandwidth of the incident pulse.

A recursion solution has been reported for chirped pulses propagating through strongly dispersive but nonabsorbing media,[7] and for non-chirped pulses in strongly dispersive and absorbing media.[7-9] Numerical calculations of pulse shapes have been reported for non-chirped pulses in dispersive, absorbing media, requiring evaluation by computer of the inverse Fourier transform for the pulse shape.[13] For situations where the strong dispersion results from an average carrier frequency lying close to an absorption frequency of the medium, frequency-dependent absorption can play an important role in determining the shape and final width of the compressed pulse.[6,7,10-12]

In this paper, closed-form analytic solutions are presented for a linearly chirped pulse propagating in an absorbing, strongly dispersive medium, where terms through cubic in frequency are retained in the frequency dependence of the wave vector $k(\omega)$. Numerical examples are given to illustrate the contribution of this cubic dispersion term to the shape of the output compressed pulse envelope, and the limitations imposed by it upon the attainable compressed pulse width.

Theory

Consider a linearly chirped pulse having average carrier frequency ω_o (rad/sec) and a Gaussian envelope of the form:

$$E(0,t) = E_o \exp\left(\frac{-2t^2}{T^2}\right)\cos\left(\omega_o t + \frac{\delta\omega_m}{2T^2}\ t^2\right) \tag{1}$$

specified at x=0 just inside the boundary of a frequency-dispersive medium. The full width at e^{-1} of peak intensity $|E_o|^2$ is T, and the range of frequencies swept over during the full width is $\delta\omega_m$ (rad/sec). The Fourier transform of E(0,t) is given by:

$$\tilde{E}(0,\omega) = \left(\frac{2\pi}{\delta\omega_o\delta\omega}\right)^{1/2} E_o \left\{ \exp\left[\frac{-2(\omega-\omega_o)^2}{\delta\omega_o(\delta\omega_o+i\delta\omega_m)} - i\,\frac{1}{2}\tan^{-1}\left(\frac{\delta\omega_m}{\delta\omega_o}\right)\right] + \exp\left[\frac{-2(\omega+\omega_o)^2}{\delta\omega_o(\delta\omega_o-i\delta\omega_m)} + i\,\frac{1}{2}\tan^{-1}\left(\frac{\delta\omega_m}{\delta\omega_o}\right)\right]\right\} \tag{2}$$

where

$$\delta\omega \equiv \left[(\delta\omega_o)^2 + (\delta\omega_m)^2\right]^{1/2} \tag{3}$$

is the full width at e^{-1} of peak for the power spectrum $|\tilde{E}(0,\omega)|^2$, and $\delta\omega_o \equiv 4/T$ is the bandwidth, similarly defined, for the power spectrum of the unmodulated pulse envelope. The pulse is assumed to propagate in the +x direction in the dispersive medium, which is characterized by complex wave vector $k(\omega)$. If the first term of $\tilde{E}(0,\omega)$ in Eq. (2) peaked in amplitude about $\omega=\omega_o$ is denoted as $\tilde{E}^{(+)}(0,\omega)$ and the second term peaked at $\omega=-\omega_o$ as $\tilde{E}^{(-)}(0,\omega)$, the output pulse waveform at position x is:

$$E(x,t) = \int_{-\infty}^{\infty} d\omega \left[\tilde{E}(0,\omega)^{(+)} e^{ik(\omega)x} + \tilde{E}(0,\omega)^{(-)} e^{-ik(\omega)x} \right] e^{-i\omega t} , \qquad (4)$$

which ensures that $E(x\to\infty,t) \to 0$ in the presence of absorption in the medium. The dispersive medium is characterized by a complex, frequency-dependent wave vector $k(\omega)$ which is assumed to be slowly varying with ω over the bandwidth of the incident pulse. The wave vector $k(\omega)$ is expressed by the Taylor series

$$k(\omega)x = k_o x + \tau_1(\omega-\omega_o) + \frac{1}{2}\left(\frac{\tau_2}{2}\right)^2(\omega-\omega_o)^2 + \frac{\tau_3{}^3}{3}(\omega-\omega_o)^3 + ... \qquad (5\text{-a})$$

about $\omega=+\omega_o$, and (5-a)

$$k(\omega)x = k_o x - \tau_1(\omega+\omega_o) + \frac{1}{2}\left(\frac{\tau_2}{2}\right)^2(\omega+\omega_o)^2 - \frac{\tau_3{}^3}{3}(\omega+\omega_o)^3 + ... \qquad (5\text{-b})$$

about $\omega=-\omega_o$, where $k_o \equiv k(\omega_o)$ and the expansion coefficients are defined as

$$\tau_1 \equiv \left.\frac{dk}{d\omega}\right|_{\omega_o} x , \qquad (5\text{-c})$$

$$\tau_2{}^2 \equiv 4\left.\frac{d^2k}{d\omega^2}\right|_{\omega_o} x , \qquad (5\text{-d})$$

and

$$\tau_3{}^3 \equiv \frac{1}{2}\left.\frac{d^3k}{d\omega^3}\right|_{\omega_o} x . \qquad (5\text{-e})$$

The purpose of this form of definition for τ_2 and τ_3 is to obtain simple parameters of the dispersive medium, having units of time, which can be compared to the incident pulse width and bandwidth for the discussions of pulse compression to follow.

The output pulse waveform at position x is evaluated to be:

$$E(x,t) = \text{Real } 2\,E_o \left(\frac{2\pi}{\delta\omega_o \delta\omega}\right)^{1/2} \exp\left(i\left[k_o x - \omega_o t - \frac{1}{2}\tan^{-1}\left(\frac{\delta\omega_m}{\delta\omega_o}\right)\right]\right)$$

$$\exp\left(\frac{a}{\tau_3}\left[\tau_1 - t + \frac{2}{3}\frac{a^2}{\tau_3}\right]\right)\ \text{Ai}\left(\frac{\tau_1 - t + \frac{a^2}{\tau_3}}{\tau_3}\right)\ , \qquad (6)$$

where for convenience we define

$$a \equiv \frac{2}{\delta\omega_o(\delta\omega_o + i\delta\omega_m)} - i\,\frac{\tau_2^2}{8}\ , \qquad (7)$$

which contains information about the initial pulse width, the applied chirp, and the quadratic dispersion parameter τ_2. Ai( ) is the well-known Airy integral.[14] Details of the derivation of Eq. (6) are given in Appendix A.

A case of particular interest occurs when τ_3 is sufficiently small that the cubic term in the expansion for $k(\omega)$ contributes only slightly to shaping of the output pulse envelope, or $\left|\tau_3^3[\tau_3-(\tau_1-t)]\right| << |a^2|$, for which $E(x,t)$ reduces to the following form:

$$E(x,t) = \text{Real } E_o \left(\frac{T}{T_x}\right)^{1/2} \exp\left(i\left[k_o x - \omega_o t + \frac{1}{2}\tan^{-1}\left(\frac{(\tau_2/T)^2}{1+\frac{\delta\omega_m}{\delta\omega_o}\left(\frac{\tau_2}{T}\right)^2}\right)\right]\right)$$

$$\exp\left(-2\,\frac{(\tau_1-t)^2}{T_x^2}\left[1 + i\left\{\frac{\delta\omega_m}{\delta\omega_o}\left[1 + \frac{\delta\omega_m}{\delta\omega_o}\left(\frac{\tau_2}{T}\right)^2\right] + \left(\frac{\tau_2}{T}\right)^2\right\}\right]\right)\ S(x,t)\ , \qquad (8)$$

where T_x is defined by:

$$T_x = T \left\{ \left[1 + \frac{\delta\omega_m}{\delta\omega_o} \left(\frac{\tau_2}{T} \right)^2 \right]^2 + \left(\frac{\tau_2}{T} \right)^4 \right\}^{1/2} \tag{9}$$

and the contribution of the cubic frequency term in $k(\omega)$ is contained entirely within the shape factor $S(x,t)$, given by:

$$S(x,t) = \exp\left(\frac{1}{3} \left[\frac{\tau_3 (\tau_1 - t)}{2a} \right]^3 \right) \left[1 + \frac{\tau_3^3 (\tau_1 - t)}{(2a)^2} \right]^{-1} . \tag{10}$$

In the limit that $\tau_3=0$, the shape factor S becomes unity and $|E(x,t)|^2$ reduces to a Gaussian pulse with full width T_x at e^{-1} of peak intensity. For this case Eq. 8 shows the peak pulse intensity is reduced or increased by a factor $(T/T_x)\exp(-2\mathrm{Im}[k_o x])$ as the output pulse becomes either dispersion broadened or compressed in width. When the applied chirp is an optimum value given by

$$\delta\omega_m \Big|_{opt} = - \delta\omega_o \left(\frac{T}{\tau_2} \right)^2 , \tag{11}$$

then the output pulse $E(x,t)$ is compressed to its narrowest possible width.

Figure 1 illustrates the compressed pulse waveform for a chirped Gaussian pulse having initial width T = 1 nsec and an applied chirp $\delta\omega_m=-100\delta\omega_o$ after the pulse has propagated through a dispersive medium for which $\mathrm{Im}(k_o x)=0$ and $\tau_2=0.1$ nsec. Both Eqs. (6) and (8) were used to calculate pulse envelopes. The approximate solution of Eq. (8) greatly simplifies the calculations for ranges of parameters such that the argument of the Airy function is very large. The solid curve for the case $\tau_3=0$ shows the compressed pulse has a Gaussian profile of full width $T_x=10$ psec at e^{-1} of peak intensity. The

broken curves illustrate the influence of the cubic term in $k(\omega)$ upon the output pulse shape for successively larger values of τ_3, with the other parameters held constant. For larger values of τ_3 the peak of the compressed pulse is diminished in height and shifted to larger delay times, and the pulse shape becomes asymmetrically broadened about the peak. Interference structure occurs in the trailing edge of each pulse for $\tau_3=0$ in accordance with the oscillatory nature of the Airy function for negative real argument.

It is apparent from Figure 1 that significant pulse shaping effects occur for τ_3 as small as 3 psec in the above example. Upon replacing the factor $(\omega-\omega_o)$ in Eq. (5-a) by the bandwidth $\delta\omega$ of the incident pulse, it is noted that the magnitude of the third order term in the series expansion for $k(\omega)$ is only about 0.3 percent of the magnitude of the second order term. Therefore, the influence of τ_3 upon the shape and height of the compressed pulse becomes quite significant for smaller values of τ_3 than might be anticipated upon examination of Eq. (5-a) alone.

Conclusion

In conclusion, it has been shown that a closed-form analytic solution may be obtained for a linearly chirped pulse which becomes temporally compressed upon propagating through a strongly dispersive medium, where terms cubic in frequency are retained in the expansion of $k(\omega)$ about the average carrier frequency. The cubic frequency dependence is shown to further delay the peak of the compressed pulse and to cause the pulse to become asymmetrically broadened about that peak. The small value of τ_3 required to influence the compressed pulse shape suggests τ_3 may easily be significant in pulse compression experiments for which the group delay changes rapidly with frequency over the bandwidth of the incident pulse.

Acknowledgements

The Airy function solution for the compressed pulse shape was suggested by A. A. Maradudin of the University of California at Irvine. The author gratefully acknowledges stimulating and helpful discussions with D. L. Mills of the University of California at Irvine.

Appendix A

Analysis of the output pulse shape from Eq. (4) requires the evaluation of inverse Fourier transform integrals of the form:

$$I = \int_{-\infty}^{\infty} dy \exp\left[i(\tau_1 - t)y - ay^2 + i \frac{\tau_3^3}{3} y^3 \right] \qquad \text{A-1}$$

where $y \equiv \omega - \omega_0$ and a is defined by Eq. (7).

Upon introducing a change in variable

$$\xi = y + i \frac{a}{\tau_3^3} \qquad \text{A-2}$$

The integral becomes:

$$I = \exp\left(\frac{a}{\tau_3^3} \left[\tau_1 - t + \frac{2}{3} \frac{a^2}{\tau_3^3} \right] \right) \int_{-\infty}^{\infty} d\xi \exp\left[i \frac{\tau_3^3}{3} \xi^3 + i\left(\tau_1 - t + \frac{a^2}{\tau_3^3} \right) \xi \right] \qquad \text{A-3}$$

The integral in Eq. (A-3) is recognizable as the Airy integral,[14] leading to the analytic expression in Eq. (6) for the pulse shape at position x.

When τ_3 is very small and the argument of the Airy function becomes very large in magnitude, it is useful to approximate Ai by the following limit:

$$\lim_{|z| \to \infty} \mathrm{Ai}(z) \simeq \frac{1}{2\pi^{1/2} z^{1/4}} \exp\left(- \frac{2}{3} z^{3/2} \right) \qquad \text{A-4}$$

where

$$z = \frac{a^2}{\tau_3^4} \left[1 + \frac{\tau_3^3}{a^2} (\tau_1 - t) \right] \quad . \qquad \text{A-5}$$

Series expansion of $z^{3/2}$ must be carried out to include terms quadratic in τ_3^3 because of the exponential factor preceeding the integral in Eq. (A-3), so that

$$z^{3/2} \simeq \frac{a^3}{\tau_3^6}\left[1 + \frac{3}{2}\frac{\tau_3^3}{a^2}(\tau_1 - t) + \frac{3}{8}\left(\frac{\tau_3^3}{a^2}(\tau_1 - t)\right)^2 + \cdots\cdots\right], \qquad \text{A-6}$$

while the expansion for $z^{1/4}$ in the denominator of Eq. A-4 may be truncated after the first order term in τ_3^3 as follows:

$$z^{1/4} \simeq \frac{a^{1/2}}{\tau_3}\left[1 + \frac{1}{4}\frac{\tau_3^3}{a^2}(\tau_1 - t) + \cdots\cdots\right] \qquad \text{A-7}$$

The resulting expression for the output pulse shape in Eq. (8) greatly reduces the computational effort for E(x,t) for ranges of parameters over which the argument of the Airy function is large in magnitude.

References

1. J. R. Klauder, A. C. Price, S. Darlington and W. J. Albersheim, Bell System Tech. J. 39, 745 (1960).
2. J. R. Klauder, Bell System Tech. J. 39, 809 (1960).
3. C. E. Cook, Proc. IRE 48, 310 (1960)
4. M. I. Skolnik, Introduction to Radar Systems (McGraw-Hill, New York, 1962) p. 493.
5. A. Laubereau and D. von der Linde, Z. Naturforsche 25A, 1626 (1976).
6. J. D. McMullen, J. Appl. Physics (to be published, manuscript No. 2509R).
7. D. G. Anderson and J. I. H. Askne, Proc. IEEE 62, 1518 (1974).
8. D. Anderson, J. Askne and M. Lisak, Proc. IEEE 63, 715 (1975).
9. D. Anderson, J. Askne and M. Lisak, Phys. Rev. A 12, 1546 (1975).
10. D. Rader, Am. J. Phys. 41, 420 (1973).
11. R. A. Fisher, Am. J. Phys. 44, 1002 (1976).
12. D. Rader, Am. J. Phys. 44, 1005 (1976).
13. G. I. Terina, Radio Engr. and Electr. Phys. 17, 475 (1972).
14. Handbook of Mathematical Functions, ed. by M. Abramowitz and I. A. Stegun (Nat. Bureau Standards, Wash. D. C.,1965) pp 446-478.

Figure Captions

Figure III-1 Waveform of compressed chirped pulse intensity with T-1 nsec, $\delta\omega_m$=-100$\delta\omega_o$, and τ_2=0.1 nsec, for various values of group dispersion τ_3=0 (——), τ_3=3 psec (----), τ_3=4 psec (-·-·-·-·), τ_3=5 psec (-··-··-··-) and τ_3=10 psec (····).

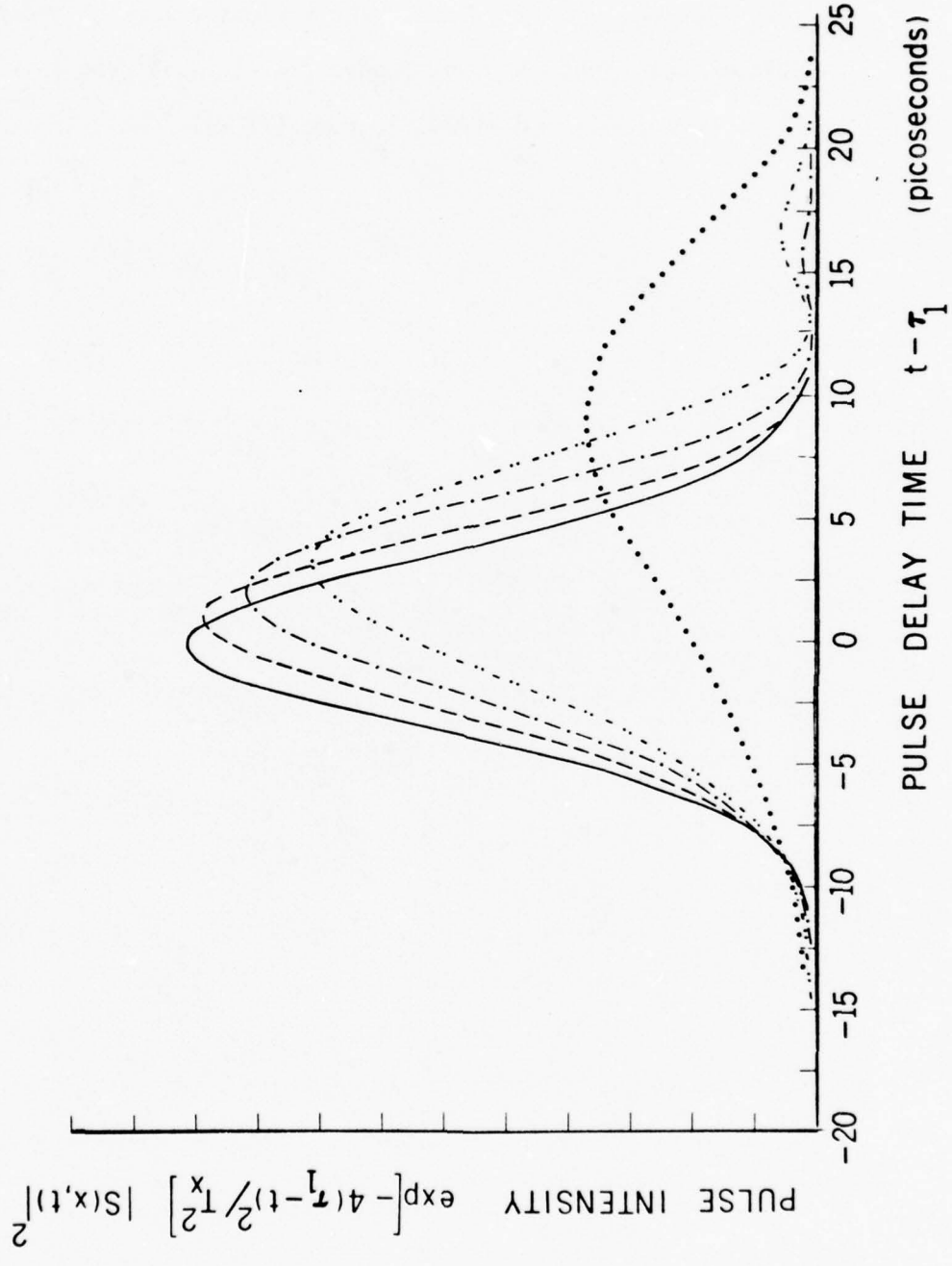
PULSE INTENSITY $\exp\left[-4(\tau_1-t)^2/T_x^2\right]$ $|S(x,t)|^2$
-20
-15
-10
-5
0
5
10
15
20
25
PULSE DELAY TIME $t-\tau_1$ (picoseconds)

Figure III-1

IV. THEORY OF SURFACE POLARITON GENERATION THROUGH GRATING COUPLERS*

D. L. Mills
Department of Physics
University of California
Irvine, California 92664

ABSTRACT

We discuss the theory of surface polariton generation by grating couplers. The emphasis is on an analysis of the manner in which the grating may modify the frequency spectrum of a shaped incident pulse. If L is the length of the portion of the grating illuminated by the incident beam, then we find the frequency spectrum of the incident pulse can be transmitted to the surface polariton undistorted if the criterion $L < V_g/\sigma$ is satisfied, where V_g is the group velocity of the surface polariton, and σ a measure of the spread of frequencies in the incident beam used to excite the surface polaritons. If this criterion is not satisfied, the frequency spectrum of the transmitted pulse will be narrower than that in the incident pulse. The treatment here provides expressions for the absolute amplitude and shape of the transmitted signal, within the framework of a method that assumes the height of the grating is small.

* Research supported by Contract DAHC04-74-C-0024
U.S. Army Research Office, Durham, North Carolina

A. Introductory Remarks

There is considerable current interest in the study of surface polaritons. These are electromagnetic surface waves[1] that under a variety of circumstances may propagate along an interface between two media, with electromagnetic fields confined to the near vicinity of the interface. For the simple case of the interface between vacuum and an isotropic dielectric with frequency dependent dielectric constant $\epsilon(\omega)$, these waves may propagate whenever $\mathrm{Re}(\epsilon(\omega)) < 0$. One may launch them through use of a prism coupling device or a grating[1],[2] and their propagation length may be in the range of 1 mm to 1 cm at 10.6μ, for selected substrates.

Since the propagation length of these waves can be reasonably long in the infrared, in principle one may contemplate incorporating them into devices. There can be substantial curvature in the surface polariton dispersion relation, and as a consequence one may consider the use of surface polaritons for signal processing operations such as compression of a chirped input pulse.[3] Experimental studies of this possibility are underway, but they are currently in an early stage.[4]

In such an operation, one envisions a chirped pulse incident on a coupler which launches a surface polariton pulse that propagates on a substrate. One is then led to inquire into the question of whether the surface polariton pulse is composed of a frequency spectrum that accurately reflects that in the input pulse. Since the response function of the grating coupler is sharply peaked about a particular frequency (that of a surface polariton) when excited by radiation incident at a fixed angle, the question seems particularly important to explore in this case.

The purpose of this paper is to present a study of the shape of the surface polariton pulse launched through use of a grating coupler excited by an incident wave with a spectrum of frequencies contained in it. We consider the specific case of a chirped input pulse, and find expressions for the absolute amplitude and shape of the output surface polariton pulse, when the height of the grating

coupler may be regarded as small. We find that if L is the length of the grating segment illuminated by the incident beam, V_g is the group velocity of the surface polariton launched from the coupler, and σ the width in frequency of the input beam (in radians/sec), then provided

$$L < V_g/\sigma \ , \qquad \text{(A-1)}$$

the frequency composition of the surface polariton generated can accurately reflect that of the input pulse. When one has instead $L > V_g/\sigma$, the frequency spectrum of the output pulse is narrower than of the input pulse. This is most unfavorable, since the coupler then acts to expand the surface polariton pulse, thus making the task of subsequently compressing the pulse more difficult.

In essence, the criterion quoted above requires one to focus the incident beam down to a size small compared to V_g/σ, if one wishes to pass the frequency spectrum in the incoming pulse faithfully on to the surface polariton pulse generated by the grating. Insertion of numbers into the criterion indicates that the focusing requirement places no serious limitation on the use of gratings, although for pulses that approach picosecond duration, one may well need to worry about this question.

The organization of this paper is as follows. In Section B , we derive an expression for the amplitude of the surface polariton produced by a linearly chirped pulse incident on a grating. This derivation leans heavily on results obtained in an earlier paper by the present author. The result obtained in Section B is of reasonable generality, and after some manipulation we cast it into a form that is useful for numerical computation. In Section C , we work out the form of the surface polariton pulse for several special limiting situations. These results, obtained in analytic form, allow the principal parameters of the problem to be isolated, and their role evaluated.

B. Derivation of an Expression for the Shape of the Output Pulse

The geometry that forms the basis of the present discussion is illustrated in Figure (1). An incident beam of finite width is presumed to strike a diffraction grating ruled on a substrate with dielectric constant $\varepsilon(\omega)$. The angle of incidence is θ_o, and to generate surface polaritons the incident radiation is p-polarized. The plane of incidence of the incident radiation is perpendicular to the grooves in the grating.

Consider the incident wave to be monochromatic with frequency ω for the moment and let d be the grating spacing. The wave vector component of the incident radiation parallel to the surface is $k_{\parallel}^{(o)} = \omega \sin\theta_o / c$, with c the velocity of light. Near the surface of the grating, the electromagnetic field of the incident wave is perturbed from the plane wave form, and acquires ripples with wave vector parallel to the surface

$$k_{\parallel}^{(n)} = \frac{\omega}{c} \sin\theta_o + \frac{2\pi}{d} n \quad ; \quad n = 0, 1, 2 \ldots \quad . \qquad (B-1)$$

Derivation of the detailed form of the field near the grating has been presented in recent works by Elson[5] and by the present author.[6] (While the main emphasis in Reference (6) differs from the question explored here, a prescription is given there for constructing the fields near the grating, and it is this prescription we have used here.)

Now let $\omega_s(k_{\parallel})$ be the dispersion relation of the surface polariton. For the semi-infinite dielectric/vacuum interface, this dispersion relation is found from[1]

$$\frac{c^2 k_{\parallel}^2}{\omega^2} = \frac{\varepsilon(\omega)}{\varepsilon(\omega) + 1} \qquad (B-2)$$

Then if θ_o and the frequency of the incident radiation are adjusted so that for some n, $\omega = \omega_s\left(k_{\parallel}^{(n)}\right)$, the grating exhibits a resonant response to the incoming

field, and a surface polariton is generated. In the present paper, we are interested in incident beams that operate within such a resonance peak.

To proceed, we introduce a convention that will be used throughout the paper. Its purpose is to keep the notation and analysis as simple as possible. The incident electric field is a vector, but we work with only a single Cartesian component. We choose the component parallel to the surface. Furthermore, we shall need only the amplitude of this component very slightly above the surface. The values of this electric field component elsewhere in space, and the Cartesian component perpendicular to the surface, are readily constructed from this information by elementary considerations. This convention allows convenient application of the results of Reference (6), since the discussion there focuses on the relation between electric field components of the various beams parallel to the surface. Also, this convention reduces the present problem to one that can be discussed with use of notation appropriate to wave propagation in one dimension.

We let $E(x,t)$ be the amplitude of the field component parallel to the surface in the incident wave. Here x is a coordinate parallel to the surface, with the x axis perpendicular to the grating grooves. We wish the electric field at each point to have the form of a chirped pulse, with gaussian envelope:

$$E = E_{(o)} \exp\left[-\frac{t^2}{2\sigma_o^2}\right] \sin\left[\omega_o\, t(1+\lambda t)\right] \quad . \qquad (B-3)$$

Here $E_{(o)}$ is the maximum field generated by the laser pulse, $2\sigma_o$ the width of the gaussian intensity envelope of the pulse, and λ is a measure of the amount of linear chirp applied to the signal. In other works,[3] the combination $\lambda\omega_o$ is denoted by $r/2$. We write Eq. (B-3) in the form

$$E = \int_{-\infty}^{+\infty} \frac{d\omega}{2\pi} E(\omega)\, e^{-i\omega t} \quad , \qquad (B-4)$$

where after a short exercise one finds

$$E(\omega) = i\left(\frac{\pi}{2}\right)^{1/2} E_{(o)} \left\{ \sigma \exp\left[-\frac{1}{2} \sigma^2 (\omega-\omega_o)^2 \right] - \sigma^* \exp\left[-\frac{1}{2} (\sigma^*)^2 (\omega+\omega_o)^2 \right] \right\} \quad , \qquad (B\text{-}5a)$$

with

$$\sigma = \sigma_o (1+i2\sigma_o^2 \lambda\omega_o)^{-1/2} \quad , \qquad (B\text{-}5b)$$

and the complex square root is chosen so that $Re(\sigma)>0$.

These expressions give the electric field at one point in the wave. To describe the spatial dependence as well as the time dependence of the incident wave, the term which involves $(\omega-\omega_o)^2$ is multiplied by $\exp\left[i\, k_{\shortparallel}(\omega) x \right]$ and that proportional to $(\omega+\omega_o)^2$ is multiplied by $\exp\left[-i\, k_{\shortparallel}(\omega) x \right]$ where

$$k_{\shortparallel}(\omega) = \frac{\omega}{c} \sin \theta_o \qquad (B\text{-}6)$$

is the component of the wave vector parallel to the surface for the Fourier component with frequency ω.

Finally, to insure the wave illuminates only a strip of width L on the surface, as illustrated in Figure (1), we multiply the final expression for $E(x,t)$ by $\theta(x+L/2) \cdot \theta(L/2-x)$, where $\theta(z)$ is the unit step function that equals +1 for positive values of its argument, and vanishes for negative values.

We write the final expression for the incident field in the form

$$E(x,t) = \int_{-\infty}^{+\infty} \frac{d\omega}{2\pi} \int_{-\infty}^{+\infty} \frac{dk_{\shortparallel}}{2\pi} E(k_{\shortparallel},\omega)\, e^{ik_{\shortparallel}x}\, e^{-i\omega t} \qquad (B\text{-}7)$$

where one has

$$E(k_{\shortparallel},\omega) = i(2\pi)^{1/2} E_{(o)} \left\{ \sigma \exp\left[-\frac{1}{2} \sigma^2 (\omega-\omega_o)^2 \right] \frac{\sin\left[\left(k_{\shortparallel}-k_{\shortparallel}(\omega)\right)\frac{L}{2} \right]}{\left(k_{\shortparallel}-k_{\shortparallel}(\omega)\right)} \right. \qquad (B\text{-}8)$$

$$-\sigma^* \exp\left[-\frac{1}{2}(\sigma^*)^2 (\omega+\omega_0)^2\right] \frac{\sin\left[\left(k_{\shortparallel}+k_{\shortparallel}(\omega)\right)\frac{L}{2}\right]}{\left[k_{\shortparallel}+k_{\shortparallel}(\omega)\right]} \Bigg\} \qquad (B-8)$$

The next task is to describe the response of the grating to the incident field in Eq. (B-7). If the amplitude u of the grooves in the grating is small, so the fields generated by the incident field may be calculated to first order in u, then we need to consider the response of the grating to the sinusoidal field $E(k_{\shortparallel},\omega)\exp[i(k_{\shortparallel}x-\omega t)]$, and the form of the output signal may be found by synthesizing the Fourier components calculated from linear response theory. This is the procedure followed here.

The interaction of the grating with a sinusoidal field proportional to $\exp[i(k_{\shortparallel}x-\omega t)]$ may be constructed from the prescription given in Section IV of Reference (6) (or from Reference (5)). One needs the amplitude of the reflected part of the incident wave and that transmitted into the substrate. These are readily calculated from the appropriate Fresnel equations. For practical purposes, we shall always have $\sigma_0\omega_0 >> 1$ and $\lambda\sigma_0 << 1$. Also, the spread in wave vector $k_{\shortparallel}$ important in the Fourier integral will be small compared to $k_{\shortparallel}(\omega)$, so long as L is long compared to the wavelength of the wave in vacuum. Under these conditions, to excellent approximation one can calculate the reflected and transmitted incident pulses by simply multiplying each Fourier component by the same Fresnel coefficient, namely that for frequency ω_0 and $k_{\shortparallel}=k_{\shortparallel}(\omega_0)$.

We shall simply quote the result for the form of the output pulse, since the prescription for computing is supplied in Section IV of Reference (6). We have made some approximations along the way, and we describe them briefly. First of all, we are interested in frequency regimes where the dielectric constant $\epsilon(\omega)$ of the substrate has negative real part. We also assume $\mathrm{Im}\left(\epsilon(\omega)\right) << |\mathrm{Re}\,\epsilon(\omega)|$, so the propagation length of the surface polariton is long. Then in all those parts of the

response function which vary smoothly with frequency, $\varepsilon(\omega)$ has been replaced by $-|\varepsilon_r(\omega_0)|$, the magnitude of its real part evaluated at ω_0. This approximation is readily avoided if desired, at the price of an increase in complexity of some of the expressions below. However, for our purposes, this approximation introduces little error.

There is one factor where this replacement cannot be made. In the calculation of the response function, one encounters the denominator[6]

$$D\left(k_{\parallel}^{(n)}, \omega\right) = 1 + \varepsilon(\omega) \frac{\alpha_0\left(k_{\parallel}^{(n)}, \omega\right)}{\alpha\left(k_{\parallel}^{(n)}, \omega\right)} , \qquad (B-9)$$

where $k_{\parallel}^{(n)} = k_{\parallel}^{(o)} + \frac{2\pi n}{d}$, d is the period of the grating, n the order of the diffracted beam under consideration, and

$$\alpha_0\left(k_{\parallel}^{(n)}, \omega\right) = \left(k_{\parallel}^{(n)2} - \frac{\omega^2}{c^2}\right)^{1/2} \qquad (B-10a)$$

$$\alpha\left(k_{\parallel}^{(n)}, \omega\right) = \left(k_{\parallel}^{(n)2} - \frac{\omega^2}{c^2}\varepsilon(\omega)\right)^{1/2}, \quad \mathrm{Re}(\alpha) > 0 \quad . \qquad (B-10b)$$

The quantity $D\left(k_{\parallel}^{(n)}, \omega\right)$ vanishes when $k_{\parallel}^{(n)} = k_s(\omega)$, with $k_s(\omega)$ the surface polariton wave vector (complex, with $\mathrm{Re}(k_s(\omega)) > 0$) calculated from the dispersion relation in Eq. (B-2)). Since, as we shall see, $D\left(k_{\parallel}^{(n)}, \omega\right)$ is in the denominator of the response function and we shall work in the near vicinity of this resonance, the full complex dielectric constant $\varepsilon(\omega)$ will be retained here. Also, in the numerator of the expressions for the diffracted fields, since we work close to the zero in $D\left(k_{\parallel}^{(n)}, \omega\right)$, wherever the factor $\varepsilon(\omega)\alpha_0\left(k_{\parallel}^{(n)}, \omega\right)/\alpha\left(k_{\parallel}^{(n)}, \omega\right)$ is encountered, it will be replaced by -1.

Then if we presume it is the n^{th} order diffracted beam that generates the surface polariton, in this beam the tangential component of the electric field $E^{(s)}(x,t)$ just above and below the surface are equal. Following Eq.(B -7) we write

$$E^{(s)}(x,t) = \int_{-\infty}^{+\infty} \frac{d\omega}{2\pi} \int_{-\infty}^{+\infty} \frac{dk_{\parallel}}{2\pi} E^{(s)}(k_{\parallel},\omega)\, e^{i\, k_{\parallel} x}\, e^{-i\omega t} \quad , \qquad (B\text{-}11)$$

where the grating response theory described above produces the expression[8]

$$E^{(s)}(k_{\parallel},\omega) = \frac{2i\, u^{(n)}\, \omega_o}{c} \quad \frac{T(\omega_o)}{D(k_{\parallel},\omega)} \quad E\left(k_{\parallel} - \frac{2\pi n}{d}\, ,\, \omega\right) \quad , \qquad (B\text{-}12)$$

where $D(k_{\parallel},\omega)$ has been defined above,

$$T(\omega_o) = \frac{\left[1+|\varepsilon_r(\omega_o)|\right]\left[\sqrt{\sin^2\Theta_o + |\varepsilon_r(\omega_o)|} - \sin\Theta_o \sqrt{|\varepsilon_r(\omega_o)|}\right]}{\sqrt{|\varepsilon_r(\omega_o)|-1}\left[|\varepsilon_r(\omega_o)|\cos\Theta_o - i\,\frac{c}{\omega_o}\,\alpha(o)\right]} \quad , \qquad (B\text{-}13a)$$

and

$$\alpha(o) = \sqrt{k_{\parallel}(\omega_o)^2 + \frac{\omega_o^2}{c^2}\,|\varepsilon_r(\omega_o)|} \quad . \qquad (B\text{-}13b)$$

Finally, if the function $u(x)$ is the grating profile, we write

$$u(x) = \sum_{n=-\infty}^{+\infty} u^{(n)} \exp\left[i\,\frac{2\pi n}{d}\,x\right] \quad . \qquad (B\text{-}14)$$

Thus, the quantity $u^{(n)}$ in Eq. (B -12) is the amplitude of the Fourier component of the grating profile shape function $u(x)$ responsible for Bragg diffracting the incident wave, to generate the surface polariton.

If the above results are collected together, then after some algebra which makes use of the identity $D(k_{\parallel}, -\omega) = D(k_{\parallel},\omega)^*$, we find

$$E^{(s)}(x,t) = -\frac{\sqrt{2}}{\pi^{3/2}} \left(\frac{u^{(n)}{}_{\omega_o}}{c}\right) E_{(o)}$$

$$\times \mathrm{Re}\left\{ \sigma\, T(\omega_o) \int_{-\infty}^{+\infty} d\omega\, e^{-\frac{\sigma^2}{2}(\omega-\omega_o)^2} e^{-i\omega t} \right. \qquad (B\text{-}15)$$

$$\left. \times \int_{-\infty}^{+\infty} \frac{dk_{\shortparallel}\, e^{ik_{\shortparallel}x} \sin\left[\left(k_{\shortparallel}-k_{\shortparallel}^{(n)}\right)\frac{L}{2}\right]}{D(k_{\shortparallel},\omega)\,[k_{\shortparallel}-k_{\shortparallel}^{(n)}]} \right\} .$$

In this expression,

$$k_{\shortparallel}^{(n)} = k_{\shortparallel}^{(o)} + \frac{2\pi n}{d} = \frac{\omega}{c} \sin\theta_o + \frac{2\pi n}{d} . \qquad (B\text{-}16)$$

The next task is to cast Eq. (B-15) into a useful form that can be evaluated for various cases of interest. We do this by making rather extensive use of the fact that we are operating very close to the surface polariton resonance in the response function $[D(k_{\shortparallel},\omega)]^{-1}$. For example, after some algebra, we may write (with no approximation)

$$\frac{1}{D(k_{\shortparallel},\omega)} = \frac{1}{1+\varepsilon(\omega)\dfrac{\alpha_o(k_{\shortparallel},\omega)}{\alpha(k_{\shortparallel},\omega)}} \qquad (B\text{-}17a)$$

$$= \frac{\alpha(k_{\shortparallel},\omega)\,[\alpha(k_{\shortparallel},\omega) - \varepsilon(\omega)\,\alpha_o(k_{\shortparallel},\omega)]}{1-\varepsilon^2(\omega)} \frac{1}{[k_{\shortparallel}^2 - k_s^2(\omega)]} \qquad (B\text{-}17b)$$

where

$$k_s^2(\omega) = \frac{\omega^2}{c^2}\left[\frac{\varepsilon(\omega)}{\varepsilon(\omega)+1}\right] \qquad (B\text{-}18)$$

is the square of the (complex) surface polariton wave vector, for a surface polariton of frequency ω. We replace $k_{\shortparallel}$ by $k_s(\omega)$ everywhere in Eq. (B-17b) save for the factor

$\left[k_{\parallel}^2 - k_s^2(\omega)\right]^{-1}$, since we shall always be close to resonance. Then again everywhere but in this resonant factor, we replace $\varepsilon(\omega)$ by $-|\varepsilon_r(\omega_o)|$, as we have earlier. We then have the approximate expression

$$E^{(s)}(x,t) = + \left(\frac{2}{\pi}\right)^{3/2} E_{(o)}\, u^{(n)} \left(\frac{\omega_o}{c}\right)^3 \frac{|\varepsilon_r(\omega_o)|^2}{\left[|\varepsilon_r(\omega_o)|-1\right]^2 \left[|\varepsilon_r(\omega_o)|+1\right]}$$

$$\cdot \mathrm{Re}\left\{ \sigma\, T(\omega_o) \int_{-\infty}^{+\infty} d\omega\; e^{-\frac{1}{2}\sigma^2(\omega-\omega_o)^2}\, e^{-i\omega t} \right. \qquad \text{(B-19)}$$

$$\left. \cdot \int_{-\infty}^{+\infty} \frac{dk_{\parallel}\, e^{ik_{\parallel}x} \sin\left[\left(k_{\parallel}-k_{\parallel}^{(n)}\right)\frac{L}{2}\right]}{\left[k_{\parallel}^2 - k_s^2(\omega)\right]\left[k_{\parallel}-k_{\parallel}^{(n)}\right]} \right\} .$$

The result in Eq. (B-19) may be used to calculate the output field anywhere in space, provided the input pulse has a frequency spectrum sufficiently narrow that the assumptions used in deriving it are correct. (A key assumption is, in essence, that $\omega_o >> 1/|\sigma|$). The interest here is in the form of the surface polariton pulse in the limit $x \to \infty$, far from the region $-L/2<x<+L/2$ where the exciting radiation strikes the grating. For $x>L/2$, the $k_{\parallel}$ integration in Eq. (B-19) may be evaluated by a straight-forward contour integration. This gives us, again for $x>L/2$

$$E^{(s)}(x,t) = 2\left(\frac{2}{\pi}\right)^{1/2} E_{(o)}\, u^{(n)} \left(\frac{\omega_o}{c}\right)^2 \frac{|\varepsilon_r(\omega_o)|^{3/2}}{\left[|\varepsilon_r(\omega_o)|-1\right]^{3/2} \left[|\varepsilon_r(\omega_o)|+1\right]}$$

$$x\ \mathrm{Re}\left\{ i\,\sigma\, T(\omega_o) \int_{-\infty}^{+\infty} d\omega\; e^{-\frac{1}{2}\sigma^2(\omega-\omega_o)^2}\, e^{i[k_s(\omega)x-\omega t]} \right. \qquad \text{(B-20)}$$

$$\left. x\ \frac{\sin\left[\left\{k_s(\omega)-k_{\parallel}^{(n)}\right\}\frac{L}{2}\right]}{\left[k_s(\omega)-k_{\parallel}^{(n)}\right]} \right\} ,$$

In essence, the expression in Eq. (B-20) is our principal result. In it, $k_s(\omega)$ is that root of Eq. (B-18) with $\mathrm{Im}(k_s(\omega))>0$. We shall examine the shape of the output pulse through study of the structure of the integrand in the next section of this paper. We conclude this section by casting the result in a more useful form. As it stands presently, the integral over ω in Eq. (B-20) would be rather tricky to evaluate by numerical methods.

To make the notation simpler, define

$$t(\omega_o) = \frac{|\varepsilon_r(\omega_o)|^{3/2}}{\left[|\varepsilon_r(\omega_o)|-1\right]^{3/2}\left[|\varepsilon_r(\omega_o)|+1\right]}\, T(\omega_o) \qquad (B-21)$$

and split the sin up into complex exponentials to write Eq. (B-20) in the form

$$E^{(s)}(x,t) = \left(\frac{2}{\pi}\right)^{1/2} E_{(o)}\, u^{(n)}\left(\frac{\omega_o}{c}\right)^2$$

$$\times \mathrm{Re}\left\{ \sigma\, t(\omega_o) \sum_{\mu=\pm 1} \mu\, e^{-i\mu \frac{\pi n L}{d}} \int_{-\infty}^{+\infty} \frac{d\omega}{k_s(\omega)-k_{\mu}^{(n)}}\, e^{-\frac{1}{2}\sigma^2(\omega-\omega_o)^2} \right. \qquad (B-22)$$

$$\left. \times\, e^{i\left[k_s(\omega)x_\mu - \omega t_\mu\right]} \right\}$$

where we have introduced

$$x_\mu = x + \mu\,\frac{L}{2} \qquad (B-23a)$$

$$t_\mu = t + \frac{L\sin\theta_o}{2c}\,\mu \quad . \qquad (B-23b)$$

Now we have $\mathrm{Im}\left(k_s(\omega)\right)>0$, as remarked earlier. We may then write

$$\frac{1}{k_s(\omega)-k_{\parallel}^{(n)}} = i\int_0^{\infty} ds\; e^{is\left[k_s(\omega)-k_{\parallel}^{(n)}\right]} \qquad (B-24)$$

so that, introducing

$$\xi_\mu(s) = x_\mu + s \qquad (B-25a)$$

$$\tau_\mu(s) = t_\mu + \frac{s}{c}\sin\theta_o \quad , \qquad (B-25b)$$

we have

$$E^{(s)}(x,t) = \left(\frac{2}{\pi}\right)^{1/2} E_{(o)}\; u^{(n)} \left(\frac{\omega_o}{c}\right)^2$$

$$x\ \mathrm{Re}\left\{ i\,\sigma\, t(\omega_o) \sum_{\mu=\pm 1} \mu\, e^{-i\frac{\pi nL}{d}} \int_0^{\infty} ds\; e^{-i\frac{2\pi ns}{d}} \right. \qquad (B-26)$$

$$\left. x \int_{-\infty}^{\infty} d\omega\; e^{-\frac{1}{2}\sigma^2(\omega-\omega_o)^2}\; e^{i\left[k_s(\omega)\xi_\mu(s)-\omega\tau_\mu(s)\right]} \right\} \quad .$$

Next examine the integral over ω. Upon writing $\omega=\omega_o+\Omega$, this integral becomes

$$I = e^{-i\omega_o\,\tau_\mu(s)} \int_{-\infty}^{+\infty} d\Omega\; e^{-\frac{1}{2}\sigma^2\,\Omega^2}\; e^{i\,k_s(\omega_o+\Omega)\,\xi_\mu(s)}\; e^{-i\Omega\,\tau_\mu(s)} \quad . \qquad (B-27)$$

Again with the presumption that the incident pulse is composed of a reasonably small spectrum of frequencies, we expand $k_s(\omega_o+\Omega)$ in a Taylor series about ω_o:

$$k_s(\omega_o+\Omega) = k_s(\omega_o) + \frac{1}{V_g}\Omega - \frac{1}{2}\beta\Omega^2 + -- \quad , \qquad (B-28)$$

where

$$\frac{1}{V_g} = \left(\frac{\partial k_s}{\partial \omega}\right)_{\omega_o} \qquad (B-29a)$$

$$\beta = -\left(\frac{\partial^2 k_s}{\partial \omega^2}\right)_{\omega_o} \qquad (B-29b)$$

In general, note that V_g and β are complex numbers, although they become real when $\varepsilon(\omega)$ is real.

After the expansion displayed in Eq. (B-28) is used, the integral over Ω in Eq. (B-27) is readily evaluated. We write the result

$$I = \frac{(2\pi)^{\frac{1}{2}}}{\sigma_\mu(s)} \; e^{i\phi_\mu(s)} \exp\left[-\frac{T_\mu^2(s)}{2\sigma_\mu^2(s)}\right] \qquad (B-30)$$

where

$$\phi_\mu(s) = k_s(\omega_o)\, \xi_\mu(s) - \omega_o\, \tau_\mu(s) \quad , \qquad (B-31a)$$

$$\sigma_\mu^2(s) = \sigma^2 + i\,\beta\,\xi_\mu(s) \quad , \qquad (B-31b)$$

$$T_\mu(s) = \tau_\mu(s) - \frac{1}{V_g}\,\xi_\mu(s) \quad . \qquad (B-31c)$$

Then after some algebra, the pulse generated by the grating has the form, with

$$t(\omega_o) = |t(\omega_o)|\, \exp(i\delta) \quad , \qquad (B-32)$$

$$E^{(s)}(x,t) = 2\, E_{(o)}\, u^{(n)} \left(\frac{\omega_o}{c}\right)^2 |t(\omega_o)|$$

$$\times\, \mathrm{Re}\left\{ i\,\sigma \sum_\mu \mu\, e^{-i\mu \frac{\pi n L}{d}}\, e^{i\left[k_s(\omega_o)\, x_\mu - \omega_o\, t_\mu + \delta\right]} \right.$$

$$\times \int \frac{ds}{\sigma_\mu(s)} \; e^{is\left[k_s(\omega_o) - k_{\shortparallel}^{(on)}\right]} \quad \exp\left[-\frac{T_\mu^2(s)}{2\sigma_\mu^2(s)}\right] \Bigg\} \quad , \qquad (B\text{-}33)$$

where we have

$$k_{\shortparallel}^{(on)} = \frac{\omega_o}{c} \sin\theta_o + \frac{2\pi n}{d} \quad . \qquad (B\text{-}34)$$

To write out $\sigma_\mu(s)$ and $T_\mu(s)$ explicitly we have

$$\sigma_\mu^2(s) = \sigma^2 + i\,\beta\, x_\mu + i\,\beta\, s \qquad (B\text{-}35a)$$

$$T_\mu(s) = \left(t_\mu - \frac{1}{V_g} x_\mu\right) - \frac{s}{V_g}\left(1 - \frac{V_g}{c}\sin\theta_o\right) \quad . \qquad (B\text{-}35b)$$

It is possible to simplify Eq. (B-33) considerably through further algebraic manipulations. To do this, define

$$\Delta k_{\shortparallel}(\omega_o) = k_s(\omega_o) - k_{\shortparallel}^{(on)} \quad , \qquad (B\text{-}36)$$

and note that one may write

$$k_s(\omega_o)\, x_\mu - \omega_o\, t_\mu - \mu\,\frac{\pi n L}{d} = k_s(\omega_o)\, x - \omega_o\, t + \frac{1}{2}\,\Delta k_{\shortparallel}(\omega_o)\,\mu\, L \quad . \qquad (B\text{-}37)$$

We also have

$$T_\mu(s) = t - \frac{x}{V_g} - \frac{1}{\tilde{V}_g}\left(s + \frac{1}{2}\,\mu\, L\right) \quad , \qquad (B\text{-}38a)$$

and

$$\sigma_\mu^2(s) = \sigma^2 + i\,\beta\left[x + s + \frac{1}{2}\,\mu\,\frac{L}{2}\right] \quad , \qquad (B\text{-}38b)$$

where

$$\tilde{V}_g = V_g\left[1 - V_g \sin\theta_o/c\right]^{-1} \quad . \qquad (B\text{-}38c)$$

Now if in each term in the sum over μ in Eq. (B-33) we write

$$\xi = s + \frac{1}{2}\mu L \quad , \tag{B-39}$$

then Eq. (B-33) becomes

$$E^{(s)}(x,t) = 2 E_{(o)} u^{(n)} \left(\frac{\omega_o}{c}\right)^2 |t(\omega_o)| \quad \mathrm{Re}\left\{ i \sigma e^{i\left[k_s(\omega_o) x - \omega_o t + \delta\right]} \right.$$

$$\left. x \sum_{\mu} \mu \int_{\frac{1}{2}\mu L}^{\infty} \frac{d\xi\, e^{i\xi\Delta k_n}}{\sigma(\xi)} \exp\left[-\frac{T^2(\xi)}{2\sigma^2(\xi)}\right] \right\} \tag{B-40}$$

where

$$T(\xi) = t - \frac{x}{V_g} - \frac{\xi}{\tilde{V}_g} \tag{B-41a}$$

and

$$\sigma^2(\xi) = \sigma^2 + i\,\beta[x+\xi] \quad . \tag{B-41b}$$

In Eq. (B-40), the sum on μ may be carried out explicitly to yield, after we let

$$\xi = \frac{1}{2} L \eta \quad , \tag{B-42}$$

$$E_s(x,t) = \frac{1}{2} E_{(o)} f\, \mathrm{Re}\left\{ i \sigma e^{i\left[k_s(\omega_o)x - \omega_o t + \delta\right]} \right.$$

$$\left. x \int_{-1}^{+1} \frac{d\eta}{\sigma(\eta)} e^{i\eta \frac{\Delta k_n L}{2}} \exp\left[-\frac{T^2(\eta)}{2\sigma^2(\eta)}\right] \right\} \quad . \tag{B-43}$$

where we define

$$f = 2 u^{(n)} L \left(\frac{\omega_o}{c}\right)^2 |t(\omega_o)| \quad . \tag{B-44}$$

The form in Eq. (B-43) should prove most convenient for numerical studies of the pulse shape, since the integral that remains covers only the finite interval from -1 to +1. In Eq. (B-43), we have

$$T(\eta) = \left(t - \frac{x}{V_g}\right) - \frac{1}{2}\,\frac{L}{\tilde{V}_g}\,\eta \qquad (B\text{-}45a)$$

and

$$\sigma^2(\eta) = \sigma^2 + i\,\beta\left[x + \frac{1}{2}L\eta\right] \quad . \qquad (B\text{-}45b)$$

It is difficult to obtain a feeling for the shape of the output pulse from the general form of Eq. (B-33). We see, however, that the output pulse can be regarded as a linear superposition of a series of chirped output pulses. The question that remains is to decide when the output pulse has a shape that reflects the frequency composition of the input pulse, and how it is modified if it does not. We address this question in Section C , through analysis of the general results here, and appeal to a simple limiting case.

C . The Frequency Spectrum of the Output Pulse; General Remarks and a Specific Example

We first consider the frequency spectrum of the output pulse, by examining the general structure of the results in section B . For this discussion, the expression in Eq. (B -20) will prove particularly useful.

Let us first inquire into the conditions under which the frequency spectrum of the surface polariton pulse launched from the grating is identical to that of the input pulse. If we examine the structure of Eq. (B -20), then we see that if L is sufficiently small, the frequency spectrum of the output pulse mimics that of the input pulse. In particular, begin by considering the extreme case where we take the li...it $L \to 0$. Regard this as a formal mathematical exercise at the moment.

As $L \to 0$, we make the replacement

$$\frac{\sin\left[(k_s(\omega)-k_{\parallel}^{(n)})\,\frac{L}{2}\right]}{\left[k_s(\omega)-k_{\parallel}^{(n)}\right]} \longrightarrow \frac{L}{2} \quad . \qquad (C-1)$$

Then Eq. (B -20) reads

$$E^{(s)}(x,t) = L\left(\frac{2}{\pi}\right)^{\frac{1}{2}} E_{(o)}\, u^{(n)} \left(\frac{\omega_o}{c}\right)^2 \frac{|\varepsilon_R(\omega_o)|^{3/2}}{\left[|\varepsilon_R(\omega_o)|-1\right]^{3/2}\left[|\varepsilon_R(\omega_o)|+1\right]}$$

$$\times\ \mathrm{Re}\left\{\sigma\, T(\omega_o) \int_{-\infty}^{+\infty} d\omega\, e^{-\frac{1}{2}\sigma^2(\omega-\omega_o)^2}\, e^{i[k_s(\omega)x-\omega t]}\right\} \quad . \qquad (C-2)$$

Quite clearly, near the grating ($x \to 0$), the frequency spectrum of the transmitted pulse is identical to that of the input pulse. As the

surface polariton pulse propagates down the grating, it will either be compressed or it will expand, depending on how the input pulse is chirped, and the detailed form of $k_s(\omega)$. The integral over ω in Eq. (C -2) is readily evaluated if the expansion for $k_s(\omega)$ in Eq. (B -28) is used. The algebra is identical to that in the recent study of pulse compression through coupling to bulk polaritons.[9] Note that it is convenient to break $T(\omega_o)$ up into a amplitude and phase, as in Eq. (B -32). One then sees that the phase angle in $T(\omega_o)$ appears simply as a constant phase shift in the output wave which does not affect the shape of the envelope.

The next step is to inquire into the criterion that must be satisfied for the use of the limit $L \to 0$ in the calculation of the output pulse shape. This condition is simply obtained.

We suppose the incident beam directed so the grating is driven at maximum efficiency. This requires the condition

$$k_s(\omega_o) = k_{\shortparallel}^{(on)} = \frac{\omega_o}{c} \sin\theta_o + \frac{2\pi n}{d} \qquad (C\text{-}3)$$

to be satisfied, or that the quantity $\Delta k_{\shortparallel}$ defined in Eq. (B-36) vanish. We presume this to be the case in what follows.

Now the width of the pulse in the frequency domain is clearly $|\sigma|^{-1}$, and we expect $\omega_o|\sigma| >> 1$. Then we make the replacement in Eq. (B -20)

$$\left(k_s(\omega) - k_{\shortparallel}^{(n)}\right) \cong k_s(\omega_o) - k_{\shortparallel}^{(on)} + (\omega-\omega_o)\frac{1}{V_g}\left(1 - \frac{V_g}{c}\sin\theta_o\right)$$

$$= (\omega-\omega_o)\frac{1}{V_g}\left(1 - \frac{V_g}{c}\sin\theta_o\right) \quad . \qquad (C\text{-}4)$$

The quantity $k_{\shortparallel}^{(on)}$ is defined in Eq. (B-34) , and the last statement follows from

Eq. (C -3). Now we see the limit $L \to 0$ is appropriate so long as the inequality

$$\frac{L}{|\sigma| V_g}\left(1-\frac{V_g}{c}\sin\theta_o\right) << 1 \qquad (C-5)$$

is satisfied. Or in terms of the quantity $\tilde{V}_g$ introduced in Eq. (B -38c), we may write the inequality in the form

$$L << |\sigma|\tilde{V}_g \quad . \qquad (C-6)$$

Note that since one will operate the grating in a frequency regime where V_g is less than c by a fair amount, if signal processing via surface polaritons is of interest, we shall have $\tilde{V}_g \cong V_g$ in this instance.

The criterion displayed in Eq. (C -6) is the principal limit on operating conditions of the grating coupler, if one wishes to produce a surface polariton pulse which faithfully reproduces the frequency spectrum of the input pulse. This limit applies to a grating operated under conditions of optimal coupling, in the sense that we have presumed the criterion in Eq. (C -3) has been met. If the criterion is not met precisely, the conclusions here remain applicable if the condition

$$L\left|k_s(\omega_o) - \frac{\omega_o}{c}\sin\theta_o - \frac{2\pi n}{d}\right| << 1 \qquad (C-7)$$

is obeyed.

One can obtain a clear feeling for the nature of the transmitted pulse by plotting the two principal factors in the integrand of Eq. (B -20), for the two cases $L << \tilde{V}_g|\sigma|$ and the opposite limit $L >> \tilde{V}_g|\sigma|$. We do this in Figure (2). The function $\sin\left[\left(k_s(\omega)-k_{\parallel}^{(n)}\right)\frac{L}{2}\right]\Big/\left[k_s(\omega)-k_{\parallel}^{(n)}\right]$ describes the response of the grating to the incident beam. As one can see from Figure 2(a), when $L << |\sigma|\tilde{V}_g$, one may

regard the grating response as flat, over the frequency regime appropriate to the input pulse. The frequency distribution in the surface polariton pulse generated by the grating then reflects that of the input pulse quite directly. On the other hand, when $L>>|\sigma|\tilde{V}_g$, as one sees from Figure 2(b), the spectral width of the pulse is broad compared to the frequency spread of the incident beam. Then in this case, as is clear from Figure 2(b), only the central component of the input pulse is passed by the grating. Then the surface polariton pulse generated by the grating has a narrower frequency spectrum than the input pulse; in coordinate space, the surface polariton pulse is longer than it would be if the inequality were reversed (if one had $L<<|\sigma|\tilde{V}_g$).

We next illustrate these points by considering a simple limiting case of the general formulae above. For simplicity, suppose we have a gaussian unchirped pulse incident on the grating. Then the quantity λ in Eq. (B-3) vanishes, while σ in Eq. (B-5b) reduces to σ_o. Suppose further we neglect the quadratic term in Eq. (B-28) by setting the coefficient β equal to zero. Then Eq. (B-43) becomes

$$E_s(x,t) = \frac{1}{2} E_{(o)} fLRe \left\{ e^{i[k_s(\omega_o)x-\omega_o t+\delta]} \right.$$
$$\left. x \int_{-1}^{+1} d\eta \, e^{i \frac{\eta \Delta k_{\parallel} L}{2}} \exp\left[- \frac{T^2(\eta)}{2\sigma_o^2} \right] \right\} \quad . \qquad (C-8)$$

If we let

$$\zeta = t - \frac{x}{V_g} \quad , \qquad (C-9)$$

then

$$E_s(x,t) = \frac{1}{2} E_{(o)} \; f \; Re \left\{ e^{i[k_s(\omega_o)x-\omega_o t+\delta]} \right.$$

$$x \int_{-1}^{+1} d\eta \; e^{+i \frac{\eta \Delta k_{\parallel} L}{2}} \exp\left[-\frac{1}{2\sigma_o^2} \left(\zeta - \frac{1}{2} \frac{L}{\tilde{V}_g} \eta \right)^2 \right] \Bigg\} \quad . \qquad (C\text{-}10)$$

For the moment, we presume the grating is operated sufficiently close to optimal coupling that the condition in Eq. (C-7) is satisfied. In the notation of Eq. (C-10), this becomes $\Delta k_{\parallel} L << 1$. In this limit the factor $\exp\left[+i \frac{\eta \Delta k_{\parallel} L}{2}\right]$ may be set to unity. Later in the section, we investigate the role of this factor, when it is retained.

The next step is to rewrite the integral over η through the identity

$$\int_{-1}^{+1} d\eta \; f(\eta) = \int_{-1}^{\infty} d\eta \; f(\eta) - \int_{1}^{\infty} d\eta \; f(\eta) \quad . \qquad (C\text{-}11)$$

Then the expression that results may be expressed in terms of the error function erf(x), defined by

$$\mathrm{erf}(x) = \frac{2}{\sqrt{\pi}} \int_0^x ds \; \exp(-s^2) \quad . \qquad (C\text{-}12)$$

We find the result

$$E^{(s)}(x,t) = \left(\frac{\pi}{2}\right)^{\frac{1}{2}} \frac{E_o \, f}{\Delta} \sin\left[k_s(\omega_o)x - \omega_o t + \delta\right]$$

$$x \left\{ \mathrm{sgn}\left(\zeta + \tfrac{1}{2}\sigma_o\Delta\right) \mathrm{erf}\left(\frac{\left|\zeta + \frac{1}{2}\sigma_o\Delta\right|}{\sqrt{2}\,\sigma_o} \right) \right. \qquad (C\text{-}13)$$

$$\left. -\mathrm{sgn}\left(\zeta - \tfrac{1}{2}\sigma_o\Delta\right) \mathrm{erf}\left(\frac{\left|\zeta - \frac{1}{2}\sigma_o\Delta\right|}{\sqrt{2}\,\sigma_o} \right) \right\} \quad ,$$

where we have introduced

$$\Delta = \frac{L}{\sigma_o \tilde{V}_g} \qquad (C\text{-}14a)$$

and we remind the reader that

$$\zeta = t - \frac{x}{V_g} \quad . \qquad (C\text{-}14b)$$

The expression in Eq. (C-13) describes a surface polariton pulse, with frequency ω_o and wave vector $k_s(\omega_o)$. The expression in curly brackets describes the envelope of the signal, which propagates with the group velocity V_g. The envelope remains undistorted as it propagates; this is a consequence of the fact that we set the curvature parameter $\beta=0$. Quite clearly, the shape of the envelope is controlled by the ratio $\Delta=L/(\sigma_o \tilde{V}_g)$, as our earlier argument suggests. We explore the two limits $\Delta<<1$ (where our earlier argument suggests the information in the incident pulse is transmitted fully to the surface polariton) and the limit $\Delta>>1$ (where the incident pulse should be lengthened.)

(i) The limit $L<<\sigma_o \tilde{V}_g$:

Here the quantity in curly brackets may be expanded, with the first order term in L retained. One finds the simple result

$$E^{(s)}(x,t) = f\, E_{(o)} \exp\left[-\frac{\zeta^2}{2\sigma_o^2}\right] \sin\left[k_s(\omega_o)x - \omega_o t + \delta\right] \quad . \qquad (C\text{-}15)$$

This describes a gaussian pulse transmitted to the substrate undistorted by the grating. Our approximations in deriving this result ignore subsequent expansion or contraction of the pulse by the curvature in the surface polariton dispersion relation. The gaussian pulse propagates with the group velocity V_g of the surface polariton.

One by-product of the present analysis is an expression for the absolute amplitude of the surface polariton which propagates on the free substrate, to the right of the area illuminated by the incident beam. Despite the number of recent investigations of the interaction of radiation with surface roughness or small amplitude structures on the surface, we have not seen such an expression derived. From Eq. (C -15), we see the ratio of the transmitted surface polariton pulse to that of the incident pulse is given by the factor f defined in Eq. (B -44). It is convenient to note that the expression for f may be rewritten to read

$$f = 2u^{(n)}\, L \left(\frac{\omega_o}{c}\right)^2 \frac{|\varepsilon|^{\frac{3}{2}} \left[\sqrt{|\varepsilon|+\sin^2\theta_o} - |\varepsilon|^{\frac{1}{2}} \sin\theta_o\right]}{\left[|\varepsilon|-1\right]^2 \left[|\varepsilon|+1\right]^{\frac{1}{2}} \left[|\varepsilon|\cos^2\theta_o+\sin^2\theta_o\right]^{\frac{1}{2}}} \quad . \qquad (C\text{-}16)$$

The expressions in Eq. (C -15) and Eq. (C -16) may be used to calculate the absolute efficiency of a grating ruled on a substrate, in the approximation that the amplitude of the grating is regarded as small. Note, as described at the beginning of this discussion, Eq. (C -15) relates the amplitude of the component of the incident field parallel to the substrate $\left(E_{(o)}\right)$ to the component of the electric field in the surface polariton parallel to the surface. The complete field of the surface polariton can be constructed by using this information in combination with Maxwell's equations

(ii) The Limit $L \gg \sigma_o \tilde{V}_g$

For general values of $L/\sigma_o \tilde{V}_g$, the electric field set up by a gaussian input pulse is given by Eq. (C -13), under the conditions used to obtain the result. To consider the limit $L \gg \sigma_o \tilde{V}_g$, introduce the coordinate

$$\bar{x} = x - V_g t \quad , \qquad (C\text{-}17a)$$

and let

$$r = V_g/\tilde{V}_g \qquad (C-17b)$$

Then except very near the ends of the pulse, when $L>>\sigma_o\tilde{V}_g$ we can make the replacement

$$\mathrm{sgn}\left(\zeta + \frac{1}{2}\sigma_o\Delta\right)\,\mathrm{erf}\left(\frac{\left|\zeta + \frac{1}{2}\sigma_o\Delta\right|}{\sqrt{2}\ \sigma_o}\right)$$

$$- \mathrm{sgn}\left(\zeta - \frac{1}{2}\sigma_o\Delta\right)\,\mathrm{erf}\left(\frac{\left|\zeta - \frac{1}{2}\sigma_o\Delta\right|}{\sqrt{2}\ \sigma_o}\right) \qquad (C-18)$$

$$\sim 2\,\Theta\left(\frac{1}{2}rL - \bar{x}\right)\Theta\left(\bar{x} + \frac{1}{2}rL\right) \quad .$$

The envelope of the pulse is now "square". Actually, the envelope does not jump discontinuously zero to unity at $\bar{x}=-r\frac{L}{2}$, and from unity to zero at $\bar{x}=+r\frac{L}{2}$. Rather, consideration of the full form in Eq. (C-13) shows the envelope makes a gradual transition from zero to unity over a region with spatial extent $\Delta\bar{x}=\sigma_o\tilde{V}_g<<L$.

Then with Eq. (C-18), except near the ends of the envelope, when $\sigma_o\tilde{V}_g<<L$ we have

$$E^{(s)}(x,t) = (2\pi)^{\frac{1}{2}}\left(\frac{\sigma_o\tilde{V}_g}{L}\right) f\, E_{(o)}\ \Theta\left(\frac{1}{2}rL - \bar{x}\right)\Theta\left(\bar{x} + \frac{1}{2}rL\right)$$

$$x\,\sin[k_s(\omega_o)x - \omega_o t + \phi] \quad . \qquad (C-19)$$

We call attention to two figures which serve to illustrate the results obtained above. In Figure 3(a) and Figure 3(b), we sketch the shape of the pulse generated by the grating for the two cases $L<<\sigma_o\tilde{V}_g$ and $L>>\sigma_o\tilde{V}_g$. In Figure (4), we plot the amplitude of the peak field in the transmitted pulse as a function of L. When

$L<\sigma_o \tilde{V}_g$, the amplitude increases linearly with L, to saturate at a value independent of L when $\sigma_o \tilde{V}_g << L$.

We conclude by exploring the effect of retaining a finite value for the parameter $\Delta k_{\parallel} L$, which was assumed very small compared to unity in the discussion above. We shall be able to explore the influence of this parameter only for the limiting value $\Delta k_{\parallel} L >> 1$, but the results give an intuitive feeling for the role of this parameter. Further investigation may employ the full form in Eq. (B-43), with the integral evaluated numerically. As before, in the present discussion, we assume an unchirped incident pulse ($\lambda=0$), and set $\beta=0$ also.

We begin with Eq. (B-43), and let

$$\tau = \frac{(t-x/V_g)}{\sqrt{2}\ \sigma_o} \quad , \qquad (C-20)$$

and we then switch the integration variable to

$$x = \frac{\eta}{2\sqrt{2}} \Delta = \frac{\eta}{2\sqrt{2}} \frac{L}{\sigma_o \tilde{V}_g} \quad . \qquad (C-21)$$

Then finally we let

$$p = \frac{\sigma_o \tilde{V}_g}{\sqrt{2}} \Delta k_{\parallel} \qquad (C-22)$$

to write the integral in Eq. (B-43) in the form

$$E_s(x,t) = \sqrt{2}\ E_{(o)} \frac{f}{\Delta} \mathrm{Re} \left\{ i \exp[ik_s(\omega_o)x - \omega_o t + \delta] \right.$$

$$\left. \times \int_{-\frac{\Delta}{2\sqrt{2}}}^{+\frac{\Delta}{2\sqrt{2}}} dx \exp\left[-(x-\tau)^2\right] \exp\left[ipx\right] \right\} \quad . \qquad (C-23)$$

Suppose now we consider the limit $\Delta<<1$, where when $\Delta k_{\shortparallel} L<<1$, we found the transmitted and incident pulse had the same shape. When $\Delta<<1$, in Eq. (C -23) the integration variable in Eq. (C -23) is confined to values small compared to unity, so we may write

$$\exp\left[-(x-\tau)^2\right] \tilde{=} \exp\left[-\tau^2+2x\tau\right] \quad . \qquad (C-24)$$

The integral is then readily evaluated to give

$$E_s(x,t) = E_{(o)}\, f \exp\left[-\tau^2\right] \left\{ \frac{2\sin\left[\frac{1}{2}\Delta k_{\shortparallel} L\right]}{\Delta k_{\shortparallel} L} \right\} \sin[k_s(\omega_o)x-\omega_o t+\delta] \quad . \qquad (C-25)$$

This expression is identical to that in Eq. (C -15), save for the appearance of the factor in curly brackets. Thus, when $\Delta<<1$, and $\Delta k_{\shortparallel} L$ is not small compared to unity, if one works off the peak in the grating response E_s is reduced in amplitude by the factor in curly brackets, but remains undistorted.

Now consider the opposite limit $\Delta>>1$. In this limit, if we presume we wish to consider finite values of τ, then the upper and lower limits of the integration in Eq. (C -23) may be replaced by $+\infty$ and $-\infty$, respectively. Again the integration may be carried out in closed form to give

$$E_s(x,t) = (2\pi)^{\frac{1}{2}} E_{(o)} \frac{f}{\Delta} \exp\left[-p^2\right] \quad \sin\left[k_s(\omega_o)x+2p\tau-\omega_o t+\delta\right] \qquad (C-26)$$

Or, to write out the explicit form of the argument of the sin function,

$$E_s(x,t) = (2\pi)^{\frac{1}{2}} E_{(o)} \frac{f}{\Delta} \exp\left[-p^2\right]$$

$$x \quad \sin\left[\left(k_s(\omega_o) - \frac{\tilde{v}_g}{v_g^2}\Delta k_{\shortparallel}\right)x-(\omega_o-\tilde{v}_g\Delta k_{\shortparallel})t+\delta\right] \quad . \qquad (C-27)$$

This result may be compared with that in Eq. (C -19). The approximation here does not allow description of the near-vicinity of the ends of the pulse. It is appropriate only for the regime $|\bar{x}| < \frac{1}{2} rL$, in the notation of Eq. (C -19). We see from Eq. (C -19) that there are two effects that arise from the finiteness of $\Delta k_{\parallel}$. Firstly, the amplitude of the transmitted pulse is reduced by the factor $\exp\left[-p^2\right]$, and its wave vector and frequency are shifted away from $k_s(\omega_o)$ and ω_o, respectively.

D. Concluding Remarks

While the principal conclusions we have reached are summarized in the introductory remarks of Section A, it may prove useful to direct the reader's attention to particular results obtained through the analysis in Section B and Section C.

We consider conversion of an incident electromagnetic pulse to a surface polariton pulse through interaction of an incident pulse with a grating, as illustrated in Figure (1). The electric field has the time profile given in Eq. (B-3). A convenient and workable expression for the form of the transmitted pulse is provided by Eq. (B-43). To derive this expression, we have presumed $\sigma_o\omega_o << 1$, i.e., the frequency spectrum of the incident pulse has width small compared to ω_o. This and the assumption that the height of the grating structure is small are our principal assumptions.

In Section C, we show that, if L is the width of the grating exposed to the incident beam, then, when $L << |\sigma|\tilde{V}_g$, the transmitted pulse has a shape and spectral composition that accurately reflects that in the incident pulse. The quantity σ is defined by Eq. (B-5b), while $\tilde{V}_g$ is given in Eq. (B-38b).

A simple expression for the shape of the transmitted pulse obtains for general values of $|\sigma|\tilde{V}_g/L$, provided we assume the grating is driven close to the peak in its frequency response. The latter assumption requires that $\Delta k\, L << 1$, where Δk is defined in Eq. (B-36).

When $\Delta k_{\shortparallel} L << 1$, the shape of the transmitted pulse is displayed in Eq. (C-13). Special limiting forms are displayed in Eq. (C-15) (the limit $L << |\sigma|\tilde{V}_g$) and in Eq. (C-19) (the limit $L >> |\sigma|\tilde{V}_g$). We note these formulas display explicit expressions for the absolute amplitude of the transmitted pulse. These results allow the efficiency of the grating to be calculated.

Finally, when $\Delta k_{\parallel} L >> 1$ (the grating is operated far from the peak in its response), Eq. (C -25) and Eq. (C -27) provide expressions for the transmitted fields, in the limits $L << \tilde{V}_g |\sigma|$ and $L >> \tilde{V}_g |\sigma|$, respectively.

To derive the expressions in Eq. (C -15) and Eq. (C -19), along with Eq. (C -25) and Eq. (C -27), we have set the parameter λ in Eq. (B -3) equal to zero, in the interest of simplicity. Thus, these special forms apply to an unchirped incident pulse of gaussian profile. It is straightforward to generalize the results to the case $\lambda \neq 0$, if desired.

References

1. See Section X of the review article by D. L. Mills and E. Burstein, Reports on Progress in Physics 37, 817 (1974).

2. J. Schoenwald, E. Burstein and J. Elson, Solid State Communications 12, 185 (1973), J. D. McMullen, Solid State Communications 17, 331 (1975).

3. A chirped input pulse is one in which the carrier frequency is modulated to vary linearly with time. The electric field in such a pulse exhibits the time variation described in Eq. (B-3) of the present paper, if the envelope is gaussian. The virtue and utility of such pulses in microwave radar systems are described by J. R. Klauder, A. C. Price, S. Darlington and W. J. Albersheim, Bell System Technical Journal 39, 745 (1960). For a description of a method of "chirping" pulses at optical frequencies, see J. A. Giordmaine, M. A. Duguay and J. W. Hansen, IEEE J. Quantum Electronics, Vol. QE-4, p 252, May 1968.

4. The work is being performed by J. D. McMullen, with support from Contract DAHC04-74-C-0024, U. S. Army Research Office, Durham, NC.

5. J. M. Elson, J. Opt. Soc. Am. 66, 682 (1976).

6. D. L. Mills, Phys. Rev. B (to be published).

7. Actually, the dielectric constant $\varepsilon(\Omega)$ is complex, as is the wave vector $k_{\parallel}$ that emerges from Eq. (B-2), if we regard the frequency Ω as real. The remarks here presume $\varepsilon(\Omega)$ real for the moment; the calculations below take account of the effect of the imaginary part of $\varepsilon(\Omega)$, although for simplicity we shall subsequently presume the real part of $\varepsilon(\Omega)$ large compared to the imaginary part.

8. The term in $E(k_{\parallel} - \frac{2\pi n}{d}, \omega)$ proportional to $\exp\left[-\frac{1}{2}(\sigma^*)^2(\omega+\omega_o)^2\right]$ should be multiplied by $T(-\omega_o)$. One may show that $T(-\omega_o) = T^*(\omega_o)$.

9. J. D. McMullen (to be published).

FIGURE CAPTIONS

Figure (IV-1) The excitation geometry that forms the basis for discussion in the paper. The incident beam is presumed to illuminate a strip of the grating of width L.

Figure (IV-2) A plot of $\exp\left[-\frac{1}{2}\sigma^2(\omega-\omega_o)^2,\right]$ and $\sin\left[(k_s(\omega)-k_{\shortparallel}^{(n)})\frac{L}{2}\right] \Big/ \left[k_s(\omega)-k_{\shortparallel}^{(n)}\right]$, for the two cases (a) $L<<\tilde{V}_g|\sigma|$ and (b) $L>>\tilde{V}_g|\sigma|$. We assume here that σ is real, and in the figure, $\Delta k_{\shortparallel}=k_s(\omega)-k_{\shortparallel}^{(n)}$.

Figure (IV-3) The shape of the surface polariton pulse generated by the grating when (a) $L<<\sigma_o\tilde{V}_g$ and (b) $L>>\sigma_o\tilde{V}_g$.

Figure (IV-4) The value of the peak field in the transmitted pulse, as a function of L.

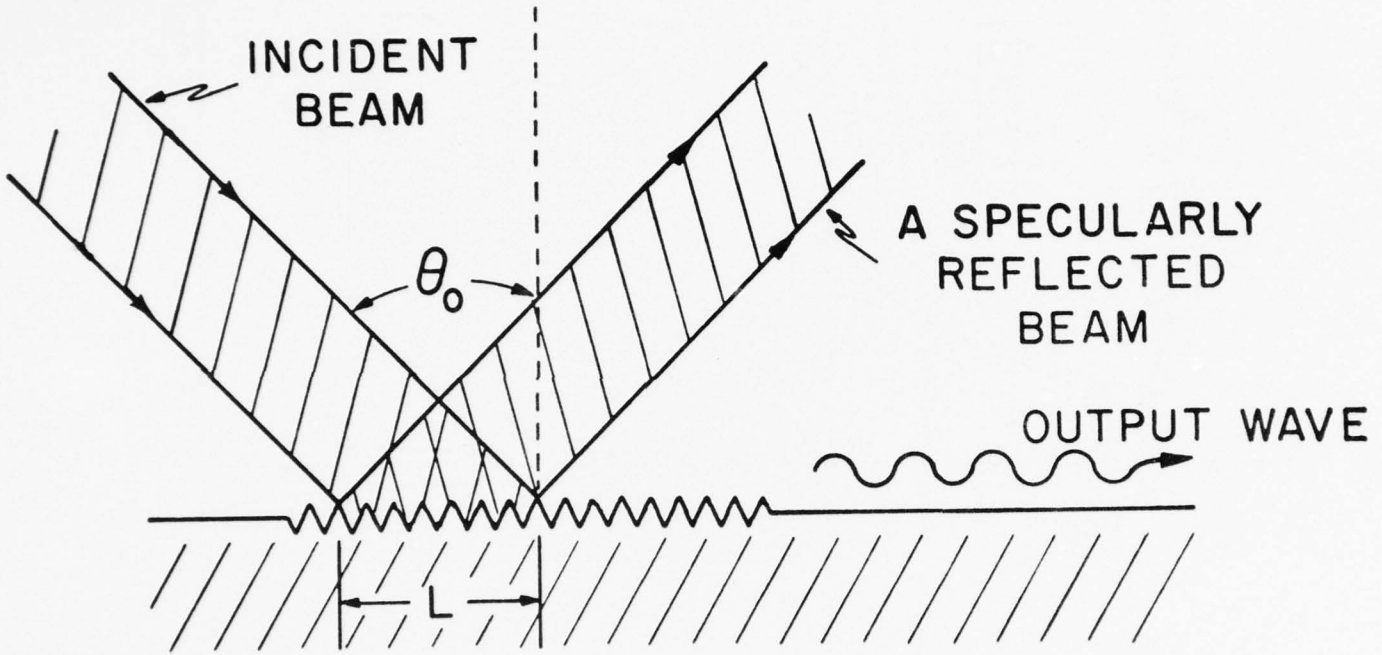
INCIDENT
BEAM
θ_o
A SPECULARLY
REFLECTED
BEAM
OUTPUT WAVE
L
SUBSTRATE, DIELECTRIC
CONSTANT $\mathcal{E}(\Omega)$

Figure IV-1

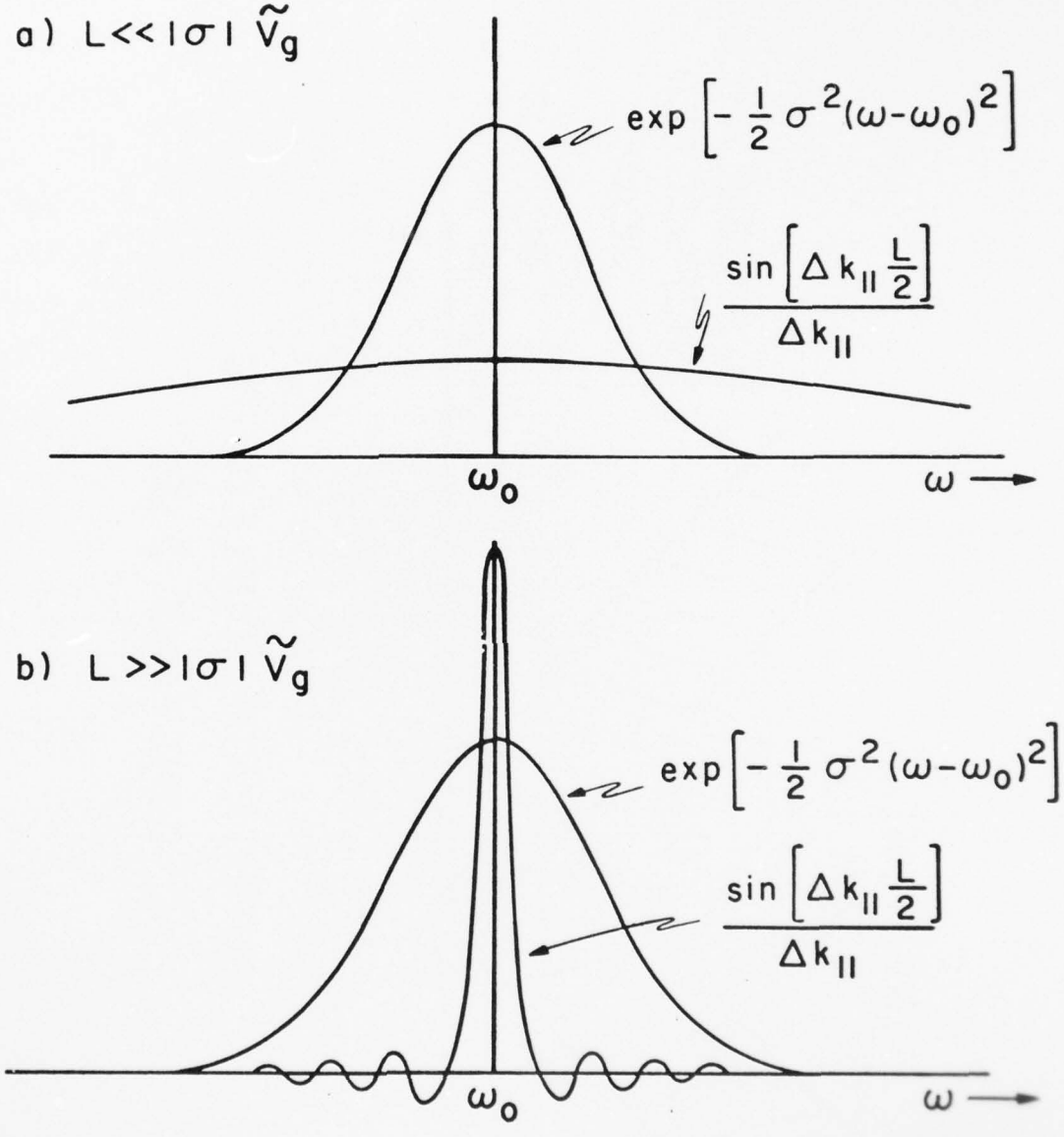
a) $L \ll |\sigma| \tilde{V}_g$
$\exp\left[-\frac{1}{2}\sigma^2(\omega-\omega_0)^2\right]$
$\frac{\sin\left[\Delta k_{\parallel}\frac{L}{2}\right]}{\Delta k_{\parallel}}$
ω_0
ω
b) $L \gg |\sigma| \tilde{V}_g$
$\exp\left[-\frac{1}{2}\sigma^2(\omega-\omega_0)^2\right]$
$\frac{\sin\left[\Delta k_{\parallel}\frac{L}{2}\right]}{\Delta k_{\parallel}}$
ω_0
ω

Figure IV-2

AD-A042 530 ROCKWELL INTERNATIONAL ANAHEIM CALIF F/G 17/9
INVESTIGATION OF SURFACE OPTICAL WAVES FOR OPTICAL SIGNAL PROCE--ETC(U)
JUN 77 J D MCMULLEN, D L MILLS DAHC04-74-C-0024
UNCLASSIFIED C77-464/501 ARO-12120.9P NL

2 OF 2
AD
A042530


END
DATE FILMED
8-77
DDC

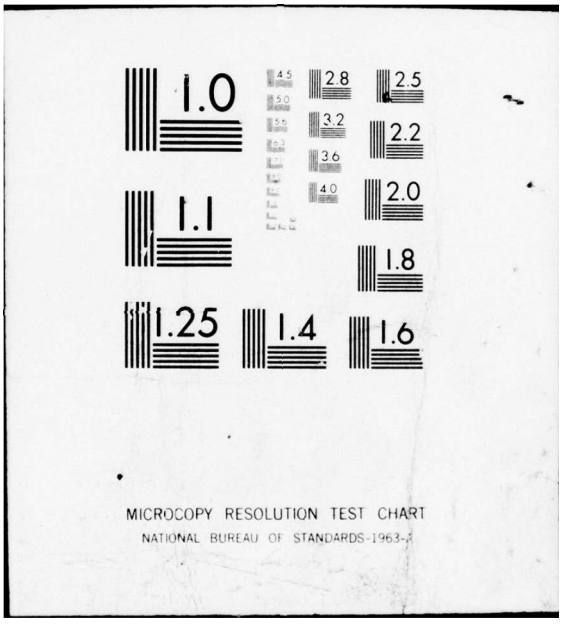
1.0
1.1
1.25
1.4
1.6
1.8
2.0
2.2
2.5
2.8
3.2
3.6
4.0
4.5
5.0
5.6
6.3
MICROCOPY RESOLUTION TEST CHART
NATIONAL BUREAU OF STANDARDS-1963-A

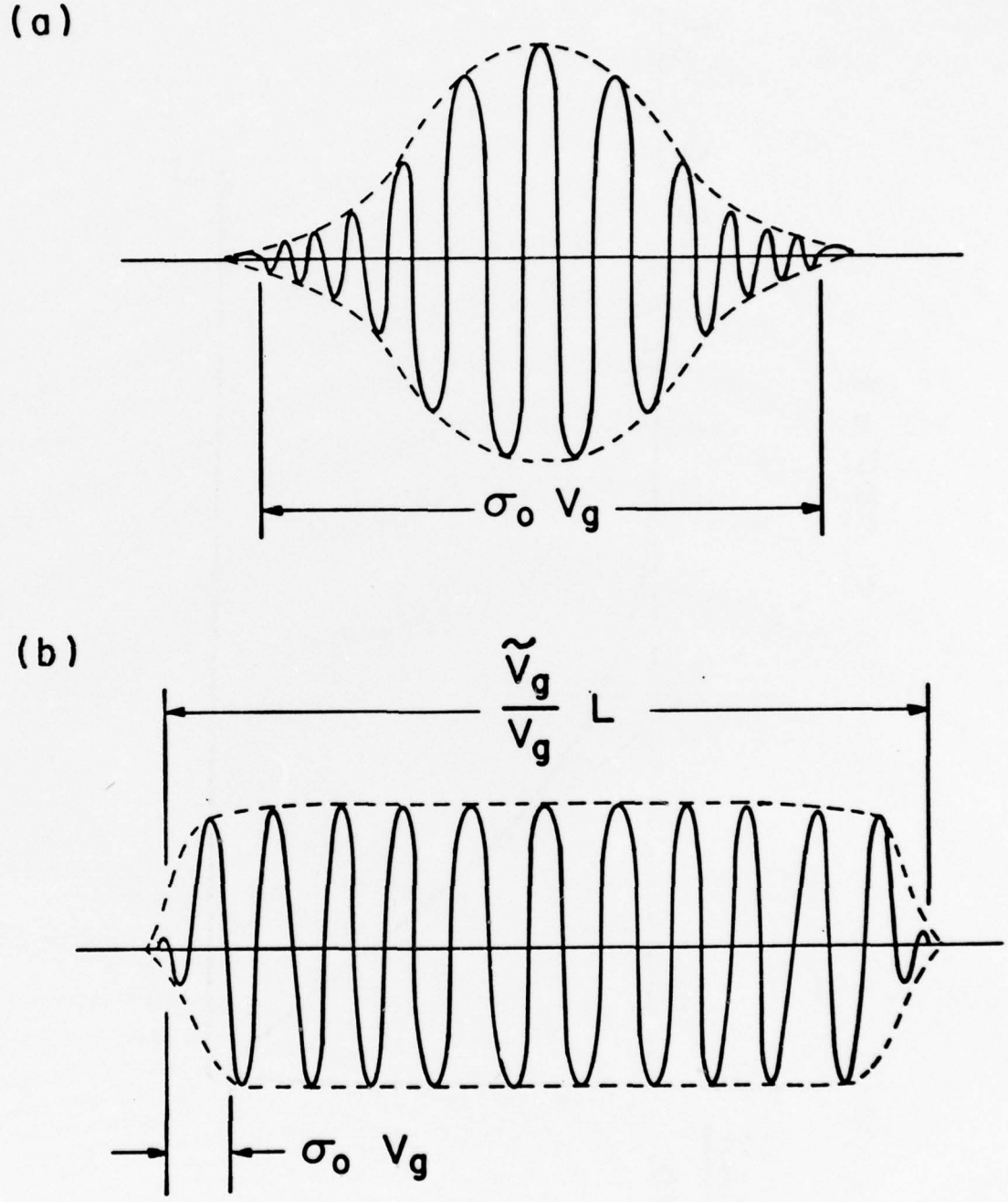

Figure IV-3

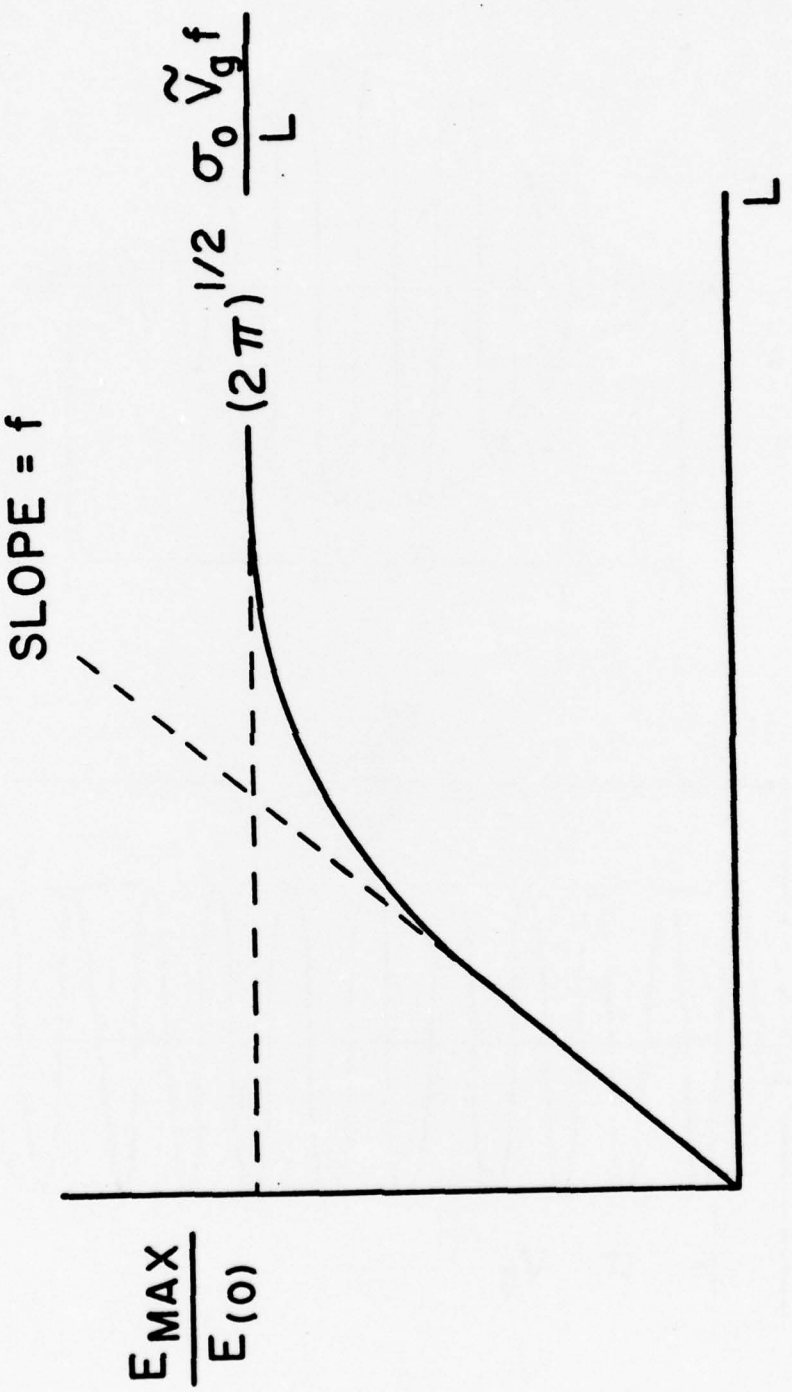

Figure IV-4

V. THEORY OF WAVE PROPAGATION IN A MEDIUM WITH TIME VARYING DIELECTRIC CONSTANT

D. L. Mills
Department of Physics
University of California, Irvine
Irvine, California 92717

General Information

One method of modifying the frequency composition of a laser pulse is to pass it through a medium with a dielectric constant that varies with time. The dielectric constant may be modulated by subjecting the medium to an external probe, such as an externally applied electric field or strain.

In these notes we examine the theory of propagation of pulses in such a medium and the interaction of incident radiation with it. Most discussions in the literature of pulse propagation in media with time-varying index of refraction are based on very simple formulae, and our aim here is to derive the results systematically. The main feature of the problem we exploit is the fact that in practical situations the time variation of the dielectric constant is slow on the time scale set by the carrier frequency of the laser pulse. In a typical case we may have 10.6 μ laser radiation (frequency 3×10^{13} Hz) which passes through a material with dielectric constant modulated by an external field at megacycle frequencies.

For simplicity, we consider a material that (in the presence of the external field that modulates the dielectric constant) is uniaxial, with the electric field vector in the laser pulse directed along a principal direction. These assumptions are made here for convenience, and the treatment is readily generalized to propagation in a medium with time-varying dielectric constant of tensor character, with electric field in the pulse of arbitrary polarization.

For the simple configuration described in the preceding paragraph, the electric field $E(x,t)$ and displacement field $D(x,t)$ are quite generally linked by the wave equation

$$\frac{\partial^2 E(x,t)}{\partial x^2} - \frac{1}{c^2} \frac{\partial^2 D(x,t)}{\partial t^2} = 0. \tag{1}$$

We presume the magnetic permeability of the material equals unity, and then the relation in Eq. (1) is independent of the manner in which $D(x,t)$ and $E(x,t)$ are related.

We assume that $D(x,t)$ and $E(x,t)$ are linked through the relation

$$D(x,t) = \varepsilon(t)\, E(x,t) \tag{2}$$

where $\varepsilon(t)$ is the dielectric constant that depends on time by virtue of the external field.

We eliminate $E(x,t)$ from Eq. (1) and find the equation satisfied by $D(x,t)$. This leads us to

$$\frac{\partial^2 D(x,t)}{\partial x^2} - \frac{\varepsilon(t)}{c^2} \frac{\partial^2 D(x,t)}{\partial t^2} = 0, \tag{3}$$

an equation which admits solutions of separable form:

$$D(x,t) = e^{ikx} d_k(t) , \tag{4}$$

where $d_k(t)$ satisfies

$$\frac{\partial^2 d_k(t)}{\partial t^2} + \frac{c^2k^2}{\varepsilon(t)}\, d_k(t) = 0 \quad . \tag{5}$$

We begin by studying the separable solutions displayed in Eq. (4), and then we examine the theory of pulse propagation in the presence of the time-varying index.

The structure of Eq. (5) is identical to the time-independent form of the Schrödinger equation which describes motion of a particle in a spatially varying potential. To see the correspondence, we replace the time variable t in Eq. (5) by the spatial coordinate x, $d_k(t)$ by $\Psi_E(x)$, the wave function of a particle of energy E, and finally $c^2k^2/\varepsilon(t)$ is replaced by $2m(E-V(x))/\hbar^2$.

To examine the nature of $d_k(t)$ for the case where $\varepsilon(t)$ varies slowly in time, we are led to pursue a method analogous to that used in quantum mechanics to describe the motion of a particle which moves in a potential that varies slowly in space. This is the WKB method.

To make the analogy with the quantum theory more direct, split the dielectric constant $\varepsilon(t)$ into a background value ε_o and a time varying portion $\Delta\varepsilon(t)[\varepsilon(t)=\varepsilon_o+\Delta\varepsilon(t)]$. Then let

$$\omega_o^2 = \frac{c^2k^2}{\varepsilon_o} \tag{6a}$$

$$\Delta_k(t) = \frac{\Delta\varepsilon(t)}{[\varepsilon_o + \Delta\varepsilon(t)]} \quad \frac{c^2k^2}{\varepsilon_o} \tag{6b}$$

to write Eq. (5) in the form

$$\frac{\partial^2 d_k(t)}{\partial t^2} + \omega_o^2 d_k(t) - \Delta_k(t) d_k(t) = 0 \quad . \tag{7}$$

We want to solve Eq. (7) under the assumption that $\Delta(t)$ varies slowly over a time interval the order of ω_o^{-1}. In essence, the method used here expands the solution in powers of (Ω/ω_o), where Ω is a frequency that characterizes the time variation of $\Delta(t)$.

To proceed, we write

$$d_k(t) = A_k(t)e^{-i\phi_k(t)} \tag{8}$$

where $A_k(t)$ and $\phi_k(t)$ are real. Upon inserting this form into Eq. (7) and equating the real and imaginary parts separately to zero, one obtains two coupled equations for $A_k(t)$ and $\phi_k(t)$. These may be arranged to read

$$\left(\frac{d\phi_k}{dt}\right)^2 = \omega_o^2 - \Delta_k(t) + \frac{1}{A_k}\frac{d^2A_k}{dt^2} \tag{9}$$

and also

$$\frac{d}{dt}\left[A_k^2\frac{d\phi_k}{dt}\right] = 0 \tag{10}$$

Suppose that $\Delta_k(t)$ is time-independent. Then Eq. (9) and Eq. (10) admit solutions of the form

$$\phi_k(t) = [\omega_o^2-\Delta_k]^{1/2}\ t \equiv \frac{ck}{\sqrt{\epsilon}}\ t \tag{11a}$$

and

$$A_k(t) = 1, \tag{11b}$$

independent of time.

We seek the solutions of Eq. (9) and Eq. (10) when $\Delta_k(t)$ varies slowly in time. This solution shall have the property that, when $\Delta_k(t)$ becomes time-independent, the solution reduces to that in Eq. (11).

We begin by eliminating $A_k(t)$ from Eq. (9). This may be done by integrating Eq. (10):

$$A_k^2(t)\dot{\phi}_k(t) = A_k^2(0)\dot{\phi}_k(0) \equiv \dot{\phi}_k(0). \tag{12}$$

In Eq. (12), $\dot{\phi}_k = d\phi_k/dt$ and we normalize the solution (arbitrarily) so that $A_k(0)=1$. From Eq. (12), we then have the (exact) result

$$A_k(t)=\left(\frac{\dot{\phi}_k(0)}{\dot{\phi}_k(t)}\right)^{1/2} . \tag{13}$$

Eq. (9) may then be written in terms of $\phi_k(t)$ alone:

$$(\dot{\phi}_k)^2 = \omega_o^2-\Delta_k(t) + \frac{1}{2}\ \frac{1}{(\dot{\phi}_k)^2}\left[\frac{3}{2}\,(\ddot{\phi}_k)^2-\dot{\phi}_k\dddot{\phi}_k\right] . \tag{14}$$

The quantity in square brackets on the right-hand side of Eq. (14) vanishes when $\Delta_k(t)$ is time independent. This follows from Eq. (11a). Thus, Eq. (14) provides a means of solving for $\phi_k(t)$ by the method of successive approximations, in the limit where $\Delta_k(t)$ varies slowly in time.

We do this by writing

$$\phi_k = \phi_k^{(o)} + \phi_k^{(1)} + \ldots \tag{15}$$

where $\phi_k^{(o)}$ satisfies

$$\left(\dot{\phi}_k^{(o)}\right)^2 = \omega_o^2 - \Delta_k(t) \equiv \frac{c^2k^2}{\varepsilon(t)} \tag{16}$$

$$\text{or} \quad \phi_k^{(o)}(t) = ck\int_o^t \frac{dt'}{\sqrt{\varepsilon(t')}} = ck\int_o^t \frac{dt'}{n(t')} \quad , \tag{17}$$

where $n(t')$ is the index of refraction of the material.

Upon inserting the complete form of Eq. (15) into Eq. (14) and keeping the terms that provide the first correction to Eq. (17), we have

$$2\,\dot{\phi}_k^{(o)}\,\dot{\phi}_k^{(1)} = \frac{1}{2}\,\frac{1}{\left(\dot{\phi}_k^{(o)}\right)^2}\left[\frac{3}{2}\left(\ddot{\phi}_k^{(o)}\right)^2 - \dot{\phi}_k^{(o)}\dddot{\phi}_k^{(o)}\right] \tag{18}$$

or, if all quantities are expressed in terms of $n(t)$,

$$\dot{\phi}_k^{(1)} = \frac{1}{4ck}\left[\ddot{n} - \frac{1}{2}\frac{(\dot{n})^2}{n}\right], \tag{19}$$

or

$$\phi_k^{(1)}(t) = \frac{1}{4ck}\int_o^t dt'\left[\ddot{n}(t') - \frac{1}{2}\,\frac{(\dot{n})^2}{n}\right]. \tag{20}$$

This correction is first order in the time variation of $n(t)$, and it provides a correction to the lowest order WKB approximation for $\phi_k(t)$, which is given in Eq. (17). We shall see that $\phi_k^{(1)}$ is of order Ω/ω_o,

where Ω is a typical modulation frequency in $\varepsilon(t)$, and ω_o the carrier frequency of the pulse that propagates through the material. We shall assess the role of this correction in modifying pulse shapes below. Note that the amplitude A(t) may be found from Eq. (13), once $\phi_k(t)$ is known to a given order in Ω/ω_o.

Further corrections to $\phi_k(t)$ may be generated by carrying out the successive approximation scheme to higher order. In this fashion, one may generate an expansion of the functions $A_k(t)$ and $\phi_k(t)$ in powers of Ω/ω_o. Note that we have yet to make any approximation that presumes $\Delta_k(t)$ in Eq. (6b) to be small in magnitude. The only assumption is that $\Delta_k(t)$ varies slowly in time. Furthermore, we have made no assumption about the specific form of the time dependence of n(t).

An Application: Pulse Propagation in the Presence of a Time Varying Index of Refraction

We consider propagation of a pulse which at time t=0 is tailored to be Gaussian in form. At t=0, the electric field is given by

$$E(x,0) = \int_{-\infty}^{+\infty} \frac{dk}{(2\pi)^{1/2}} \; E(k)e^{ikx} \quad , \tag{21}$$

where we choose

$$E(k) = \frac{E_o}{(2\sigma)^{1/2}} \; \exp\left[- \frac{1}{4\sigma} \; (k-k_o)^2 \; \right] , \tag{22}$$

so that the explicit form of E(x,0) is

$$E(x,0) = E_o \; \exp[-\sigma x^2 + ik_o x] \tag{23}$$

Upon noting that at time t, we have $E(x,t) = D(x,t)/\varepsilon(t)$, the field $E(x,t)$ in the pulse may be written in the form

$$E(x,0) = \frac{\varepsilon(0)}{\varepsilon(t)} \int_{-\infty}^{+\infty} \frac{dk}{(2\pi)^{1/2}} \; E(k)A_k(t)e^{ikx}e^{-i\phi_k(t)} \quad . \qquad (24)$$

We examine the explicit form of the pulse for the case where the time varying part $\Delta\varepsilon(t)$ of the dielectric constant is small. In the notation of Figure (6b), we have $\Delta\varepsilon(t) << \varepsilon_o$. For all times, we may then replace the ratio $\varepsilon(o)/\varepsilon(t)$ in Eq. (24) by unity. Also, for small $\Delta\varepsilon(t)$, the amplitude $A_k(t)$ may be approximated by unity. It is the time-dependent phase factor $\phi_k(t)$ that plays the greatest role in affecting the pulse shape, in this limit. We concentrate on the behavior of $\phi_k(t)$ and its influence on the pulse shape. Rather than work with $\varepsilon(t)$, we consider instead the time varying index of refraction $n(t)$, and write

$$n(t) = n_o + \Delta n(t), \qquad (25)$$

$\Delta n(t) << n_o$ always.

For $\phi_k^{(o)}(t)$, we have

$$\phi_k^{(o)}(t) = ck \int_o^t \frac{dt'}{n_o + \Delta n(t)} \cong \frac{ck}{n_o} - \frac{ck}{n_o^2} \int_o^t dt \; \Delta n(t) \qquad (26)$$

If we presume the index of refraction is modulated in a sinusoidal fashion,

$$\Delta n(t) = \Delta n \cos(\Omega t+\phi), \tag{27}$$

then

$$\phi_k^{(o)}(t) = \frac{ck}{n_o}\left[t - \frac{\Delta n}{n_o}\frac{1}{\Omega}\{\sin(\Omega t+\phi)-\sin(\phi)\}\right]. \tag{28}$$

If Δn is small, in $\phi_k^{(1)}$ the term in $(\dot{n})^2$ may be ignored to give

$$\phi_k^{(1)}(t) = \frac{1}{4ck}\left[\dot{n}(t)-\dot{n}(o)\right] = -\frac{\Omega\Delta n}{4\omega}\left[\sin(\Omega t+\phi)-\sin(\phi)\right] \tag{29}$$

so that, with $\omega=ck$,

$$\phi_k^{(o)}(t) + \phi_k^{(1)}(t) = \frac{\omega}{n_o}\left[t - \frac{\Delta n}{n_o}\left(1+\frac{n_o^2\Omega^2}{4\omega^2}\right)\left(\frac{\sin(\Omega t+\phi)-\sin(\phi)}{\Omega}\right)\right]. \tag{30}$$

We can see from this expression that the effect of including the finite rate of change of n(t) (i.e., the effect of retaining $\phi_k^{(1)}$) is small, and leads to no qualitative change in the behavior of the pulse. The term in $\phi_k^{(1)}$ leads to the contribution to the right-hand side of Eq. (30) proportional to Ω^2/ω^2. This has precisely the same time variation as the term in $\phi_k^{(o)}(t)$ proportional to Δn, and leads to no new effects of a qualitative nature. Under typical operating conditions, the ratio $n_o^2\Omega^2/\omega^2$ is very small indeed.

A short pulse which propagates in a material where the index is modulated slowly may have a time duration short compared to the period $T=2\pi/\Omega$ of the external field which modulates the index of refraction. Then we may calculate the form of the pulse by expanding the right-hand side of Eq. (30) for

small times about t=0. If we do this and keep track of the influence of the term proportional to Ω^2, we have

$$\phi_k(t) \cong \frac{\omega}{n_o}\ \tau_1(t) + \frac{n_o \Omega^2}{\omega}\ \tau_2(t) + \cdots \quad , \tag{31}$$

where

$$\tau_1(t) = t\left[1 + \frac{\Delta n}{n_o}\cos(\phi) + \frac{\Delta n}{2n_o}\sin(\phi)\Omega t - \frac{1}{6}\frac{\Delta n}{n_o}\cos(\phi)\,(\Omega t)^2 + \cdots\right] \tag{32a}$$

and

$$\tau_2(t) = \frac{\Delta n t}{4n_o}\left[\cos\phi + \frac{1}{2}\sin(\phi)\Omega t - \frac{1}{6}\cos(\phi)\,(\Omega t)^2 + \cdots\right] . \tag{32b}$$

If we recall that $\omega = ck$, then for $E(x,t)$ we have

$$E(x,t) = \frac{E_o}{2(\pi\sigma)^{1/2}} \int_{-\infty}^{+\infty} dk\ e^{-\frac{(k-k_o)^2}{4\sigma}}\ e^{ik\left[x - \frac{c\tau_1}{n_o}\right]} e^{-i\frac{n_o\Omega^2}{ck}\ \tau_2} . \tag{33}$$

We let

$$k = k_o + \kappa \tag{34a}$$

$$s = x - \frac{c\tau_1}{n_o} \tag{34b}$$

and presume $\sigma/k_o \ll 1$, so only values of κ small compared to k_o are important. Physically, this means in real space the packet is many wavelengths long. We then can write

$$\frac{n_o\Omega^2\tau_2}{ck} \cong \frac{n_o\Omega^2\tau_2}{ck_o} - \frac{n_o\Omega^2\tau_2}{ck_o^2}\,\kappa + \frac{n_o\Omega^2\tau_2}{ck_o^3}\,\kappa^2 + \cdots \tag{35}$$

so that

$$E(x,t) = \frac{E_o e^{ik_o s}\; e^{-i\frac{n_o\Omega^2}{ck_o}\tau_2}}{2(\pi\sigma)^{1/2}} \int_{-\infty}^{+\infty} dk \exp\left[-\frac{\kappa^2}{4\sigma} - i\frac{n_o\Omega^2\tau_2}{ck_o^3}\,\kappa^2\right] \tag{36}$$

$$\times \exp\left[i\kappa\left\{s + \frac{n_o\Omega^2}{ck_o^2}\,\tau_2\right\}\right] .$$

Define the quantity

$$\Delta = \frac{4n_o\Omega^2\tau_2}{ck_o^2} = 4n_o\left(\frac{\Omega}{\omega_o}\right)^2 c\tau_2 \tag{37}$$

where $\omega_o = ck_o$.

Then upon integrating Eq. (36), and introducing

$$\tilde{s} = s + \frac{1}{4}\Delta = x - \frac{c\tau_1}{n_o} + \frac{1}{4}\Delta \quad , \tag{38a}$$

and $\tilde{\sigma}$ defined by $\frac{1}{\tilde{\sigma}} = \frac{1}{\sigma} + i\frac{\Delta}{k_o}$, (38b)

we have

$$E(x,t) = \left(\frac{\tilde{\sigma}}{\sigma}\right)^{1/2} E_o \exp\left[-\tilde{\sigma}(\tilde{s})^2\right]\; e^{ik_o\left(\tilde{s} - \frac{1}{2}\Delta\right)} . \tag{39}$$

The quantity Δ provides a measure of the effect of the finite frequency Ω of the modulation rate of $\Delta n(t)$ on the shape of the propagating pulse. This effect shifts the centroid or "center of gravity" of the pulse through appearance of Δ in Eq.(38). This effect leaves the shape of the pulse unchanged.

The influence of Δ on the shape of the pulse is found from the appearance of the factor of Δ in the expression for $\tilde{\sigma}$, which controls the width of the pulse. We have for $|E(x,t)|^2$ the expression

$$|E(x,t)|^2 = \frac{|E_o|^2}{\left[1 + \left(\frac{\sigma\Delta}{k_o}\right)^2\right]^{\frac{1}{2}}} \exp\left[-\frac{2\sigma(\tilde{s})^2}{\left(1 + \left(\frac{\sigma\Delta}{k_o}\right)^2\right)}\right] \quad . \tag{40}$$

As the pulse propagates, the effect of the presence of Δ is to broaden the pulse. Notice that Δ increases linearly with the time, starting at zero, if our approximation $\Omega t << 1$ is meaningful. If we call $\Delta x(t)$ width of the pulse at time t, then Eq.(40) leads us to

$$\Delta x(t) = \left[\Delta x(0)^2 + \left(\frac{\Delta}{k_o\ \Delta x(0)}\right)^2\right]^{\frac{1}{2}} \quad . \tag{41}$$

If $x(t)=ct/n_o$ is the distance the pulse has traveled in the material, we have

$$\Delta \cong \left(\frac{\Omega}{\omega_o}\right)^2 \Delta n \cos(\phi)\ x(t) \tag{42}$$

and we may finally write

$$\Delta x(t) = \left[\Delta x(o)^2 + \left(\frac{\Omega}{\omega_o}\right)^4 \left(\frac{c}{k_o}\right)^2 \left(\frac{x(t)}{\Delta x(o)}\right)^2 (\Delta n)^2 \cos^2 \phi \right]^{\frac{1}{2}} \tag{43}$$

$$\equiv \Delta x(o) \, [1 + f]^{\frac{1}{2}}$$

where

$$f = \left(\frac{\Omega}{\omega_o}\right)^4 \left(\frac{c}{k_o \, \Delta x(0)}\right)^2 \left(\frac{x(t)}{\Delta x(0)}\right)^2 (\Delta n)^2 \cos^2 \phi \quad . \tag{44}$$

If the amplitude Δn of the modulation of the index of refraction remains fixed, but the modulation frequency Ω is increased, the pulse broadening rapidly becomes more severe; it is not possible to narrow the pulse by manipulating any parameters which enter the present discussion.

Under practical circumstances, the amount of broadening that occurs is miniscule, as some numbers show.

Consider a 10μ pulse in a medium where the index of refraction is modulated at 10^{10} Hertz, a very high modulation rate indeed. (This is higher than one can use in practice.) Then $(\Omega/\omega_o)^4 \cong 8 \times 10^{-15}$. Let the pulse be of 0.1 nanoseconds duration, so $\Delta x = c\Delta t \cong 3$ cm. If the pulse propagates 10 cm in the material, then $(x(t)/\Delta x(o))^2 \sim 10$. Finally, for these numbers $c/\omega_o \Delta x(o) \sim 5 \times 10^{-5}$, and f is incredibly tiny.

Our conclusion is that to extraordinary precision, the shape of the pulse may be described by ignoring $\phi_k^{(1)}$ and the tiny pulse broadening effects incorporated in it. We need only retain $\phi_k^{(o)}(t)$ for a pulse

with <u>any</u> envelope shape, to excellent approximation

$$E(x,t) = \int_{-\infty}^{+\infty} \frac{dk}{(2\pi)^{1/2}} E(k) \exp\left[ik\left(x - c\int_0^t \frac{dt'}{n(t')}\right)\right]$$

$$\equiv E\left(x - c\int_0^t \frac{dt'}{n(t')}\ ,\ 0\right) \quad . \tag{45}$$

This formula reproduces the results of the elementary description of pulse chirping.

<u>Reflection of Monochromatic Incident Radiation From The Surface of a Material With Time Varying Index of Refraction</u>

In the preceeding two sections the solutions of Maxwell's equations were examined for propagation in a medium with index of refraction $n(t)$ that varies slowly in time compared with the carrier frequency of the wave. If we write $n(t)$ in the form

$$n(t) = n_o + \Delta n \cos(\Omega t + \phi) , \tag{46}$$

as in Eq. (27), and assume $\Delta n << n_o$, then in the material we can construct characteristic solutions $E_k(x,t)$ of the form

$$E_k(x,t) = \exp[i(kx - \omega_k t + \lambda_k(t))] , \tag{47}$$

where $\omega_k = ck/n_o$ and

$$\lambda_k(t) = \frac{\omega_k}{\Omega} \frac{\Delta n}{n_o} \{\sin(\Omega t + \phi) - \sin(\phi)\} . \tag{48}$$

The expression in Eq. (47) describes the space and time variation of the electric field in the wave when $\Omega << \omega_k$, and when $\Delta n << n_o$, two conditions very well satisfied in the situations of interest here. In Section I and Section II the corrections to the form in Eq. (47) were obtained explicitly, and their role assessed, with the conclusion that for our purposes the effects of the corrections are quite insignificant.

In this section we discuss the reflection of an incident monochromatic plane wave at the surface of a semi-infinite material with the time varying index in Eq. (47). This will enable us to discuss in Section IV the nature of pulse propagation in such a medium, when a shaped pulse is incident on the surface. The objective is to assess whether an unchirped pulse may be compressed or altered in shape if it strikes the surface at some selected time t_o.

The problem we face here is to devise a manner in which a monochromatic incident wave may be matched across the boundary to characteristic solutions of the form displayed in Eq. (47). For our discussion it will prove extremely useful to make a Fourier decomposition of the expression in Eq. (47). This may be done through use of the relation

$$\exp[i z \sin\theta] = \sum_{n=-\infty}^{+\infty} e^{in\theta} J_n(z) \quad , \tag{49}$$

where $J_k(z) = (-1)^k J_{-k}(z)$ is the Bessel function of order k. Through application of this identity with $\theta = \Omega t + \phi$, the characteristic solution in Eq. (47) may be decomposed into its Fourier components:

$$E_k(x,t) = \exp[ikx - i\lambda_k \sin(\phi)] \sum_{n=-\infty}^{+\infty} e^{in\phi} e^{-i(\omega_k - n\Omega)t} J_n(\lambda_k), \tag{50}$$

where we define

$$\lambda_k = \frac{\Delta n}{n_o} \quad \frac{\omega_k}{\Omega} \quad . \tag{51}$$

We introduce the frequency $\omega_{kn} = \omega_k - n\Omega$ to write Eq. (50) in the more compact form

$$E_k(x,t) = \exp[ikx - i\lambda_k \sin(\phi)] \sum_{n=-\infty}^{+\infty} e^{in\phi} \; e^{-i\omega_{kn} t} \; J_n(\lambda_k) \; . \tag{52}$$

The magnetic field associated with the solution in Eq. (52) will be required for use in the boundary conditions. The magnetic field $H_k(x,t)$ is readily computed from Maxwell's Equations through use of the $\nabla \times \vec{E}$ equation. A short calculation gives

$$H_k(x,t) = \exp[ikx - i\lambda_k \sin(\phi)] \sum_{n=-\infty}^{+\infty} \eta_{kn} \; e^{in\phi} \; e^{-i\omega_{kn} t} \; J_n(\lambda_k) \; , \tag{53}$$

where

$$\eta_{kn} = \frac{ck}{\omega_{kn}} \; . \tag{54}$$

We now turn to the boundary value problem. The material with the time varying index of refraction (Eq. (46)) is presumed perpendicular to the x axis, semi-infinite in extent, with surface in the plane x=0. The material lies in the half-space $x > 0$. The electric field in all waves is parallel to the z axis.

We presume the incident wave has frequency ω_o and wave vector $k_o = \omega_o/c$, where c is the vacuum velocity of light. The electric field in the incident wave is

$$E^{(0)}(x,t) = +E_0^{(0)} \; \exp(ik_o x - i\omega_o t), \tag{55}$$

and the magnetic field is

$$H^{(0)}(x,t) = + E_0^{(0)} \exp(ik_o x - i\omega_o t) \quad . \tag{56}$$

We shall match this incident wave to waves of the form given in Eq. (52) and Eq. (53) across the boundary surface x=0, through use of the tangential E and tangential H boundary condition. While the form of the incident wave is at the control of the experimenter, so to speak, in general we may expect the reflected wave to contain radiation not only at the incident frequency ω_o but also at the harmonics

$$\omega_{on} = \omega_o - n\Omega \tag{57}$$

that appear in Eq. (52). Thus, we take the reflected wave (in vacuum) to have the form

$$E^{(R)}(x,t) = + \sum_{n=-\infty}^{+\infty} E_n^{(R)} \exp(-ik_{on} x - i\omega_{on} t) \tag{58}$$

$$H^{(R)}(x,t) = - \sum_{n=-\infty}^{+\infty} E_n^{(R)} \exp(-ik_{on} x - i\omega_{on} t) \quad . \tag{59}$$

The amplitudes $E_0^{(R)}$, $E_{\pm 1}^{(R)}$, etc. are to be found by matching the incident and reflected waves to solutions in the material with the form displayed in Eqs. (52) and (53).

It is readily verified that we cannot satisfy the boundary conditions by matching a single eigensolution like that in Eq. (52) to the vacuum waves. Suppose we consider the wave in Eq. (52) with the wave vector k adjusted so that as $\Delta n \to 0$, the solution reduces to a wave with frequency ω_o equal to that of the incident wave. If the wave in Eq. (52) is multiplied by the prefactor $\hat{\boldsymbol{\varepsilon}}_o^>$, and with $\Delta n \neq 0$ we match its Fourier component of frequency ω_o to those of the incident wave, and to the same Fourier

component of the reflected wave, then the amplitude $\mathcal{E}_o^>$ is determined uniquely by the two electromagnetic boundary conditions. Then a single amplitude $E_n^{(R)}$ cannot be chosen for the Fourier component of the reflected wave of frequency ω_{on}, $n \neq 0$, which will satisfy both tangential E and tangential H boundary conditions.

To proceed, we must match the waves in vacuum not to a single wave of the form given in Eq. (52), but instead to a linear combination of them. We proceed as follows.

Let $E_m^>(x,t)$ be that eigenwave of the material which, as the time varying part $\Delta n(t)$ of the index of refraction is set to zero, reduces to a plane wave of frequency $\omega_m = \omega_o + m\Omega$, where m is an integer. If we define

$$k_m = \frac{n_o}{c} \omega_m \tag{60}$$

and

$$\omega_{mn} = \omega_o + m\Omega - n\Omega , \tag{61}$$

we then have, with $\eta_{mn} = ck_m/\omega_{mn}$,

$$E_m^>(x,t) = E_m^> \exp[ik_m x - i\lambda_{k_m} \sin(\phi)] \sum_{n=-\infty}^{+\infty} e^{in\phi} e^{-i\omega_{mn}t} J_n(\lambda_{k_m}), \tag{62}$$

$$H_m^>(x,t) = E_m^> \exp[ik_m x - i\lambda_{k_m}\sin(\phi)] \sum_{n=-\infty}^{+\infty} \eta_{mn} e^{in\phi} e^{-i\omega_{mn}t} J_n(\lambda_{k_m}) , \tag{63}$$

and the electric and magnetic fields in the material are found by superimposing these waves:

$$E^>(x,t) = \sum_{m=-\infty}^{+\infty} E_m^>(x,t) \tag{64}$$

$$H^>(x,t) = \sum_{m=-\infty}^{+\infty} H_m^>(x,t) . \tag{65}$$

The coefficients $E_m^>$ are to be found from the electromagnetic boundary conditions. We turn to the form of the boundary conditions.

We first equate the amplitudes of the electric and magnetic fields which vary with time like $\exp(-i\omega_o t)$, then turn to the "side band" fields with frequency $\exp(-i\omega_{on} t)$.

Note that in Eq. (62) and Eq. (63) the terms with n=m describe fields which oscillate like $\exp(-i\omega_o t)$. Thus, conservation of tangential components of E leads to the requirements

$$E_0^{(0)} + E_0^{(R)} = \sum_{m=-\infty}^{+\infty} E_m^> \exp[-im\phi - i\lambda_{k_m} \sin\phi] J_m(\lambda_{k_m}) , \qquad (66)$$

and

$$E_0^{(0)} - E_0^{(R)} = \sum_{m=-\infty}^{+\infty} E_m^> \eta_{m;m} \exp[-im\phi - i\lambda_{k_m} \sin\phi] J_m(\lambda_{k_m}) . \qquad (67)$$

We next match components that vary in time like $\exp[-i(\omega_o - p\Omega)t]$ to obtain, since only the reflected wave appears in this channel,

$$E_p^{(R)} = \sum_{m=-\infty}^{+\infty} E_m^> \exp[i(p+m)\phi - i\lambda_{k_m} \sin\phi] J_{m+p}(\lambda_{k_m}) , \qquad (68)$$

and

$$-E_p^{(R)} = \sum_{m=-\infty}^{+\infty} E_m^> \eta_{m;m+p} \exp[i(p+m)\phi - i\lambda_{k_m} \sin\phi] J_{m+p}(\lambda_{k_m}) . \qquad (69)$$

Our task is to solve this infinite set of equations. In general, this seems very difficult. However, in constructing the characteristic solution in Eqs. (47) and (48), we have presumed that the frequency Ω that describes the rate of modulation of the dielectric constant is very small compared to ω_o. We can exploit this assumption again to simplify Eqs. (66) through (69) to the point where the solution is evident. Indeed, it is not worthwhile to consider any limit other than that for which $\Omega << \omega_o$ without re-examining the form of the characteristic solution in Eq. (47).

When $\Omega << \omega_o$ in the quantity η_{mn} defined above in Eq. (62), we may with little error replace ω_{mn} by $\omega_{mo} = \omega_o + m\Omega$. When this is done, $\eta_{mn} = n_o$, the index of refraction of the undisturbed medium. We also replace λ_{k_m} by $\lambda_{k_o} = \omega_o \Delta n/(n_o\Omega) \equiv \lambda_o$ to make λ_{k_m} independent of m. Both of these approximations are well justified for the extremely small values of Ω/ω_o relevant to contemporary experiments.

These assumptions greatly simplify the structure of the boundary condition equations. We introduce

$$\varepsilon_m^> = \exp[im\phi - i\lambda_o \sin(\phi)] \quad E_m^> \tag{70}$$

and

$$\varepsilon_p^{(R)} = E_p^{(R)} \exp(-ip\phi) \tag{71}$$

to cast the equations in the form

$$E_o + \varepsilon_o^{(R)} = \sum_{m=-\infty}^{+\infty} \varepsilon_m^> J_m(\lambda_o) \tag{72}$$

$$E_o - \varepsilon_o^{(R)} = n_o \sum_{m=-\infty}^{+\infty} \varepsilon_m^> J_m(\lambda_o) \tag{73}$$

$$\varepsilon_p^{(R)} = \sum_{m=-\infty}^{+\infty} \varepsilon_m^> J_{p+m}(\lambda_o) \quad (p \neq 0) \tag{74}$$

and

$$-\varepsilon_p^{(R)} = n_o \sum_{m=-\infty}^{+\infty} \varepsilon_m^> J_{p+m}(\lambda_o) \quad (p \neq 0)\ . \tag{75}$$

Eqs. (74) and (75) can be satisfied only if we require

$$\sum_{m=-\infty}^{+\infty} \varepsilon_m^> J_{m+p}(\lambda_o) \equiv 0 \quad , \quad p \neq 0 \tag{76}$$

and thus also

$$\varepsilon_p^{(R)} = E_p^{(R)} \equiv 0, \quad p \neq 0\ . \tag{77}$$

The result in Eq. (77) is perhaps surprising. Even though the index of refraction of the substrate varies with time, so a monochromatic incident wave excites a non-monochromatic disturbance in the medium; the reflected wave is perfectly harmonic with frequency equal that of the incident wave. Indeed, we shall see shortly that the reflection coefficient has the value appropriate to the undisturbed medium with $\Delta n = 0$. Thus, through study of the reflected radiation, one cannot tell that the dielectric constant of the substrate is modulated in time. This conclusion is true only when $\Omega << \omega_0$; presumably the amplitudes $E_p^{(R)}$ are of order Ω/ω_0 or smaller. Also, as one sees from Section I, we have presumed in addition that $\Delta n/n_0$ is small; for example, the prefactor $\epsilon(0)/\epsilon(t)$ in Eq. (24) and the amplitude $A_k(t)$ have been set to unity.

The requirement in Eq. (76) allows one to guess the form of $\epsilon_m^>$. One may do this by noting the Bessel function addition theorem (identity 9.1.75 on page 363 of Abramowitz and Stegun)

$$J_p(\lambda_1 - \lambda_0) = \sum_{m=-\infty}^{+\infty} J_m(\lambda_0)\, J_{m+p}(\lambda_1). \qquad (\lambda_0 < \lambda_1) \qquad (78)$$

If we take the limit $\lambda_0 \to \lambda_1$ and presume that $p \neq 0$, then we obtain the statement

$$J_p(0) = \sum_{m=-\infty}^{+\infty} J_m(\lambda_o)\, J_{m+p}(\lambda_o) \equiv 0 \quad , \qquad (79)$$

upon noting $J_p(x)$ vanishes as x^p.

The statement in Eq. (79) tells us we may take

$$\epsilon_m^> = \epsilon^> J_m(\lambda_o) \quad , \qquad (80)$$

with $\varepsilon^{>}$ found from Eq. (72) and Eq. (73). Then Eq. (76) is satisfied identically, and noting that

$$\sum_{m=-\infty}^{+\infty} J_m^2 \ (\lambda_o) \ = \ 1 \tag{81}$$

(use Eq. (79) with p = 0, with $J_0(0) = 1$), Eq. (72) and Eq. (73) become simply

$$E_o \ + \ \varepsilon_o^{(R)} \ = \varepsilon^{>} \tag{82}$$

and

$$E_o \ - \ \varepsilon_o^{(R)} \ = \ n_o \ \varepsilon^{>} \ , \tag{83}$$

or

$$\varepsilon^{>} = 2/(1 + n_o) \ .$$

When the results above are assembled the electric field in the medium is given by the double sum

$$E^{>}(x,t) = \frac{2E_o}{1+n_o} \sum_{m=-\infty}^{+\infty} \sum_{n=-\infty}^{+\infty} \exp[ik_m x - i(m-n)\phi - i\omega_{mn} t] \ J_m(\lambda_o) \ J_n(\lambda_o) \ . \tag{84}$$

Through use of the identity in Eq. (49), the fact that $\omega_{nm}=\omega_o+(m-n)\Omega$, and $k_m=n_o(\omega_o+m\Omega)/c$, both sums in Eq. (84) may be evaluated in closed form, to express $E^{>}(x,t)$ in terms of elementary functions. The result is

$$E^{>}(x,t) = \frac{2E_o}{1+n_o} \exp\Big[ik_o x - i\omega_o t\Big] \exp\left[i\lambda_o\left\{\sin[\Omega t+\phi] - \sin\left[\Omega\left(t - \frac{n_o x}{c}\right)+\phi\right]\right\}\right] \ . \tag{85}$$

In what follows, it will be convenient to use the notation

$$\overline{c} = \frac{c}{n_o} \tag{86}$$

$$\tau(x,t) = \frac{\Delta n}{\Omega n_o}\left\{\sin\left[\Omega\left(t-\frac{x}{\bar{c}}\right)+\phi\right]-\sin[\Omega t+\phi]\right\} \tag{87}$$

so that Eq. (85) becomes

$$E^{>}(x,t) = \frac{2E_o}{1+n_o}\exp\left[-i\omega_o\left\{t+\tau(x,t)-\frac{x}{\bar{c}}\right\}\right] \quad . \tag{88}$$

This is the final result of the present section.

As $x \to o$, notice that $\tau(x,t) \to o$. Thus, the fields in the transmitted wave are monochromatic near the surface. This accounts for the fact that for our level of approximation, the reflected wave is monochromatic. "Sidebands" of the sort present in the characteristic solution of Eq. (47) require a distance $\Delta x \approx \bar{c}/\Omega$ to build up to full amplitude. This suggests that if one wishes to "chirp" or otherwise manipulate a pulse, the thickness of the modulator *should not be smaller than* $\bar{c}/\Omega$ *in the propagation* direction, if the incident pulse is to be modulated in the optimum fashion.

In the next section, we consider a pulse incident from the vacuum onto the substrate, and study the form of the transmitted signal through use of the result in Eq. (88) as the basic building block.

Transmission of a Pulse Through a Medium with Time Varying Index

We wish now to examine the propagation of a pulse through the medium with time varying index. We suppose a pulse of some prearranged shape is incident from the vacuum, to strike the surface of the material.

From the fact that Maxwell's equations are linear, and in view of our conclusion that just inside the surface the transmitted wave excited by an incident monochromatic wave is also monochromatic, we may solve the pulse

propagation problem easily. We simply decompose the incident pulse at the surface into its frequency components, assign to each frequency a wave with amplitude, time and space variation given in Eq. (88), then synthesize the result to find the transmitted pulse profile. We do this here and explore the behavior of the transmitted pulse for two cases: a pulse with delta function profile and a Gaussian pulse.

Let the incident pulse at x=0 (just to the left of the boundary) have the time profile $E_o(0,t)$ and write

$$E_o(0,t) = \int_{-\infty}^{+\infty} \frac{d\omega}{2\pi} \; E_o(\omega)\, e^{-i\omega t} \quad . \tag{89}$$

It then follows from Eq. (88) that the transmitted pulse has the form

$$E^{>}(x,t) = \frac{2}{1+n_o} \int_{-\infty}^{+\infty} \frac{d\omega}{2\pi} \; E_o(\omega) \exp\left[-i\omega\left\{t + \tau(x,t) - \frac{x}{c}\right\}\right], \tag{90}$$

which may be written in the very simple form

$$E^{>}(x,t) = \frac{2}{1+n_o} \; E_o\left(0, t + \tau(x,t) - \frac{x}{c}\right) \quad . \tag{91}$$

All information about the change in shape of the pulse is contained in the factor $\tau(x,t)$ in Eq. (91). Consider two cases:

(a) <u>A Delta Function Pulse:</u>

Suppose the incident pulse has the form of a delta function which strikes the surface at time t_o. Then,

$$E_o(0,t) = E_o\, \delta\,(t-t_o) \quad , \tag{92}$$

so that

$$E^{>}(x,t) = \frac{2E_o}{1+n} \; \delta\left(t + \tau(x,t) - \frac{x}{c} - t_o\right) \quad . \tag{93}$$

The pulse remains a delta function, and its position $x(t)$ at time t is found by solving the equation

$$x(t) = \bar{c}(t - t_o) + \bar{c}\ \tau(x(t),t) \quad . \tag{94}$$

Suppose for the moment that $\Omega x/\bar{c}$ is small compared to unity. Then, in Eq. (94), $\tau(x,t)$ may be replaced by

$$\tau(x,t) \approx -x\ \frac{\Delta n}{\bar{c} n_o}\ \cos[\Omega t + \phi] \quad , \tag{95}$$

and Eq. (94) becomes, with $\bar{c} = c/n_o$

$$\left[1 + \frac{\Delta n}{n_o}\ \cos[\Omega t + \phi]\right] x(t) = \frac{c}{n_o}\ (t - t_o) \quad ,$$

or

$$x(t) = \frac{c}{n(t)}\ (t - t_o) \quad . \tag{96}$$

As long as $\Omega x/\bar{c}$ is small compared to unity, in $n(t)$ the time t may be replaced by t_o. Hence, the delta function pulse propagates with a velocity controlled by the value of the index of refraction it sees when it strikes the surface. This result, which is an obvious one, holds only for values of x such that $\Omega x/\bar{c} \ll 1$. Otherwise, one must solve Eq. (94) fully. Notice that the largest possible value $\tau(x,t)$ can assume is $2\ \Delta n/n_o\Omega$. Hence, the greatest amount by which the position of the delta function pulse can differ from the ballistic trajectory $\bar{c}(t - t_o)$ appropriate to the undisturbed medium is $2\bar{c}\Delta n/n_o\Omega$, which is a very small displacement for typical values of Δn and Ω.

(b) A Gaussian Pulse:

Now we examine the behavior of a Gaussian pulse incident on the medium. Let the pulse have carrier frequency ω_o, width Δ, and suppose it strikes the

surface at time t_o. For the incident pulse we have

$$E_o(0,t) = E_o \exp\left[-i\omega_o(t - t_o) - \frac{(t-t_o)^2}{\Delta^2}\right] \quad . \tag{95}$$

The shape of the transmitted pulse is then, from Eq. (90),

$$E^{>}(x,t) = \frac{2E_o}{1+n_o} \exp\left[-i\omega_o\psi(x,t) - \frac{1}{\Delta^2}\ \psi^2(x,t)\right] \quad , \tag{96}$$

where

$$\psi(x,t) = t - t_o - \frac{x}{c} + \tau(x,t) \quad . \tag{97}$$

Before we examine the nature of the pulse described by Eq. (96), a word about the order of magnitude of various quantities is appropriate. The width of the input pulse is Δ, and $T = 2\pi/\Omega$ is the period of the field which modulates the index of refraction of the material. We shall always have $T >> \Delta$, so $\tau(x,t)$ is slowly varying over a time interval the order of Δ. This allows the discussion of the pulse shape to be presented in simple terms.

Let us sit at one position x, and examine the time profile of the pulse as it passes by. The magnitude of the electric field reaches its maximum at a time $t_c(x)$ found from the condition

$$\psi(x,t_c(x)) = 0 \quad . \tag{98}$$

Since $\tau(x,t)$ varies slowly over intervals the order of Δ, one may study the time profile of the pulse by expanding $\psi(x,t)$ in a Taylor series about $t_c(x)$:

$$\psi(x,t) = (t - t_c(x)) \left(\frac{\partial\psi}{\partial t}\right)_{t_c(x)} + \frac{1}{2} \left(\frac{\partial^2\psi}{\partial t^2}\right)_{t_c(x)} (t - t_c(x))^2 + \tag{99}$$

$$+ \ . \ . \ .$$

We use this expansion and retain only terms in the exponent of Eq. (96) quadratic in $(t - t_c(x))$. Note that

$$\left(\frac{\partial\psi}{\partial t}\right)_{t_c(x)} = 1 + \left(\frac{\partial\tau}{\partial t}\right)_{t_c(x)} \tag{100}$$

$$\left(\frac{\partial^2\psi}{\partial t^2}\right)_{t_c(x)} = \left(\frac{\partial^2\tau}{\partial t^2}\right)_{t_c(x)} . \tag{101}$$

If we define

$$\Delta(x) = \Delta\left[1 + \left(\frac{\partial\tau}{\partial t}\right)_{t_c(x)}\right]^{-1} , \tag{102}$$

$$\omega_o(x) = \omega_o\left[1 + \left(\frac{\partial\tau}{\partial t}\right)_{t_c(x)}\right] , \tag{103}$$

$$r(x) = \frac{\omega_o}{2\pi}\left(\frac{\partial^2\tau}{\partial t^2}\right)_{t_c(x)} , \tag{104}$$

then, $E^{>}(x,t)$ becomes

$$E^{>}(x,t) = \frac{2E_o}{1+n_o}\exp\left[-\frac{(t - t_c(x))^2}{\Delta^2(x)}\right]$$

$$\exp\left[-i\omega_o(x)(t - t_c(x)) - i\pi r(x)(t - t_c(x))^2\right] . \tag{105}$$

Since $\tau(x,t)$ vanishes as $x \to 0$, $\Delta(x)$ reduces to Δ, $r(x)$ vanishes, and $\omega_o(x)$ reduces to ω_o.

The expression in Eq. (105) describes a Gaussian pulse with width $\Delta(x)$ different than that of the incident pulse. Its frequency is shifted from that of the incident, and the presence of $r(x)$ shows it has been "chirped".

We find

$$\frac{\partial \tau}{\partial t} = \frac{\Delta n}{n_o} \left\{ \cos \left[\Omega \left(t - \frac{x}{\bar{c}} \right) + \phi \right] - \cos[\Omega t + \phi] \right\} \tag{106a}$$

$$\cong \frac{\Delta n}{n_o} \sin[\Omega t + \phi] \frac{\Omega x}{\bar{c}} , \tag{106b}$$

where the last statement is valid when $\Omega x/\bar{c} << 1$. Also,

$$\frac{\partial^2 \tau}{\partial t^2} = \frac{\Delta n \Omega}{n_o} \left\{ \sin[\Omega t + \phi] - \sin \left[\Omega \left(t - \frac{x}{\bar{c}} \right) + \phi \right] \right\} \tag{107a}$$

$$\cong \frac{\Delta n \Omega}{n_o} \cos[\Omega t + \phi] \frac{\Omega x}{\bar{c}} , \tag{107b}$$

where again the second statement is valid for $\Omega x/\bar{c}$.

These results show that the width of the pulse is given by, for $\Omega x/\bar{c} < 1$,

$$\Delta(x) \cong \Delta \left[1 - \frac{1}{n_o} \left(\frac{\partial n}{\partial t} \right)_{t_o} \frac{x}{\bar{c}} \right]^{-1} , \tag{108}$$

so the pulse may be either broadened or narrowed, depending on the sign of the time derivative of the index of refraction when the pulse strikes the surface. When $(\partial n/\partial t)_{t_o}$ is negative, the pulse narrows. The trailing edge of the pulse strikes the medium at a time for which the index is smaller than when the leading edge strikes the surface. Thus, the trailing edge "catches up" with the leading edge.

The result in Eq. (108) applies only when $\Omega x/\bar{c}$ is small compared to unity. More generally, we have

$$\Delta(x) = \Delta[1 + f(x)]^{-1} . \tag{109}$$

From Eq. (106) it is evident that f(x) does not increase indefinitely, but rather its maximum possible value is $2\Delta n/n_o$. Since $\Delta n/n_o$ is small compared to unity, the fractional amount by which a pulse can be compressed by this mechanism is quite small.

For the chirp parameter r(x), again when $\Omega x/\bar{c}$ is small compared to unity, one obtains

$$r(x) = \frac{\omega_o \Omega \Delta n}{2\pi n_o} \cos[\Omega t + \phi] \frac{\Omega x}{\bar{c}} , \qquad (110)$$

with r(x) assuming a maximum possible value $\omega_o \Omega \Delta n/\pi n_o$. The rate of chirp r(x) rises linearly with x near the surface, as one sees from Eq. (110), to assume its maximum value at a distance the order of $\bar{c}/\Omega$ from the surface. Thus, the ability to "chirp" a pulse will be inhibited by use of a sample that is too thin.

VI. Theory of Second Harmonic Generation by Surface Polaritons on Metals†

D. L. Mills
Department of Physics
University of California
Irvine, California
U.S.A. 92717

ABSTRACT

We discuss the theory of second harmonic generation by surface polaritons which propagate on the surface of a nearly free electron metal, with emphasis on the infrared frequency range.

RESUMÉ

Nous discutons la théorie de production de la deuxième harmonique par polaritons de surface sur les metaux dans la théorie des electrons presque libres, en mettant l´ accent sur les fréquences infra-rouge.

†Research supported by Contract DAHC04-74-C-0024, U. S. Army Research Office; Durham, NC

I. Introductory Remarks

While there has been considerable interest in the study of surface polariton propagation on a variety of materials[1], rather little attention has been devoted to nonlinear interactions between these waves.

One does not expect nonlinear effects to be large, unless the process in question proceeds under conditions of near phase matching. One example of such a process has been proposed by Maddox and Mills[2], in a study of nonlinear interactions between surface polaritons on the surface of doped (n type) zinc blend semiconductors. For a range of carrier concentrations with plasma frequency below that of the LO phonon, one may mix two waves on the lower branch of the two branch dispersion relation to produce an output wave very near a point on the upper branch. This process has subsequently been reinvestigated by Bonsall and Maradudin[3], who find an appreciable output.

In this note, we discuss a second nonlinear process which proceeds under conditions of near phase matching. This is second harmonic generation by surface polaritons that propagate on metal surfaces. For frequencies well below the plasma frequency ω_p of the conduction electrons, the dispersion relation is nearly linear. Thus, the driven output wave of frequency 2ω and wave vector $2k_{//}$, where ω and $k_{//}$ are the frequency and wave vector (parallel to the surface) of the initial wave, has a wave vector very close to that of the freely propagating surface polariton, of frequency 2ω.

However, it is unclear at the outset whether or not one can expect appreciable second harmonic generation for this case. At these low frequencies, the fields in the wave extend quite far into the vacuum, while in the medium where the nonlinear mixing occurs, the fields are nonzero only within the

small skin depth; nearly all the wave energy is stored in the vacuum, where no harmonic generation occurs. On the other hand, for driving fields of given magnitude, the nonlinear currents within the skin depth and at the metallic surface increase dramatically as the frequency is lowered.[5] The present study has been motivated by the above remarks, and by an experimental search for the second harmonic of a surface polariton propagating on copper metal, at the CO_2 laser frequency.[6]

II. Theoretical Derivation of the Second Harmonic Intensity

In a recent paper, Rudnick and Stearn[5] have presented a phenomenological description of the second harmonic currents generated at the surface of a simple metal, and within its skin depth, when the metal is irradiated with an electromagnetic wave of frequency ω. Their prescription forms the basis of the present study. We note that at the infrared frequencies of interest here, interband processes should make a negligible contribution to the second harmonic intensity.

We presume a plane, semi-infinite metal in the half space $z < o$. The incident surface polariton (frequency ω, wave vector $k_{//}$) propagates parallel to the x axis, with fields $E^{(\omega)}_{x,z}(z)\exp(ik_{//}x-i\omega t)$. The frequency dependent dielectric constant of the model metal is $\varepsilon(\omega) = \varepsilon_\infty - \omega_p^2/\omega^2$, which is real and presumed negative at both ω, and also 2ω. Indeed, in the infrared frequency regime, $\varepsilon(\omega) \cong -\omega_p^2/\omega^2$ and $|\varepsilon(\omega)| >> 1$, a condition[7] we use below to simplify the final result substantially.

Rudnick and Stearn describe three contributions to the second harmonic current density $\vec{j}^{(2\omega)}(\vec{x})$. These are

(i) a surface current normal to the surface which we write

$$j^{(2\omega)}_{sz}(\vec{x}) = \frac{i3e\omega_p^2 a}{16\pi m\omega^3}\ \delta(z+)\left(E^{(\omega)}_z\ (0-)\right)^2 e^{i2k_{//}x}\, e^{-i2\omega t} \qquad (1)$$

where a is a dimensionless constant of order unity, m the conduction electron mass, $\delta(z+) = \delta(z-\varepsilon)$ where ε is a positive infinitesimal, and $E_z^{(\omega)}(0-)$ the z component of the incident field just below the surface of the metal.

(ii) a surface current parallel to the surface given by

$$j_{sx}^{(2\omega)}(\vec{x}) = i\,\frac{be\omega_p^2}{4\pi m\omega^3}\,E_z^{(\omega)}(0-)\,E_x^{(\omega)}(0-)\,\delta(z+)\,e^{i2k_{//}x}\,e^{-i2\omega t} \qquad (2)$$

where b is a dimensionless constant of order unity, and

(iii) a volume current that exists throughout the skin depth

$$\vec{j}_v(\vec{x}) = \frac{ie\omega_p^2}{16\pi m\omega^3}\,\vec{\nabla}\left(\vec{E}^{(\omega)}(z)\cdot\vec{E}^{(\omega)}(z)\,e^{i2k_{//}x}\right)\,e^{-i2\omega t}\ . \qquad (3)$$

To construct the fields associated with the second harmonic, we insert the total current density given by Eqs. (1) - (3) into Maxwell's equation, and use the Green's function method[8] to find the electric field in the wave. Since the Green's function method has been employed in several recent calculations, in this note we omit a description of the details and present only the final result.

In the vacuum above the crystal, there is a second harmonic field given by

$$E_x^{(2\omega)}(\vec{x}) = \frac{1}{i}\,\varepsilon(2\omega)\,\exp[i2k_{//}x - i2\omega t - \alpha_0(2\omega)z] \qquad (4)$$

with $E_z^{(2\omega)}(\vec{x}) = 2ik_{//}\,E_x^{(2\omega)}/\alpha_0(2\omega)$, where $\alpha_0(2\omega) = [4k_{//}^2 - 4\omega^2/c^2]^{\frac{1}{2}} \cong 2\omega/\,|\varepsilon(2\omega)|^{\frac{1}{2}}c$, with the approximate form of $\alpha_0(2\omega)$ valid when $|\varepsilon(2\omega)| >> 1$. The amplitude $\varepsilon(2\omega)$ is given by, in the limit appropriate to the present discussion,

$$\varepsilon(2\omega) = \frac{e\,\omega_p^2\,\delta(\omega)}{m\omega c^3}\;\frac{\gamma(\omega)}{\Delta(\omega)}\;E_o^2\;, \tag{5}$$

where $\delta(\omega)\cong c/\omega_p$ is the skin depth for the incident surface polariton, $\Delta(\omega) = \alpha(2\omega) + \varepsilon(2\omega)\,\alpha_o(2\omega)$, with $\alpha_o(2\omega)$ defined above and $\alpha(2\omega) = [4k_{//}^2 - 4\varepsilon(2\omega)\omega^2/c^2]^{\frac{1}{2}}$, E_o is the magnitude of the electric field component of the incident surface polariton parallel to the surface, evaluated at the surface, and finally $\gamma(\omega)$ is a dimensionless number given by

$$\gamma(\omega) = 2b\text{-}a\left(\frac{\varepsilon(2\omega)}{\varepsilon(\omega)}\right)^{\frac{1}{2}} - \frac{1}{2}\left(\frac{\varepsilon(\omega)}{\varepsilon(2\omega)}\right)^{\frac{1}{2}}\;. \tag{6}$$

In the limit of interest here, ($|\varepsilon(\omega)|$ and $|\varepsilon(2\omega)| >> 1$), one may show that $\Delta(\omega)$ is well approximated by $\Delta(\omega) \cong |\varepsilon(2\omega)|^{\frac{3}{2}}/L_c(\omega)$, where $L_c(\omega) = [2k_{//}(\omega) - k_{//}(2\omega)]^{-1}$ is a coherence length that controls the strength of the non-linear interaction. In the formula for $L_c(\omega)$, $k_{//}(\omega)$ is the wave vector of a surface polariton of frequency ω (this equals that of the incident surface polariton), while $k_{//}(2\omega)$ is that of a surface polariton of frequency 2ω.

From the form of $\gamma(\omega)$, with the constants a and b of order unity, one sees the volume currents contribute to the non-linear mixing (third term of Eq. (7)) on equal footing with the surface currents. This is in contrast to second harmonic generation from plane waves incident on the boundary, where the contribution from the volume currents is small.[5] Also, note for a perfectly phase-matched interaction, $2k_{//}(\omega) \equiv k_{//}(2\omega)$ and $L_c(\omega)$ becomes infinite. In our derivation, we have implicitly assumed the distance of travel L of the incident wave on the surface is long compared to $L_c(\omega)$. In the limit $L << L_c(\omega)$, in the formulae, $L_c(\omega)$ should be replaced by L.[9]

In addition to the fields in the vacuum above the metal, there are non-zero second harmonic fields within the metal. Here one has a driven wave (fields proportional to $\exp[i2k_{//}x+2\alpha(\omega)z]$ where $\alpha(\omega)=[k_{//}^2-\omega^2\varepsilon(\omega)/c^2]^{\frac{1}{2}}$) and a wave with amplitude proportional to $\exp[i2k_{//}x+\alpha(2\omega)z]$. These fields are non-zero only within the skin depth, and are similar in magnitude to the fields in the vacuum, which extend into the vacuum a distance very much larger than the skin depth. The fields in the skin depth thus carry only a very small fraction of the energy in the second harmonic fields, and we ignore their contribution to the energy flow calculated below.

We presume that the incident surface polariton propagates along the surface in a strip of width d, and the second harmonic fields are confined to a strip of the same width. If $I_{(2\omega)}$ is the energy per unit time which flows along the surface in the second harmonic, and $I_{(\omega)}$ that in the incident wave, we find

$$I_{2\omega} = \frac{64\pi}{d}\frac{e^2}{m^2e^5}\left(\frac{\omega_p}{\omega}\right)^4 \frac{\alpha_o(\omega)^6}{\alpha_o(2\omega)^3}\ \delta(\omega)^2\ \frac{|\gamma(\omega)|^2}{|\Delta(\omega)|^2}\ I_{(\omega)}^2 \qquad (7)$$

In our limit $|\varepsilon(\omega)| >> 1$ and $|\varepsilon(2\omega)| >> 1$, this result becomes

$$I_{(2\omega)} = \frac{8\pi}{d}\frac{e^2\omega_p^4}{m^2c^8\omega}\ \frac{\delta(\omega)^2 L_c(\omega)^2}{|\varepsilon(2\omega)|^{\frac{1}{2}}|\varepsilon(\omega)|^3}\ |\gamma(\omega)|^2\ I_{(\omega)}^2, \qquad (8)$$

which is the final result of the present section.

We remind the reader that to obtain Eq. (8), we have begun with a general expression for the output fields, and utilized a series of approximations valid when both $|\varepsilon(\omega)|$ and $|\varepsilon(2\omega)|$ are large compared to unity. The

input wave and output radiation are associated with the nearly linear portion of the surface polariton dispersion curve. Our presumption is that only this frequency regime is of potential interest, since only there is the interaction nearly phase matched.

III. Concluding Remarks and Numerical Estimates

We first simplify Eq. (8) further by presuming that $\varepsilon(\omega) = \varepsilon_\infty - \omega_p^2/\omega^2$, and $\omega << \omega_p$ so in fact $\varepsilon(\omega) \cong -\omega_p^2/\omega^2$. For the skin depth, one has $\delta(\omega) \cong c/\omega_p$ independent of frequency, while the coherence length $L_c(\omega) \cong c\omega_p^2/3\omega^3$. Finally, $|\gamma(\omega)|^2$ approaches the frequency independent limit $|\gamma|^2$, where $\gamma = (4b-a-2)/2$. Eq. (8) then reduces to

$$I_{(2\omega)} = \frac{64\pi}{9d} \frac{e^2\omega^2}{m^2c^4\omega_p^3} |\gamma|^2 I_{(\omega)}^2 \quad . \tag{9}$$

The result in Eq. (9) shows that, as ω decreases, for fixed input power, the energy per unit time carried by the second harmonic decreases as ω^2. The coherence length $L_c(\omega)$ does not increase fast enough as ω decreases to overwhelm the rapidly increasing factors $|\varepsilon(2\omega)|^{\frac{3}{2}}$ and $|\varepsilon(\omega)|^3$ in Eq. (8). These two factors have their origin in the fact that, as ω decreases, a progressively smaller fraction of the energy in both the driving wave and the second harmonic are stored in the medium where the non-linear mixing occurs.

For Cu metal, one has $\hbar\omega_p \cong 10$eV, and for a surface polariton at the CO_2 laser frequency, $\hbar\omega = 0.1$eV. Thus, $\omega/\omega_p \cong 10^{-2}$ and the coherence length $L_c(\omega) \cong 0.5$cm. This means the standard two-prisms ATR geometry[4], with prisms about 0.5cm apart, should prove close to an optimum geometry to observe the second harmonic; the attenuation length of the waves is about 0.5cm in practice, so spacing the prisms this distance apart also places them about $L_c(\omega)$ apart.

If $I_{(2\omega)}$ and $I_{(\omega)}$ are both expressed in watts, and the beam width d is in cm, Eq. (9) gives the quantitative estimate

$$I_{(2\omega)} \simeq \frac{3\times10^{-19}}{d} |\gamma|^2 I_{(\omega)}^2 \quad . \tag{10}$$

To see whether the second harmonic is detectable in the infrared, consider the numbers appropriate to McMullen's attempt to observe the second harmonic. The CO_2 laser employed here had an irradiance of 50 megawatts/cm^2, in a spot diameter of 100 microns. Thus, we take d = 100 microns = 10^{-2} cm, while the total energy in the incident beam is the irradiance multiplied by the spot area; after the beam reflects off the coupling prism, about 10% of this energy is carried by the surface polariton. Thus, we estimate $I_{(\omega)} \simeq 380$ watts, and Eq. (10) gives $I_{(2\omega)} \simeq (5\times10^{-12}) |\gamma|^2$ watts. If 10% of the energy in the second harmonic exits from the output prism, one should find $(0.5\times10^{-12}) |\gamma|^2$ watts at the detector. The limit of detectability in this experiment was about 10^{-12} watts.

While the numerical value of γ is unknown, but presumably the order of unity, the present calculation suggests that the results of the experiment outlined above were inconclusive; with a bit of luck, the second harmonic might have been detected. The theory shows the second harmonic output to be modest, but of detectable magnitude.

IV. Acknowledgements

I am grateful to Dr. J. D. McMullen for a number of discussions of this problem.

REFERENCES

1. See Section X of the article by D. L. Mills and E. Burstein, Reports on Progress in Physics 37, 817 (1974).
2. R. Maddox and D. L. Mills (unpublished). A summary of this work may be found in R. Maddox thesis (University of California, Irvine, 1975).
3. L. Bonsall and A. A. Maradudin (to be published). These authors have corrected an important algebraic error in Reference 2.
4. J. Schoenwald, E. Burstein and J. Elson, Solid State Communications 12, 185 (1973).
5. J. Rudnick and E. Stearn, Phys. Rev. B4, 4274 (1971).
6. J. D. McMullen (private communication).
7. If $|\varepsilon(\omega)|$ is not large compared to unity, the condition of near phase matching is not met.
8. A. A. Maradudin and D. L. Mills, Phys. Rev. B11, 1392 (1975).
9. D. L. Mills, Phys. Rev. B12, 4036 (1975).